REMARKS

Claims 1, 2, 4, 6, 10-12, 14-16, 19, 20, 35, 39, 46-48, 53, 60, 66 to 73 were pending in the present application. Claims 35, 39, 46-48, 53, 60, and 66 are withdrawn from consideration. Claim 11 has been amended to recite that the amino acid "substitution is a substitution of a first amino acid with a second amino acid wherein the first amino acid and the second amino acid are both within the same one of the following groups of amino acids: (i) Alanine, Serine, and Threonine; (ii) Aspartic acid and Glutamic acid; (iii) Asparagine and Glutamine; (iv) Arginine and Lysine; (v) Isoleucine, Leucine, Methionine, and Valine; or (vi) Phenylalanine, Tyrosine, and Tryptophan." The amendment to claim 11 is supported in the specification as originally filed, *e.g.*, at page 31, paragraph 100, and Table 2 at page 31. Claim 67 has been amended to specify that the length of the contiguous nucleotide sequence is at least 500 nucleotides. Support for this amendment can be found in the specification as originally filed, *e.g.*, at page 6, line 8. Claims 68 and 69 have been canceled without prejudice. Applicants reserve the right to prosecute the subject matter of these claims in one or more related continuation, continuation-in-part, and/or divisional applications.

No new matter has been introduced. Claims 1, 2, 4, 6, 10-12, 14-16, 19, 20, 35, 39, 46-48, 53, 60, 66, 67, and 70 to 73 are pending in the present application upon entry of the present amendment.

STATEMENT OF THE SUBSTANCE OF THE INTERVIEW

A telephonic interview in connection with the above-identified patent application was held on September 21, 2006 with Patent Examiner Stacy Brown Chen and Applicants' representatives Dr. Jacqueline Benn and Dr. Sebastian Martinek participating. Applicants and Applicants' representatives thank Patent Examiner Chen for her courtesy during the interview.

Topics of the discussion were 1) the rejection of claims 67-71 under 35 U.S.C. 102(b) over Karron et al.; 2) the rejection of claim 11 under 35 U.S.C. 112, second paragraph; and 3) the rejection of claims 1, 2, 4, 6, 10-12, 14-16, 19, and 20 under 35 U.S.C. 112, first paragraph, for failing to comply with the written description requirement.

Dr. Benn stated that Applicants propose to amend claim 67 to recite "at least 500 contiguous nucleotides of SEQ ID NO:1." Dr. Benn further stated that an alignment between the nucleotide sequence that encodes the amino acid sequence of Karron and the

corresponding nucleotide sequence of the viral strain of the present invention revealed that there is no contiguous stretch of sequence identity that is at least 500 nucleotides long. Examiner Chen stated that if the alignment data are correct, Karron would not anticipate the present invention as claimed in amended claim 67.

Dr. Benn continued to discuss the rejection of claim 11 for the recitation of the term "conservative." Dr. Benn stated that Applicants proposed to amend the claim by removing the term conservative and, in its place, recite the conservative amino acid exchanges listed in Table 2 of the specification. Examiner Chen replied that that amendment should overcome the rejection.

Dr. Benn then began the discussion of the written description rejection by a brief description of the present invention: Applicants had discovered a new strain of respiratory syncytial virus (RSV) and analyzed its sequence. Dr. Benn continued to state that many other strains of RSV and their respective sequences were known in the art and that the skilled artisan can determine which structures of Applicants' new strain of RSV should be maintained and which can be modified simply by comparing the sequence of the presently claimed virus with the sequences of known RSV strains. Such sequence comparisons to determine conserved, and therefore likely essential, core-structures of a virus are routine.

Dr. Martinek stated that the legal standard for written description is illustrated in a recent decision by the Federal Circuit: *Invitrogen v. Clontech*, 429 F.3d 1052 (Fed. Cir. 2005). Dr. Martinek briefly summarized this case. The subject of the invention was a genetically engineered reverse transcriptase. The inventors had discovered that a modified reverse transcriptase enzyme with DNA polymerase activity but without RNase H activity had certain beneficial properties. Polypeptides with DNA polymerase activity and substantially reduced RNase H activity were claimed. The claimed polypeptides were further only identified as being encoded by a modified reverse transcriptase nucleotide sequence, wherein the nucleotide sequence is derived from a retrovirus, yeast, Neurospora, Drosophila, primates, or rodents. But no sequence information was recited. Further, the patents-in-suit disclosed only mutants from a single virus. Nevertheless, the Federal Circuit upheld the trial court's determination that the written description requirement had been met. The rational for the decision was that the sequences of reverse transcriptase genes were known, that the genes of different species share significant homologies, and that there was a known correlation between RNase H activity of reverse transcriptase and the structure of the gene encoding the reverse transcriptase.

Examiner Chen stated that from the information available to her, Applicants disclosed a partial structure, namely by reciting a percentage of sequence identity to a disclosed sequence, but failed to disclose which parts are sufficient to obtain the recited function.

Dr. Martinek recited a passage from the Guidelines for Examination of Patent Applications Under the 35 U.S.C. 112 ¶ 1, "Written Description Requirement" (published in the January 5, 2001 Federal Register at Volume 66, Number 4, p. 1099-1111) that states that the written description requirement can be complied with by providing "functional characteristics coupled with a known or disclosed correlation between structure and function." Dr. Martinek stated that in the present case the functional characteristics were disclosed, namely infectivity and replication, and that the correlation between structure and function was known in the art. Dr. Benn continued to state that Applicants could provide several pre-filing publications to demonstrate the state of the art. In particular, publications showing sequence alignments among different RSV strains from which functional conclusions were drawn could be provided.

Examiner Chen stated that this information would be helpful, and that Applicants should also cite the *Invitrogen* case in their response. Examiner Chen concluded that once Applicants had filed their response, she would discuss the written description issue with a quality assurance specialist.

Change of Correspondence Address

Applicants had submitted a Revocation and Power of Attorney on October 25, 2005 and requested that all future correspondence be directed to the new Attorneys of record and that their attorney docket number be used in future correspondence from the U.S. Patent and Trademark Office. Since the outstanding Office Action of June 26, 2006 has been mailed to the previous representative of Applicants, the present representatives for Applicants submit herewith a Change of Correspondence Address form PTO/SB/122.

The Rejections under 35 U.S.C. § 112, Second Paragraph, Should Be Withdrawn

Claim 11 is rejected under 35 U.S.C. § 112, second paragraph, for indefiniteness. In particular the claims have been rejected because the claim term "conservative" is unclear.

In response, claim 11 has been amended to delete the term "conservative," and to list conservative amino acid substitutions. Because the term "conservative" has been deleted

from the claim, the rejection under 35 U.S.C. § 112, second paragraph, for indefiniteness, should be withdrawn.

The Rejections under 35 U.S.C. § 112, First Paragraph, Should Be Withdrawn

Claims 1, 2, 4, 6, 10, 11, 12, 14, 15, 16, 19, 20, and 20 are rejected under 35 U.S.C. § 112, first paragraph, for insufficient written description. The claims are directed to biosequences and sequences with certain degrees of sequence identities to those biosequences. The Examiner argues that these claimed genera of biosequences are very large, a representative number of species has not been disclosed, no portion of the biosequence that must be conserved to obtain an infectious and replicating RSV has been taught. Applicants respectfully disagree.

Applicants had previously argued that the specification discloses biosequences and degrees of sequence identity between the disclosed sequence and the claimed sequences. The specification further discloses that the claimed sequences encode infectious, replicating viruses (SEQ ID NO:1 and homologs thereof) or are components of an infectious, replicating virus (SEQ ID NO:2-11). The correlation between the structure and function of viral genomes (SEQ ID NO:1) and of the protein components of viruses (SEQ ID NO:2-11) is well-known in the art. In response, the Examiner contends in the present Office Action that the "[o]ne of skill in the art would not know how to modify SEQ ID NO:1 such that a sequence of any less than 100% identity would encode an infectious, replicating respiratory syncytial virus without having to experiment with different mutations . . .." Page 5, lines 5-8 of the present Office Action.

Applicants would like to reiterate that *Invitrogen v. Clontech*, 429 F.3d 1052 (Fed. Cir. 2005; attached as Exhibit A) is applicable to the present situation. In *Invitrogen*, the patents-in-suit disclose genetically engineered reverse transcriptase. The reverse transcriptase has two enzymatic activities: DNA polymerase activity and RNase H activity. The inventors of the patents-in-suit developed mutant reverse transcriptase with DNA polymerase activity but without RNase H activity.[1] The claims are directed to polypeptides with DNA polymerase activity and substantially reduced RNase H activity, wherein the polypeptide is encoded by a modified reverse transcriptase nucleotide sequence, wherein the nucleotide sequence is derived from a retrovirus, yeast, Neurospora, Drosophila, primates, or

[1] A copy of one of the patents-in-suit, U.S. Patent 6,063,608, is attached as Exhibit B.

rodents. The disclosure of representative species in the patents-in-suit, however, is limited to several deletion mutants of Moloney murine leukemia virus reverse transcriptase. Additionally, it is noted that the claims do not recite any biosequence information. Nevertheless, the Federal Circuit upheld the trial court's determination that the written description requirement had been met. The rational for the decision was that the sequences of reverse transcriptase genes were known, that the genes of different species share significant homologies, and that there was a known correlation between RNase H activity of reverse transcriptase and the structure of the gene encoding the reverse transcriptase. *Id.* at 1072-1073.

Similarly, in the present case, the genomic viral sequence and several viral protein sequences for RSV B 9320 are disclosed in the application. Homologous sequences in other strains of RSV were known in the art. It was further well-known that sequence alignments between homologous sequences reveal conserved regions, and that such conserved regions are more likely to be essential to the function of the protein than other regions of the protein.

Smith *et al.*, 2002 (Protein Engineering 15(5):365-371; "Smith;" attached as Exhibit E) is an example of how sequence alignments of the F protein can be used to determine three-dimensional structures and thereby derive locations of certain functional components in a protein (see Table 1). Smith had employed a technology called "homology modeling" to determine the three-dimensional structure of the F protein of an RSV by sequence comparison with the equivalent protein of Newcastle disease virus. The resulting three-dimensional model is shown in Figure 2 at page 370 of Smith. Functional aspects of the F protein, such as the stalk of the protein and certain antigenic sites, are indicated. Similarly, the skilled could align the sequence of the F protein, or any other protein, of the RSV strain of the present invention and deduce a three-dimensional model and thereby determine which amino acids are at essential positions in the molecule and should not be altered, and which can be modified.

Garcia, 1994 (J. Virol. 68(9):5448-5459; "García;" attached as Exhibit F) published an alignment of the G proteins of many different RSV isolates. One sequence alignment is shown in Figure 2 at page 5451. Locations of amino acid variability are indicated in the figure. The skilled artisan would readily deduce that these locations can be modified without losing the viability of the resulting virus. And vice versa, amino acids that are conserved among different RSV isolates and strains, would be expected to be important for virus viability. For example, the location of the four cysteines of the G-protein's ectodomain are

indicated in Figure 2 of García are indicated. The skilled artisan would know to leave these intact if proper folding and function of the G-protein of the virus of interest was desired.

Additionally, structure-function analyses had been conducted for different RSV sequences. For example, Fearns *et al.*, 2000 (J. Virol. 74(13):6006-6014; "Fearns;" attached as Exhibit C) conducted a functional analysis of the promoters of human RSV by determining the effects of increasingly larger deletions in the viral genome. By aligning the sequence of the virus used in Fearns with the sequence of the presently claimed viral strain, the skilled artisan would know which portions of the viral promoter are essential and should be maintained and which portions could be deleted while retaining viral replication.

Similarly, Zimmer *et al.*, 2002 (J. Virol. 76(18):9218-9224; "Zimmer;" attached as Exhibit D) conducted a structure function analysis relating to proteolytic processing of the F protein. In particular, Zimmer showed that mutations in one of the cleavage sites of the F protein abolished proteolytic processing at that site and the resulting virus, although viable, showed a reduced cytopathic effect. Again, the skilled artisan could align the sequence of the F protein of the presently claimed viral strain with the sequence of the F protein used in Zimmer and deduce the analogous amino acid substitutions that would be expected to result in the same effect.

The above examples illustrate that the skilled artisan was familiar with the structural basis of different aspects of viral functions.

The present application, thus, provides a structure, namely the viral genomic sequence of RSV B 9320 coupled with percentages of sequence identity, and functional characteristics. The correlation between structure and function was well-known in the art.

Because the factual situation is very similar to the present situation and because the rational the led to the holding in *Invitrogen* squarely applies to the present case, Applicants request that the rejection under 35 U.S.C. § 112, first paragraph, be withdrawn.

The Rejections under 35 U.S.C. § 102 over Karron Should Be Withdrawn

Claims 67-71 are rejected under 35 U.S.C. § 102(b) as anticipated by Karron *et al.* (1997, PNAS USA 94:13961-13966, "Karron"). In particular, the Examiner asserts that Karron teaches a nucleotide sequence that is 99.4% identical to SEQ ID NO:9.

First, it is noted that claim 67 has been amended to specify that the length of the contiguous nucleotide sequence is at least 500 nucleotides.

The sequence that has been deposited by Karron at accession number O42050 is an amino acid sequence. In contrast, the rejected claims are directed to polynucleotides. Applicants have obtained the nucleotide sequence that encodes the amino acid at accession number O42050 and aligned it with the nucleotide sequence that encodes SEQ ID NO:9 (Exhibit G). This alignment reveals that there is no contiguous region of sequence identity between these two nucleotide sequences that is at least 500 nucleotides long. Thus, Karron does not teach all the limitations of claim 67, and the rejection under 35 U.S.C. § 102(b) as anticipated by Karron should accordingly be withdrawn.

Conclusion

Applicants respectfully submit that all of the pending claims are now in condition for allowance. If there are any remaining concerns, the Examiner is invited to call the undersigned to schedule an interview.

It is believed that no fee is due in connection with this Amendment other than that for the extension of time; however, in the event any additional fee is required, please charge the required fee to Jones Day Deposit Account No. 50-3013.

Entry of the remarks made herein is respectfully requested.

Respectfully submitted, by: Jacqueline Bon
Reg No. 43,492

Date: September 25, 2006

Laura A. Coruzzi 30,742
Laura A. Coruzzi (Reg. No.)

JONES DAY
222 East 41st Street
New York, New York 10017
212-326-3939

JOURNAL OF VIROLOGY, July 2000, p. 6006–6014 Vol. 74, No. 13
0022-538X/00/$04.00+0

Functional Analysis of the Genomic and Antigenomic Promoters of Human Respiratory Syncytial Virus

RACHEL FEARNS,[1] PETER L. COLLINS,[1]* AND MARK E. PEEPLES[1,2]

Laboratory of Infectious Diseases, National Institute of Allergy and Infectious Diseases, Bethesda, Maryland 20892-0720[1] and Department of Immunology and Microbiology, Rush-Presbyterian-St. Luke's Medical Center, Chicago, Illinois 60612[2]

Received 9 February 2000/Accepted 12 April 2000

The promoters involved in transcription and RNA replication by respiratory syncytial virus (RSV) were examined by using a plasmid-based minireplicon system. The 3′ ends of the genome and antigenome, which, respectively, contain the 44-nucleotide (nt) leader (Le) and 155-nt trailer-complement (TrC) regions, should each contain a promoter for RNA replication. The 3′ genome end also should have the promoter for transcription. Substitution for the Le with various lengths of TrC demonstrated that the 3′-terminal 36 nt of TrC are sufficient for extensive (but not maximal) replication and that when juxtaposed with a transcription gene-start (GS) signal, this sequence was also able to direct transcription. It was also shown that the region of Le immediately preceding the GS signal of the first gene could be deleted with either no effect or with a slight decrease in transcription initiation. Thus, the TrC is competent to direct transcription even though it does not do so in nature, and the partial sequence identity it shares with the 3′ end of the genome likely represents the important elements of a conserved promoter active in both replication and transcription. Increasing the length of the introduced TrC sequence incrementally to 147 nt resulted in a fourfold increase in replication and a nearly complete inhibition of transcription. These two effects were unrelated, implying that transcription and replication are not interconvertible processes mediated by a common polymerase, but rather are independent processes. The increase in replication was specific to the TrC sequence, implying the presence of a nonessential, replication-enhancing *cis*-acting element. In contrast, the inhibitory effect on transcription was due solely to the altered spacing between the 3′ end of the genome and GS signal, which implies that the transcriptase recognizes the first GS signal as a promoter element. Neither the enhancement of replication nor the inhibition of transcription was due to increased base-pairing potential between the 3′ and 5′ ends. The relative strengths of the Le and TrC promoters for directing RNA synthesis were compared and found to be very similar. Thus, these findings highlighted a high degree of functional similarity between the RSV antigenomic and genomic promoters, but provided a further distinction between promoter requirements for transcription and replication.

Human respiratory syncytial virus (RSV) is a member of the family *Paramyxoviridae* of the order *Mononegavirales*, the nonsegmented negative-strand RNA viruses (35). The genome of RSV (strain A2) is 15,222 nucleotides (nt) in length and encodes 11 proteins. Three proteins are associated with the nucleocapsid: the major RNA-binding nucleocapsid N protein, the P phosphoprotein, and the major polymerase subunit L (21, 32, 42). The RSV N, P, and L proteins together with the RNA genome are the virus-specific components required for RNA replication (19, 43). Processive transcription requires, in addition, the transcription antitermination protein, M2-1 (11, 15, 20).

In some aspects of transcription and replication, RSV resembles prototype mononegaviruses such as Sendai virus (SeV) and vesicular stomatitis virus (VSV) (reviewed in references 12, 26, and 39). The genome is tightly bound by N protein to form the nucleocapsid, which is the template for the viral polymerase. The 3′ and 5′ ends of the genome consist of short extragenic leader (Le) and trailer (Tr) regions, respectively (29). Genome transcription is initiated at the genomic promoter located at the 3′ (Le) end (13) and involves a sequential stop-start mechanism in which the polymerase is guided by conserved *cis*-acting signals present at the ends of each gene to produce a series of subgenomic mRNAs (24). The RSV transcription signals are the 10-nt gene start (GS) and 12- to 13-nt gene end (GE) signals found at the beginning and end, respectively, of each gene (25). It is not known whether the RSV Le region is transcribed into a short positive-sense Le RNA, comparable to those of VSV and SeV.

In RNA replication, the genome is copied into a complete positive-sense encapsidated intermediate called the antigenome; hence, the 3′ and 5′ ends of the antigenome are the Tr complement (TrC) and Le complement (LeC), respectively. The antigenome is the template for the synthesis of progeny genome. In the case of RSV, the Le and TrC regions are 81% identical for the first 26 nt, after which there is no apparent relatedness (Fig. 1) (29). This likely represents a conserved promoter at the 3′ end of the genome and antigenome. It might also represent a conserved encapsidation signal at the 5′ end of these molecules, although as yet there is no evidence for this signal for RSV (33).

The early events in mononegavirus transcription and RNA replication are not well understood. A widely held view is that a common polymerase initiates at a single promoter, copies the Le region, and somehow commits to either stop-start transcription or readthrough replication. The availability of soluble N protein to direct cosynthetic encapsidation of the nascent positive-sense product is thought to switch the polymerase to readthrough replication (4, 23). According to this model, transcription and RNA replication are interconvertible processes. However, an alternative possibility is that transcription and

* Corresponding author. Mailing address: 7 Center Dr. MSC 0720, Bethesda, MD 20892-0720. Phone: (301) 496-3481. Fax: (301) 496-8312. E-mail: pcollins@niaid.nih.gov.

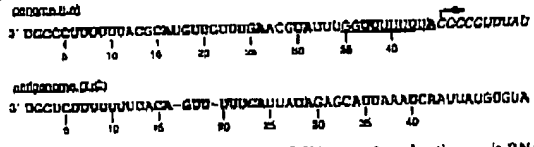

FIG. 1. Sequences of the 3' termini of RSV genomic and antigenomic RNA (Le and TrC, respectively). The first 52 nt of the TrC sequence are shown with gaps introduced to maximize sequence alignment with the Le sequence, and nucleotide assignments that are identical in Le and TrC are shown in boldface. The last 10 nt of Le are underlined, the GS signal is italicized, and the transcription initiation site is indicated with an arrow. Note that the Le contains a C residue at position 4. Both the C and G assignments have been identified at this position in biologically derived virus.

replication are independent processes that involve different versions of the polymerase and/or different *cis*-acting initiation signals. In this case, transcription need not necessarily initiate at the 3' genomic terminus. In this respect, there is some evidence that transcription can be initiated directly at the GS signal of the first gene of VSV (7).

While it appears that certain features of transcription and replication are shared among the mononegaviruses, RSV has its own distinct features. For example, processive transcription requires an antitermination factor, the M2-1 protein, which is not found in most other mononegaviruses. Two additional proteins, NS1 and M2-2, which exist only for the *Pneumovirus* genus, have been implicated in regulating RNA synthesis (2, 3, 22). Deletion of the M2-2 gene reduces RNA replication and augments RNA transcription. Unlike other paramyxoviruses, RSV replication does not require the genome nucleotide length to be a multiple of 6 (36). Furthermore, the *cis*-acting signals involved in initiation of replication and transcription appear to be mostly or entirely confined to the extragenic regions and the first GS signal (10, 24), whereas for other paramyxoviruses, these signals extend into the adjacent genes (30, 38).

The present study investigates the *cis*-acting sequences involved in RSV transcription and RNA replication and, in particular, examines and compares the genomic and antigenomic promoters contained in the Le and TrC regions, respectively.

MATERIALS AND METHODS

cDNAs. Minigenome plasmids C41, C2, and 2G have been described previously (15, 19, 33). Each encoded minigenome contains in 3'-to-5' order the 44-nt RSV Le, the 10-nt NS1 GS signal, the upstream 29 nt of the nontranslated region of the NS1 gene, a 669-nt negative-sense copy of the chloramphenicol acetyltransferase (CAT) open reading frame (ORF), the last 12 nt of the nontranslated region of the L gene, the 12-nt L GE signal, and the 155-nt Tr region. Minigenome 2G differs in that it contains a C-to-G mutation (negative sense) at position 2 relative to the 5' end of the Tr. Each cDNA is bordered at the 5' end relative to the encoded minigenome by three G residues and the T7 RNA polymerase promoter (the G residues improve efficiency of initiation by the T7 RNA polymerase) and at the 3' end with a self-cleaving ribozyme: the hammerhead ribozyme in C2 and 2G (19) and the hepatitis delta virus ribozyme in C41 (34). Plasmid C4 contains minigenome C2 in the opposite orientation with respect to the ribozyme and T7 RNA polymerase promoter and so encodes a positive-sense miniantigenome. Minigenome plasmids A36 to A147 were prepared by PCR-amplifying portions of the RSV Tr sequence with C41 plasmid as a template. The negative-sense primer contained a portion of the hepatitis delta ribozyme sequence, including an *Rsr*II site, and hybridized to the end of the Tr region. The positive-sense primer contained a *Bsr*XI site and hybridized within the Tr region to generate Tr fragments of 36, 57, 77, 97, 117, or 147 nt. The PCR products were digested with *Rsr*II and *Bsr*XI and inserted into the *Rsr*II-*Bsr*XI window of minigenome C41, which contains an *Rsr*II site within the ribozyme and a naturally occurring *Bsr*XI site within the Le (the *Bsr*XI recognition sequence spans nt 35 to 46). Plasmids B36 to B147 were constructed by the method of Byrappa et al. (5): minigenome plasmids A36 to A147 were used as templates for PCR amplification by using a positive-sense phosphorylated primer whose 5' end lay 42 nt from the Tr terminus and a negative-sense phosphorylated primer whose 5' end lay at the end of the L GE signal. The PCR product was gel purified and ligated. Plasmids C61, C81, and C101 were prepared by inserting oligonucleotide duplexes into the *Bsr*XI site of plasmid C2, resulting in heterologous insertions of 17, 37, or 57 nt. These insertions regenerated the end of the Le and the NS1 GS signal. Each insert included a unique *Afl*II site. Minigenome plasmids C121 and C151 were prepared by inserting 20 and 30 nt into the *Afl*II site within C101 by using oligonucleotide duplexes consisting of sequence randomly chosen from the RSV N gene. Plasmids D36 to D97 were generated by using A36 to A97 as templates in a PCR (5), a phosphorylated positive-sense primer whose 5' end lay at the first G residue of the NS1 GS signal, and a phosphorylated negative-sense primer whose 5' end lay at position 34 of the Le. Plasmids E36 to E97 were constructed by transferring the Tr region of plasmid 2G into plasmids A36 to A97 by using *Nco*I, which restricts within the CAT ORF, and *Hin*dIII, which restricts between the plasmid backbone and the T7 RNA promoter. Minigenome plasmid F1 was generated from plasmid C41 by PCR mutagenesis (5) to insert a hammerhead ribozyme (1) and a sequence GGGACGG, which allows optimal transcription by the T7 RNA polymerase, between the Tr and the T7 RNA polymerase promoter. Minigenome F3 was constructed in a similar manner with a version of C41 that contains a G rather than a C at position 4 of the Le (negative sense). Minigenome plasmids F2 and F4 were prepared from F1 and F3, respectively, by using PCR to replace the Tr region with LoC sequence. The LoC sequence contained a G at position 4 relative to the 3' end of the antigenome.

Transfections. Monolayers of HEp-2 cells in six-well dishes were simultaneously infected with 10 PFU (per cell) of vaccinia virus vTF7-3 (provided by Thomas Fuerst and Bernard Moss), which expresses the T7 RNA polymerase (18), and transfected with the following mixture of plasmids per well of a six-well dish: 0.2 μg of minigenome DNA, 0.4 μg of pTM1 N, 0.2 μg of pTM1 P, 0.1 μg of pTM1 M2-1, and 0.1 μg of pTM1 L (Fig. 2 to 7) or 0.2 μg of minigenome DNA, 0.4 μg of pTM1 N, 0.2 μg of pTM1 P, and 0.1 μg of pTM1 L (Fig. 8), as described previously (19). Control transfections lacking L or all support plasmids received pTM1 plasmid with no insert so that the amount of transfected DNA was equivalent in each well. Twenty-four hours later, the transfection-infection mixture was replaced with OptiMem containing 2% fetal bovine serum and actinomycin D (Calbiochem) at 2 μg/ml. The actinomycin D-containing medium was removed after 2 h, replaced with fresh OptiMem containing 2% fetal bovine serum, and incubated for a further 24 h. Each transfection reaction was set up in duplicate: RNA was directly extracted from cells from one of the wells, and the cells in the other well were lysed with nonionic detergent and incubated with micrococcal nuclease (MCN) prior to RNA purification to digest unencapsidated RNA, as described previously (14).

RNA isolation, oligo(dT) chromatography, and Northern blot hybridization. RNA was extracted by dissolving cell pellets or MCN-treated cell lysates in Trizol reagent (Life Technologies) according to the supplier's protocol, except that the RNAs were extracted with phenol-chloroform and ethanol precipitated after the isopropanol precipitation. Oligo(dT) chromatography was performed with an Oligotex mRNA mini kit (Qiagen) according to the manufacturer's instructions, except that the RNA was denatured by being heated to 95°C prior to addition of the Oligotex suspension. RNA representing 1/10 of one well of cells was analyzed by electrophoresis in a 1.5% agarose gel containing 0.44 M formaldehyde, transferred to nitrocellulose (Schleicher & Schuell), and fixed by UV cross-linking (Stratagene). Negative-sense or positive-sense ^{32}P-labelled CAT-specific riboprobe was synthesized by T7 RNA polymerase from *Xho*I-digested C2 cDNA or *Nco*I-digested C4 cDNA, respectively and hybridized to the Northern blot in a mixture of 6× SSC (1× SSC is 0.15 M NaCl plus 0.015 M sodium citrate), 5× Denhardt's solution, 0.5% sodium dodecyl sulfate (SDS), and 200 μg of sheared DNA per ml at 65°C for 12 h. The blots were washed in 2× SSC–0.1% SDS at room temperature for 30 min and then at 65°C for 2 h and then in 0.1× SSC–0.1% SDS at 65°C for 15 to 30 min. The blot shown in Fig. 4D was hybridized with a 5' ^{32}P-labelled, negative-sense, Le-specific oligonucleotide probe (5'-GG TTTATGCAAGTTTGTTGTACGCATTTTTTCCCGT) in a solution of 5× SSC, 5× Denhardt's solution, 0.1% SDS, 0.05% sodium pyrophosphate at 52°C for 12 h. The blot was washed in 6× SSC for 30 min. PhosphorImager analysis was carried out with a PhosphorImager 445 SI (Molecular Dynamics).

Primer extension analysis of RNA. Oligo(dT)-purified or total RNA representing one-third to one-half of a well of cells or 5 pmol of RNA transcribed in vitro from plasmid C4 by T7 RNA polymerase was annealed to an excess of 5' ^{32}P-labelled, negative-sense, CAT-specific oligonucleotide probe (5'-GGGATA TATCAACGGTGGTATATCCAGTGT) in 1× SuperScript II buffer (Life Technologies) by heating the mixture to 95°C for 5 min and placing it at room temperature for 15 min. One-half of the RNA-DNA hybrid was utilized as a template in a reverse transcriptase reaction using SuperScript II reverse transcriptase (Life Technologies) according to the supplier's reaction conditions, except that the reaction was carried out at 37°C for 1 h. The cDNA was extracted with phenol-chloroform and precipitated with ethanol and resuspended in 20 μl of a mixture of 95% formamide, 20 mM EDTA, 0.05% bromophenol blue, and 0.05% xylene cyanol. Ten microliters of this cDNA was electrophoresed on a 5% LongRanger (J. T. Baker) polyacrylamide gel and analyzed by autoradiography and phosphorimaging. As a molecular length marker, a dideoxy C sequencing reaction was carried out with the same oligonucleotide as a primer and with C41 plasmid as a template for T7 Sequenase (Amersham).

RESULTS

Effects of replacing Le with TrC. RNA synthesis from the RSV genomic and antigenomic promoters was compared by using a plasmid-based, intracellular system in which a genome analog (minigenome) containing a CAT reporter gene is coexpressed with RSV nucleocapsid and polymerase proteins. The RNAs synthesized by the reconstituted RSV polymerase are detected by Northern blotting. Minigenome C41 represents the wild-type genome and contains at its 3′ end the first 86 nt of the RSV genome, including the 44-nt Le, the NS1 GS signal, and the nontranslated region of the NS1 gene, and at its 5′ terminus, the last 179 nt of the genome, including the nontranslated region of the L gene, the L GE signal, and the 155-nt Tr (Fig. 2A). To examine the promoter activity of the TrC region, we constructed a series of minigenomes in which the first 34 nt of Le sequence were replaced with various lengths of TrC sequence ranging from 36 to 147 nt (minigenomes A36 to A147). The 10 nt that lie immediately upstream of the NS1 GS signal were left intact to avoid disruption of possible *cis*-acting elements preceding this GS signal (Fig. 2A).

Plasmids encoding minigenome C41 or A36 to A147 were transfected together with support plasmids into cells which had been infected with a vaccinia virus encoding T7 RNA polymerase to drive plasmid expression. Total intracellular RNA was harvested at 48 h and analyzed by Northern blot hybridization with a negative-sense riboprobe to detect antigenome and mRNA generated by the RSV polymerase. To further distinguish the encapsidated antigenome, cell extracts from duplicate transfection wells were treated with MCN prior to RNA purification. As described previously (15), minigenome C41 generated a large amount of mRNA and a small amount of antigenomic RNA (Fig. 2B and C, lane 3). Similarly minigenome A36 generated both antigenome and mRNA (Fig. 2B and C, lane 4). Thus the first 36 nt of TrC contain a promoter that can direct transcription in addition to replication when juxtaposed with the Le-NS1 junction sequence. As the length of TrC sequence was increased (minigenomes A57 to A147), the level of antigenome increased, although minigenomes containing more than 97 nt of TrC sequence yielded somewhat less than the maximal level (Fig. 2B and C). In contrast, mRNA synthesis decreased significantly, such that the mRNA synthesized from minigenomes A97 to A147 was barely detectable (Fig. 2B, lanes 7 to 9). Thus, increasing the amount of TrC sequence augmented replication and reduced transcription.

It was important to confirm that the level of plasmid-supplied minigenome RNA was equivalent in each transfection reaction. Therefore parallel transfections were carried out in the absence of the L expression plasmid, and the accumulation of plasmid-supplied minigenome was analyzed by Northern blotting with a positive-sense probe. This analysis showed that a similar amount of plasmid-supplied minigenome RNA accumulated in each transfection (Fig. 2D). However, examination of MCN-treated RNA showed that there was a progressive change in the pattern of MCN-resistant input minigenome with increasing length of added TrC sequence (Fig. 2E, lanes 3 to 8). Minigenomes C41, A36, and A57 could be observed as abundant single bands (Fig. 2E, lanes 2 to 4), but minigenomes A77 to A147 appeared as less-abundant multiple bands, mostly of slightly reduced length (Fig. 2E, lanes 5 to 8). This suggested that one or both termini of these RNA molecules were incompletely encapsidated and hence subject to digestion by MCN and that encapsidation overall was much less efficient. The results presented below indicated that this was due to the high degree of terminal complementarity of these minigenomes, which probably promoted panhandle structure formation and

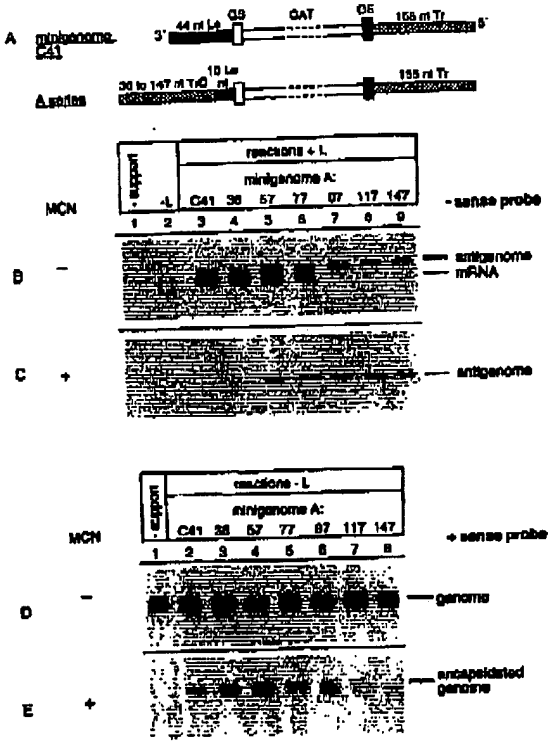

FIG. 2. Effect of replacing the 3′ 34 nt of Le with increasing lengths of TrC. (A) Structures (not to scale) of minigenome C41, representing wild-type RSV, and minigenomes A36 to A147, which are designated according to the length of the added TrC sequence. GS or GE signals are indicated with open or solid boxes, respectively. (B and C) Northern blots of positive-sense RNAs synthesized by the reconstituted RSV polymerase. HEp-2 cells were infected with vaccinia virus vTF7-3 and simultaneously transfected with plasmids that encode minigenome C41 (lanes 1, 2, and 3) or minigenomes A36 to A147 (lanes 4 to 9, as indicated) together with pTM1 support plasmids expressing N, P, and M2-1 (lane 2) or N, P, M2-1, and L (lanes 3 to 9) proteins. Lane 1 received empty pTM1 expression plasmid. Forty-eight hours later, the cells were processed directly for RNA purification (B), or lysates were prepared and treated with MCN to destroy unencapsidated RNA (C). The blots were hybridized with a negative-sense, CAT-specific riboprobe. (D and E) Northern blot analyses of plasmid-supplied minigenome template. HEp-2 cells were infected with vTF7-3 and transfected with plasmids that encode minigenome C41 (lanes 1 and 2) or minigenomes A36 to A147 (lanes 3 to 8, as indicated) together with plasmids expressing N, P, and M2-1 proteins (lanes 2 to 8) or with empty pTM1 plasmid (lane 1). L plasmid was omitted from all reactions, and hence the only source of minigenome RNA was plasmid. Forty-eight hours later, the cells were processed directly for RNA purification (D) or lysed and treated with MCN followed by RNA purification (E). The RNAs were detected with a positive-sense, CAT-specific riboprobe.

inhibited encapsidation of the termini. The relatively lower levels of full-length, encapsidated minigenome generated from plasmids A97 to A147 would account for the relatively lower levels of antigenome produced in these transfections, as described above (Fig. 2B and C).

The amounts of antigenome and mRNA generated from the minigenomes that were encapsidated efficiently (C41, A36, and A57) were quantitated by PhosphorImager analysis. This analysis showed that minigenome A36 produced amounts of antigenome and mRNA similar to those of minigenome C41, whereas minigenome A57 generated approximately twofold more antigenome and one-third less mRNA.

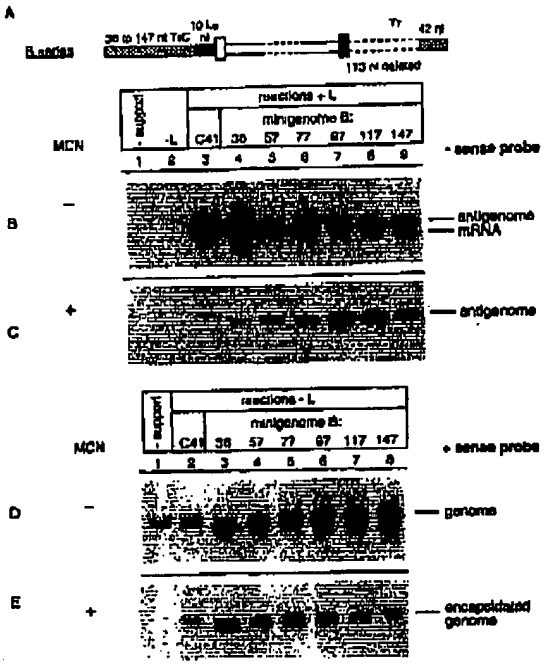

FIG. 3. Effect of replacing Le with increasing lengths of TrC under conditions in which terminal complementarity is limited to 42 nt. (A) Structure of a series of minigenomes, B36 to B147, in which the 3' 34 nt of Le have been replaced by the indicated length of TrC sequence (as in minigenome series A shown in Fig. 2) and the Tr has been truncated to the 5' 42 nt, thus limiting terminal complementarity. (B and C) Northern blots of positive-sense RNAs synthesized by the reconstituted RSV polymerase. Parallel wells of cells were transfected with plasmid C41 (lanes 1 to 3) or minigenomes B36 to B147 (lanes 4 to 9, as indicated) together with plasmids expressing N, P, and M2-1 (lane 2) or N, P, M2-1, and L (lanes 3 to 9). Lane 1 received empty pTM1 expression plasmid. The blots show total (B) or MCN-resistant (C) RNA, detected by hybridization with a negative-sense CAT probe. (D and E) Northern blot analysis of plasmid-derived minigenome template. Cells were transfected with plasmid C41 (lanes 1 and 2) or plasmids encoding minigenomes B36 to B147 (lanes 3 to 8, as indicated) without support plasmids (lane 1) or with N, P, and M2-1 plasmids (lanes 2 to 8). The blots show total (C) or MCN-resistant (D) RNA, detected by hybridization with a positive-sense CAT probe.

TrC nt 77 to 97 enhance replication independently of increased terminal complementarity. Increasing the length of TrC sequence used to replace Le might have affected the pattern of positive-sense RNA synthesis either directly, as a consequence of its primary sequence or increased length compared to that of Le, or indirectly, by increasing the degree of terminal complementarity and potential interaction between the genome ends, or both. Terminal complementarity has been shown to affect transcription and replication by VSV (40, 41). To distinguish between these possibilities, minigenomes were constructed that were similar to those described above, but contained only the 5'-proximal 42 nt of Tr sequence (B series of minigenomes [Fig. 3A]). Thus, these minigenomes have increasing amounts of TrC sequence at the 3' terminus, but share the same degree of terminal complementarity.

Figure 3B and C show Northern blots of total and MCN-resistant, positive-sense RNA generated by the RSV polymerase. Note that in panel B, lane 5 is underloaded in this particular experiment, as was confirmed by repeat experiments. This analysis showed that, as with minigenomes containing complete Tr, antigenome levels increased and mRNA levels decreased with increasing length of TrC. For minigenomes B57 to B147, these effects cannot be attributed to increasing terminal complementarity and therefore must be due to the primary sequence or increased length of the introduced TrC segment.

Figure 3D and E are Northern blots of the control transfections showing the accumulation of total and MCN-resistant, plasmid-supplied minigenome, respectively. In contrast to the situation seen with minigenomes containing complete Tr, each minigenome was observed as a single, discrete band following MCN treatment, indicating that each of these minigenomes was completely encapsidated. This result indicated that it was the high level of terminal complementarity of minigenomes A77 to A147 that inhibited encapsidation (Fig. 2E).

Because each transfection received completely encapsidated minigenome, this experiment allowed us to measure the effect of different lengths of TrC sequence on antigenome accumulation. The RNA bands in panel C were quantitated by using a PhosphorImager and adjusted according to the values for panel E to account for the minor variation in input encapsidated RNA. This analysis showed that increasing the length of TrC from 36 to 97 nt augmented antigenome levels approximately fourfold and that increasing the length of TrC from 97 to 147 nt caused a further minor increase in antigenome synthesis.

The effect of TrC on RNA replication is independent of its effect on transcription. To determine if the effects of increasing TrC were sequence or spacing dependent, minigenomes were constructed in which a spacer sequence was inserted at the end of the Le region, such that the length of the 3' extragenic region was similar to that in the minigenomes used in Fig. 2 and 3 (C series, Fig. 4A). These minigenomes differ slightly from those used in the experiments described above, because their 3' terminus is generated by a hammerhead ribozyme rather than the hepatitis delta virus ribozyme, a technical point which would not influence the results. However, so that the minigenome backbones within the experiment were consistent, minigenome C2 was used as a positive control instead of minigenome C41.

Analysis of the positive-sense RNAs generated from these minigenomes showed that, similar to the findings with increasing the length of TrC, increasing the length of the 3' extragenic region caused a decrease in mRNA synthesis, particularly if the length was increased above 101 nt (Fig. 4B). This result indicates that the inhibition of transcription due to increasing the length of TrC is not sequence specific, but rather is an effect of increased length of the 3' extragenic region.

Increasing the Le length from the wild-type 44 nt to 61 nt (compare lanes 2 and 3) caused a slight increase in the level of antigenome; however, further increases in Le length had no significant effect on replication (Fig. 4C and D). This contrasted with the findings for minigenomes containing imported TrC (Fig. 2 and 3). Thus, the increase in antigenome synthesis caused by increasing the length of TrC was specific to the TrC sequence. To confirm that the lack of increase in antigenome was not due to suboptimal replication conditions (e.g., insufficient soluble N protein), a parallel reaction was carried out with minigenome A147 (Fig. 4B and C, lane 8). This minigenome produced significantly more antigenome than any of the C series of minigenomes, demonstrating that conditions were not restrictive for replication.

A subgenomic RNA species of greater size than monocistronic CAT mRNA was generated from the C series of mini-

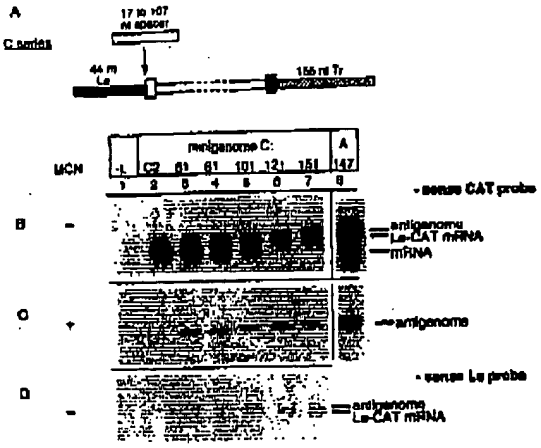

FIG. 4. Insertion of a heterologous spacer into the Le region has differentiated effects on transcription and replication. (A) Structures (not to scale) of the C series of minigenomes, in which a spacer sequence was inserted at the indicated position in the Le region, resulting in Le regions of 61 to 151 nt (C61 to C151, designated according to the final length of the Le). (B, C, and D) Northern blot analyses of positive-sense RNAs synthesized by the RSV polymerase. Cells were transfected with plasmids expressing minigenome C2 (lanes 1 and 2), minigenomes C61 to C151 (lanes 3 to 7, as indicated), or minigenome A147 (lane 8), together with plasmids expressing N, P, and M2-1 (lane 1) or N, P, M2-1, and L (lanes 2 to 8). Panels B and D show total intracellular RNA, and panel C shows MCN-resistant intracellular RNA. The RNAs were detected with a negative-sense, CAT-specific riboprobe (B and C) or negative-sense, Le-specific oligonucleotide probe (D).

genomes (Fig. 4B). Northern blotting with an oligonucleotide probe specific for the positive-sense Le transcript (Fig. 4D) identified this species as a Le-CAT readthrough mRNA, which had been described previously both with minigenomes and with authentic RSV infection (9, 24). The Le-CAT mRNA levels did not diminish with increasing Le length and thus paralleled the antigenome levels. Le-CAT mRNA was not detected in samples treated with MCN, indicating that it was not encapsidated (Fig. 4C).

The 10 nt of Le that immediately precede the CS signal are not essential for accurate transcription initiation. As described above, TrC sequence juxtaposed to the last 10 nt of Le and the GS signal directed transcription. To examine if the 10 Le nt are necessary for transcription to occur, we compared minigenomes in which they were deleted (minigenomes D36 to D97) to minigenomes A36 to A97.

Minigenomes which contained 57, 77, or 97 nt of TrC sequence yielded similar amounts of mRNA and antigenome, irrespective of the presence of the 10 Le nt (Fig. 5B and C, compare lanes 3, 4, and 5 to lanes 8, 9, and 10). This demonstrated that these nucleotides are not required for transcription or RNA replication. However, minigenomes that contained 36 nt of TrC sequence produced significantly less mRNA and slightly more antigenome if the last 10 nt of Le were deleted, suggesting that this region does play a minor role in regulating transcription and/or replication.

It was important to confirm that the mRNA synthesized in the absence of the 10 nt of Le was initiated correctly at the NS1 GS signal. Polyadenylated RNA, isolated from the total RNA shown in Fig. 5B, lanes 2, 3, 7, and 8, was analyzed by primer extension (Fig. 6) to determine if it was initiated at the NS1 GS signal. Control reactions were carried out with total RNA derived from minigenomes A36 and D36 and antigenome RNA synthesized in vitro by T7 RNA polymerase to indicate the origin of the antigenome RNAs generated from those minigenomes (Fig. 6, lanes 2, 3, and 9).

This analysis showed that almost all of the polyadenylated RNA synthesized from minigenomes D36 and D57 was initiated at the NS1 GS signal (indicated by an open arrowhead), similarly to the polyadenylated RNA derived from minigenomes A36 and A57 (compare lanes 7 and 8 to 5 and 6), and only a barely detectable amount was initiated at the genome 3′ end (Le-CAT readthrough mRNA, indicated by solid arrowheads). This result demonstrates that the last 10 nt of Le are not required for accurate transcription initiation at the NS1 GS signal.

Comparison of promoter strength of TrC to that of Le. It was of interest to directly compare the strengths of the genomic promoter in Le and the antigenomic promoter contained in TrC. This could not be done reliably in the preceding experiments because they employed minigenomes which were competent for amplification by the reconstituted RSV polymerase. Specifically, the minantigenome which is produced serves in turn as a template to produce progeny minigenome. As we have described previously (14, 33), this amplifies the plasmid-supplied minigenome template 5- to 50-fold, depending on the efficiency of reconstituted replication in any particular experiment. Thus, any mutation which affects the efficiency of antigenome synthesis can drastically affect the level of minigenome template, complicating evaluation of mutations. This problem can be overcome by blocking amplification by introducing one of several point mutations into the Tr region (33), one example being a C-to-G substitution at the penultimate nucleotide (Fig. 7A). This mutation does not significantly affect encapsidation or template activity of the plasmid-supplied minigenome, but the minantigenome it encodes is inactive as a template for the progeny minigenome.

Figure 7B shows mRNA and antigenome generated from

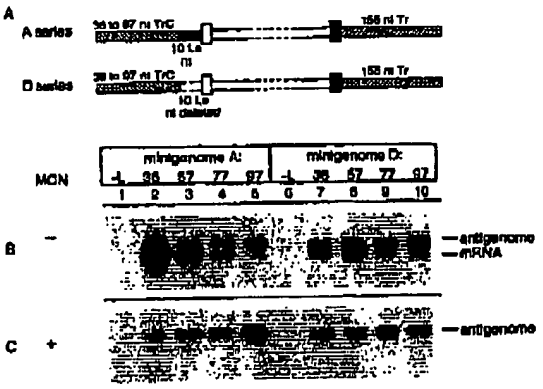

FIG. 5. The last 10 nt of Le (nt 34 to 44) are dispensable for transcription and RNA replication. (A) Structures of minigenomes A36 to A97, as described in Fig. 2, and their derivatives D36 to D97, from which the last 10 nt of the Le region between the TrC sequence and the GS signal have been deleted. (B and C) Northern blot analyses of positive-sense RNAs synthesized from minigenomes A36 (lanes 1 and 3), A57 to A97 (lanes 3 to 5), D36 (lanes 6 and 7), or D57 to D97 (lanes 8 to 10). Cells were transfected with the indicated minigenome together with plasmids expressing N, P, and M2-1 (lanes 1 and 6) or N, P, M2-1, and L (lanes 2 to 5 and 7 to 10). Panel B shows total intracellular RNA, and panel C shows MCN-resistant intracellular RNA. The RNAs were detected with a negative-sense, CAT-specific riboprobe.

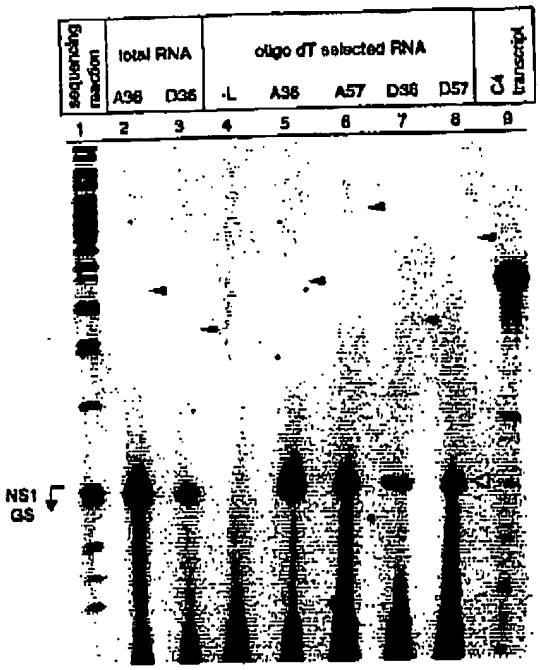

FIG. 6. The last 10 nt of Le (nt 34 to 44) are not necessary for correct transcription initiation at the NS1 GS signal. Primer extensions were carried out by using templates of total RNA derived from transfections with minigenome A36 (lane 2) or D36 (lane 3) or oligo(dT)-purified RNA derived from transfections with minigenome A36 (lanes 4 and 5), A57 (lane 6), D36 (lane 7), or D57 (lane 8). Lane 4 is a negative control in which the transfection reaction mixture did not contain L plasmid. Lane 9 is a positive control using minlantigenomic RNA synthesized from C4 plasmid in vitro by T7 RNA polymerase. The size of this primer extension product is 1 nt longer than that of A36, consistent with its predicted structure. Lane 1 is a ddC sequencing reaction carried out with minigenome C41 as a template; the position of the first 4 nt (CCCC) of the NS1 GS signal is indicated. Solid arrowheads indicate the positions of cDNAs generated from RNAs initiated at the minigenome 3' terminus, which are barely detectable in lanes 5 to 8, and a large open arrowhead indicates the position of cDNAs generated from RNAs initiated at the NS1 GS signal.

minigenomes containing either Le or 36 to 77 nt of TrC and Tr containing the 2G mutation. Control reactions demonstrated that each reaction received a similar amount of MCN-resistant minigenome RNA (data not shown). This analysis demonstrated that the minigenome containing 36 nt of TrC generated slightly more antigenome (less than twofold) than the minigenome containing Le. However, the two minigenomes generated essentially the same amount of total positive-sense RNA, since the antigenome comprised only a small fraction. As the length of TrC was increased to 57 and 77 nt, the total amount of RNA synthesized decreased due to a reduction in mRNA transcription. There was a minor increase in antigenome levels associated with the increase in TrC length from 36 to 57 nt, but this was not reciprocal to the decrease in transcription. Thus, these data show that the promoters contained within the 3'-terminal regions of TrC and Le direct essentially the same amount of total positive-sense RNA synthesis.

Promoter activity of Le under conditions of enhanced terminal complementarity. Previously it had been shown that increasing the complementarity within the terminal 50 nt of VSV augments replication and inhibits transcription (40, 41). Although the result shown in Fig. 3 addressed the role of terminal complementarity beyond 42 nt, this experiment did not examine the importance of complementarity within the terminal 42 nt. To examine this, minigenome C41 was modified by replacing the Tr region with the 44-nt complement of Le (LeC), creating minigenome F2 (Fig. 8A). This increased the amount of terminal complementarity from 27 of 44 nt (61%) to 43 of 44 nt (98%), with the single mismatch being at position 4 (see below). We also placed a ribozyme between the T7 promoter and the 5' end of the minigenome so that both ends of the minigenome were generated by self-cleaving ribozymes, which leave correct ends. This made it possible to place the T7 promoter in an optimal sequence context for efficient T7-mediated RNA synthesis and obviated effects on T7 promoter efficiency due to changes in the minigenome 5' end (33). This modification precluded the need for nonviral G residues at the 5' end of the minigenome. A version of C41 containing the second ribozyme was constructed and designated minigenome F1 (Fig. 8A).

The F1 and F2 minigenomes were complemented with the N, P, and L plasmids, and the synthesis of positive-sense and negative-sense RNA was monitored. The two minigenomes expressed similar amounts of positive-sense RNA (Fig. 8B, lanes 3 and 6). Because the transfections did not contain M2-1, some of the mRNA was truncated and migrated as a smear below the full-length mRNA. Parallel samples which were treated with MCN prior to RNA purification confirmed the synthesis of comparable amounts of encapsidated minlantigenome (Fig. 8C, lanes 3 and 6). Encapsidated negative-sense RNA also was analyzed, which showed that F1 synthesized slightly more minigenome than F2 (Fig. 8D, lanes 3 and 6). In comparison, very little minigenome was detected when L plasmid was omitted (Fig. 8D, lanes 2 and 5), which showed that reconstituted RSV replication was very efficient and was re-

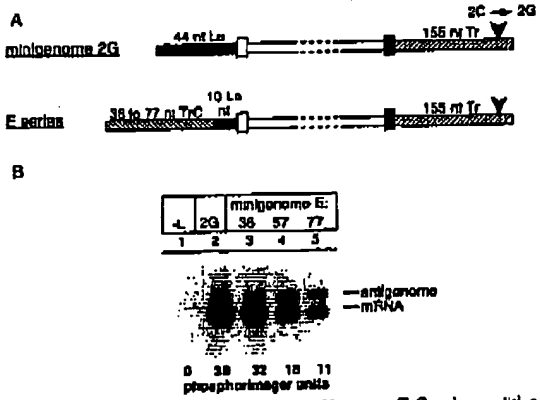

FIG. 7. Analysis of the promoter strength of Le versus TrC under conditions in which the minigenome template was not amplified. (A) Diagram (not to scale) of a series of minigenomes, E36 to E77, in which the 3' 34 nt of Le have been replaced by the indicated length of TrC sequence (as in series A, Fig. 2) and the penultimate nucleotide of the Tr region has been changed from a C to a G residue. (B) Northern blot analysis of positive-sense RNAs synthesized from minigenome 2G, which contains the complete Le (lanes 1 and 2), or minigenomes E36 to E77 (lanes 3 to 5). For comparison, the same nucleotide substitution was introduced into minigenome C41 containing the wild-type Le (Fig. 2), creating minigenome 2G. Cells were transfected with plasmids expressing the indicated minigenome and plasmids expressing N, P, and M2-1 (lane 1) or N, P, M2-1, and L (lanes 2 to 5). The RNAs were analyzed by Northern blotting with a negative-sense, CAT-specific riboprobe. The total amount of RNA in each lane is indicated in arbitrary PhosphorImager units.

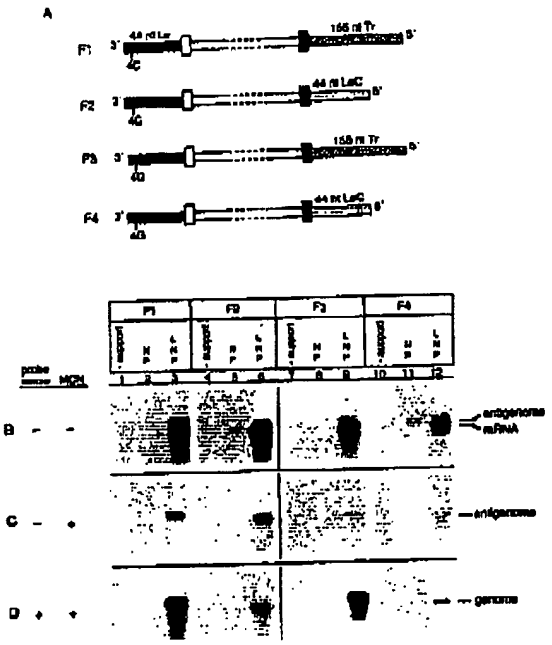

FIG. 8. Transcription and replication of minigenomes in which the Tr was replaced by the complement of the Le (LeC). (A) Structures (not to scale) of minigenomes F1 to F4. Each minigenome contains a 44-nt Le at the 3′ terminus. minigenomes F1 and F3 contain the complete 155-nt Tr at the 5′ terminus, and minigenomes F2 and F4 contain the 44-nt LeC sequence at the 5′ terminus. The 3′ Le sequence of minigenomes F1 and F2 differs from that of F3 and F4 by a single nucleotide substitution at position 4; hence, both naturally occurring assignments are represented. (B and C) Northern blot analyses of positive-sense RNAs synthesized by the reconstituted RSV polymerase. Parallel wells of cells were transfected with minigenome F1 (lanes 1 to 3), F2 (lanes 4 to 6), F3 (lanes 7 to 9), or F4 (lanes 10 to 12) together with plasmids expressing N and P (lanes 2, 5, 8, and 11) or N, P, and L (lanes 3, 6, 9, and 12). Lanes 1, 4, 7, and 10 received empty pTM1 expression plasmid. The blots show total (B) or MCN-resistant (C) RNA detected by hybridization with a negative-sense CAT probe. (D) Northern blot analysis of MCN-resistant minigenome RNA detected by hybridization with a positive-sense CAT probe.

sponsible for most of the encapsidated intracellular minigenome. Thus, increasing the amount of terminal complementarity did not dramatically affect the activities of either the genomic or antigenomic promoters.

Position 4 in the Le has two naturally occurring assignments. The 4C assignment (negative sense), which was present in all of the preceding minigenomes used in this paper, results in increased antigenome synthesis in the minireplicon system (M.E.P., R.F., and P.L.C., unpublished data, and see below). The 4G assignment is more common in biologically derived viruses. We constructed minigenomes F3 and F4, which were the same as minigenomes F1 and F2, except that the Le contained the G assignment at position 4 (Fig. 8A). Minigenome F4 thus had 100% complementarity in the terminal 44 nt. Minigenome F3 synthesized slightly more positive-sense RNA and encapsidated miniantigenome and substantially more encapsidated minigenome than did F4 (Fig. 8B, C, and D, compare lanes 9 and 12). Thus, the increased complementarity did not augment synthesis. The reduced amount of antigenome synthesized by F3 and F4 (Fig. 8C, lanes 9 and 12) compared to that synthesized by F1 and F2 (lanes 3 and 6) is due to the 4C mutation.

DISCUSSION

The control of transcription and replication is a central, unresolved issue in the molecular biology of mononegaviruses. In this study, we compared the genomic and antigenomic promoters of RSV to distinguish the *cis*-acting requirements for replication and transcription. The promoter contained within TrC was shown to resemble that of Le in being able to direct efficient transcription in addition to replication, when juxtaposed with a GS signal (Fig. 2, 3, 5, 6, and 7). The two promoters also were essentially identical with regard to promoter strength (Fig. 7). The sequence similarity between Le and TrC lies at the 3′ termini, which share 81% nucleotide identity for the first 26 nt, after which there is no significant similarity (Fig. 1). It is likely that the 21 conserved nt include the important elements of a functionally conserved promoter, with the caveat that transcription requires, in addition, a downstream GS signal (24). The remainder of the Le and TrC appeared to have sequences which modified these activities, but were not essential and had an impact that was on the order of only severalfold. In addition, we showed that Le-specific sequence is not required for accurate transcription initiation at the first GS signal (Fig. 6).

These findings differ in some ways from those described for model mononegaviruses. For example, the TrC of SeV can direct transcription (6), as described here for RSV, but that of VSV apparently does not (41). Furthermore, both of these model viruses appear to have Le sequence essential for transcription located immediately before the first GS signal (6, 28, 41), whereas there is no evidence for such a signal here for RSV.

Given the greater intracellular accumulation of genome compared to antigenome in cells infected with this group of viruses, it had been suggested that the antigenomic promoter is substantially more powerful than the genomic promoter. Direct comparison of the strengths of the genomic and antigenomic promoters, in a situation in which slight differences would not be exaggerated by genome amplification, showed that the RSV genomic and antigenomic core promoters directed similar amounts of positive-sense RNA synthesis (Fig. 7). In this experiment, we were comparing TrC with an Le that contained a C residue at position 4. Since there are two naturally occurring assignments at this position, we have also used the 2G minigenome backbone to compare the promoter strengths of these two Le sequences and found that a minigenome containing a C residue synthesizes twofold more antigenome RNA than a minigenome containing a G at this position (M.E.P., R.F., and P.L.C., unpublished observations), an effect that seems small, but apparently increases exponentially under conditions permissive for template amplification.

Increasing the length of inserted TrC sequence increased replication and decreased transcription. The effect on replication could not be duplicated with heterologous, non-TrC sequence (Fig. 4), indicating that it depended on a specific TrC sequence element. This appeared to lie between nt 36 and 97, but was not further defined (Fig. 3). Similarly it has been shown for VSV, SeV, and rabies virus that the primary sequence of the TrC region is more efficient at directing replication than the Le (6, 16, 17, 27, 37). There are several possible mechanisms by which sequences within TrC could enhance replication: (i) expediting polymerase binding to the promoter and/or initiation of RNA synthesis; (ii) promoting encapsidation of the nascent RNA, which could facilitate replication

processivity; (iii) stabilizing naked, nascent RNA, which might be important if encapsidation lags behind RNA synthesis.

The downregulatory effect on transcription caused by increasing lengths of TrC sequence was due to the increased length of the 3′ extragenic region. This was demonstrated by inserting nonspecific spacer sequence into the Le region; mRNA synthesis decreased significantly as the length of spacer was increased (Fig. 4), similar to the situation seen with increasing length of TrC. This result suggests that efficient transcription depends on appropriate spacing between important *cis*-acting elements, presumably the 3′ element and the first GS signal.

The changes in transcription and replication caused by substituting for Le with TrC sequence could not be attributed to the increasing degree of terminal complementarity, because minigenomes in which terminal complementarity was consistent behaved similarly to minigenomes in which terminal complementarity was increased (compare Fig. 2 and 3). Furthermore, comparison of minigenomes containing Tr or LeC sequence at the 5′ terminus indicated that the degree of terminal complementarity had no discernible effect on transcription or replication (Fig. 8). These results are consistent with findings for SeV, which indicated that increasing terminal complementarity did not affect replication (37), but contrast with observations made for VSV (40, 41), which indicated that increasing terminal complementarity augmented replication at the expense of transcription.

In these experiments, as well as others described previously (24, 25), there was no evidence of a direct inverse relationship between transcription and RNA replication, as would be expected if these two processes were in balance (e.g., Fig. 7). Although increasing length of the TrC increased replication and decreased transcription, these effects appeared to be coincidental and unrelated. Previous studies of other mononegaviruses have not clarified whether transcription and replication are competitive; some experiments indicated that the ability of a minigenome to direct transcription was not related to its replication efficiency (6, 28), but other experiments indicated an inverse relationship between the two processes (41). The data presented here suggest that for RSV, transcription and replication are for the most part independent rather than competitive, interconvertible processes. There may be some situations in which transcription efficiency affects replication efficiency and/or vice versa (Fig. 5), but this likely is an effect of two independent processes sharing the same template.

The data presented in this paper suggest the following model for RSV transcription and replication. A single *cis*-acting element contained within the first 26 nt of the Le is utilized for both transcription and replication initiation. During replication, the polymerase binds to this sequence and initiates RNA synthesis directly at the 3′ end of the genome. During transcription, the polymerase contacts the 3′ element, but initiates RNA synthesis directly at the first GS signal, possibly by contacting the 3′ element and the GS signal simultaneously.

This model of transcription initiation eliminates the requirement for a transcription termination site before the first GS signal and is consistent with our finding that the Le sequence immediately upstream of the NS1 GS signal is not required for accurate transcription initiation. It also accounts for the lack of a direct inverse relationship between transcription and replication. This model also accommodates our previous finding that increasing the intracellular concentration of N protein augments replication without inhibiting transcription (14). It is possible that encapsidation is necessary for replication, at either the initiation or elongation stage, and therefore increasing the intracellular concentration of N protein does enhance replication efficiency (as determined by synthesis of complete antigenome and genome). However, since transcription is a distinct process, mRNA synthesis is unaffected by N protein concentration. If this model is correct, transcription and replication could be mediated by two separate pools of polymerase which have different conformations allowing them to bind the common promoter element at the 3′ terminus, but then recognize different initiation sites. This is consistent with evidence that VSV transcription and replication are mediated by two subsets of polymerase, differentiated by posttranslational modification (8, 31).

One important postulate of this model is that the Le 3′ terminus contains a common element for initiation of transcription and replication. We are currently testing this proposal by carrying out saturation mutagenesis of the Le region to identify the nucleotide requirements for antigenome and mRNA synthesis.

ACKNOWLEDGMENTS

We thank Myron Hill and Ena Camargo for technical assistance; Michael Teng for helpful discussion; and Michael Teng, Christine Krempl, Alison Bermingham, Brian Murphy, and Robert Channock for critical reviews of the manuscript.

REFERENCES

1. Absehuler, M. E., R. Tritz, and A. Rampel. 1992. A method for generating transcripts with defined 5′ and 3′ termini by autocatalytic processing. Gene 122:85–90.
2. Atreya, P. L., M. E. Peeples, and P. L. Collins. 1998. The NS1 protein of human respiratory syncytial virus is a potent inhibitor of minigenome transcription and RNA replication. J. Virol. 72:1452–1461.
3. Bermingham, A., and P. L. Collins. 1999. The M2-2 protein of human respiratory syncytial virus is a regulatory factor involved in the balance between RNA replication and transcription. Proc. Natl. Acad. Sci. USA 96: 11259–11264.
4. Blumberg, B. M., M. Leppert, and D. Kolakofsky. 1981. Interaction of VSV leader RNA and nucleocapsid protein may control VSV genome replication. Cell 23:837–845.
5. Byrappa, S., D. K. Gavin, and K. C. Gupta. 1995. A highly efficient procedure for site-specific mutagenesis of full-length plasmids using Vent DNA polymerase. Genome Res. 5:404–407.
6. Calain, P., and L. Roux. 1995. Functional characterization of the genomic and antigenomic promoters of Sendai virus. Virology 212:163–173.
7. Chuang, J. L., and J. Perrault. 1997. Initiation of vesicular stomatitis virus mutant polR1 transcription internally at the N gene in vitro. J. Virol. 71: 1466–1473.
8. Chuang, J. L., R. L. Jackson, and J. Perrault. 1997. Isolation and characterization of vesicular stomatitis virus polR revertants: polymerase readthrough of the leader-N gene junction is linked to an ATP-dependent function. Virology 229:57–67.
9. Collins, P. L., and G. W. Wertz. 1985. Nucleotide sequences of the 1B and 1C nonstructural protein mRNAs of human respiratory syncytial virus. Virology 143:442–451.
10. Collins, P. L., M. A. Mink, and D. S. Stec. 1991. Rescue of synthetic analogs of respiratory syncytial virus genomic RNA and effect of truncations and mutations on the expression of a foreign reporter gene. Proc. Natl. Acad. Sci. USA 88:9663–9667.
11. Collins, P. L., M. G. Hill, J. Cristina, and H. Grosfeld. 1996. Transcription elongation factor of respiratory syncytial virus, a nonsegmented negative-strand RNA virus. Proc. Natl. Acad. Sci. USA 93:81–85.
12. Collins, P. L., K. McIntosh, and R. M. Chanock. 1990. Respiratory syncytial virus, p. 1313–1351. *In* B. N. Fields, D. M. Knipe, and P. M. Howley (ed.), Fields virology, 3rd ed. Raven Press, New York, N.Y.
13. Dickens, L. E., P. L. Collins, and G. W. Wertz. 1984. Transcriptional mapping of human respiratory syncytial virus. J. Virol. 52:364–369.
14. Fearns, R., M. E. Peeples, and P. L. Collins. 1997. Increased expression of the N protein of respiratory syncytial virus stimulates minigenome replication but does not alter the balance between the synthesis of mRNA and antigenome. Virology 238:188–201.
15. Fearns, R., and P. L. Collins. 1999. Role of the M2-1 transcription antitermination protein of respiratory syncytial virus in sequential transcription. J. Virol. 73:5852–5864.
16. Finke, S., and K.-K. Conzelmann. 1997. Ambisense gene expression from recombinant rabies virus: random packaging of positive- and negative-strand ribonucleoprotein complexes into rabies virions. J. Virol. 71:7281–7288.
17. Finke, S., and K.-K. Conzelmann. 1999. Virus promoters determine inter-

ference by defective RNAs: selective amplification of mini-RNA vectors and rescue from cDNA by a 3′ copy-back ambisense rabies virus. J. Virol. 73: 3818–3825.
18. Fuerst, T. R., E. G. Niles, F. W. Studier, and B. Moss. 1986. Eukaryotic transient-expression system based on recombinant vaccinia virus that synthesizes bacteriophage T7 RNA polymerase. Proc. Natl. Acad. Sci. USA 83: 8122–8126.
19. Grosfeld, H., M. G. Hill, and P. L. Collins. 1995. RNA replication by respiratory syncytial virus (RSV) is directed by the N, P, and L proteins; transcription also occurs under these conditions but requires RSV superinfection for efficient synthesis of full-length mRNA. J. Virol. 69:5677–5686.
20. Hardy, R. W., and G. W. Wertz. 1998. The product of the respiratory syncytial virus M2 gene ORF1 enhances readthrough of intergenic junctions during viral transcription. J. Virol. 72:520–526.
21. Huang, Y. T., P. L. Collins, and G. W. Wertz. 1985. Characterization of the ten proteins of human respiratory syncytial virus: identification of a fourth envelope associated protein. Virus Res. 2:157–173.
22. Jin, H., X. Cheng, H. Z. Y. Zhou, S. Li, and A. Seddiqui. 2000. Respiratory syncytial virus that lacks open reading frame 2 of the M2 gene (M2-2) has altered growth characteristics and is attenuated in rodents. J. Virol. 74: 74–82.
23. Kingsbury, D. W. 1974. The molecular biology of paramyxoviruses. Med. Microbiol. Immunol. 160:73–83.
24. Kuo, L., H. Grosfeld, J. Cristina, M. G. Hill, and P. L. Collins. 1996. Effect of mutations in the gene-start and gene-end sequence motifs on transcription of monocistronic and dicistronic minigenomes of respiratory syncytial virus. J. Virol. 70:6892–6901.
25. Kuo, L., R. Fearns, and P. L. Collins. 1997. Analysis of the gene start and gene end signals of human respiratory syncytial virus: quasi-templated initiation at position 1 of the encoded mRNA. J. Virol. 71:4944–4953.
26. Lamb, R. A., and D. Kolakofsky. 1996. *Paramyxoviridae*: the viruses and their replication, p. 1177–1204. *In* B. N. Fields, D. M. Knipe, and P. M. Howley (ed.), Fields virology, 3rd ed. Raven Press, New York, N.Y.
27. Li, T., and A. K. Pattnaik. 1997. Replication signals in the genome of vesicular stomatitis virus and its defective interfering particles: identification of a sequence element that enhances DI RNA replication. Virology 232: 248–259.
28. Li, T., and A. K. Pattnaik. 1999. Overlapping signals for transcription and replication at the 3′ terminus of the vesicular stomatitis virus genome. J. Virol. 73:444–452.
29. Mink, M. A., D. S. Stec, and P. L. Collins. 1991. Nucleotide sequence of the 3′ leader and 5′ trailer regions of human respiratory syncytial virus genomic RNA. Virology 185:615–624.
30. Murphy, S. K., and G. D. Parks. 1999. RNA replication for the paramyxovirus simian virus 5 requires an internal repeated (CGNNNN) sequence motif. J. Virol. 73:805–819.
31. Pattnaik, A. K., L. Hwang, T. Li, N. England, M. Mathur, T. Das, and A. K. Banerjee. 1997. Phosphorylation within the amino-terminal acidic domain I of the phosphoprotein of vesicular stomatitis virus is required for transcription but not for replication. J. Virol. 71:8167–8175.
32. Peeples, M., and S. Levine. 1979. Respiratory syncytial virus polypeptides: their location in the virion. Virology 95:137–145.
33. Peeples, M. E., and P. L. Collins. 2000. Mutations in the 5′ trailer region of a respiratory syncytial virus minigenome which limit RNA replication to one step. J. Virol. 74:146–155.
34. Perrotta, A. T., and M. D. Been. 1991. A pseudoknot-like structure required for efficient self-cleavage of hepatitis delta virus RNA. Nature 350:434–436.
35. Pringle, C. R. 1991. The order Mononegavirales. Arch. Virol. 117:137–140.
36. Samal, S. K., and P. L. Collins. 1996. RNA replication by a respiratory syncytial virus RNA analog does not obey the rule of six and retains a nonviral trinucleotide extension at the leader end. J. Virol. 70:5075–5082.
37. Tapparel, C., and L. Roux. 1996. The efficiency of Sendai virus genomic replication: the importance of the RNA primary sequence independent of terminal complementarity. Virology 225:163–171.
38. Tapparel, C., D. Maurice, and L. Roux. 1998. The activity of Sendai virus genomic and antigenomic promoters requires a second element past the leader template regions: a motif (GNNNNN)$_3$ is essential for replication. J. Virol. 72:3117–3128.
39. Wagner, R. R., and J. K. Rose. 1996. *Rhabdoviridae*: the viruses and their replication, p. 1121–1135. *In* B. N. Fields, D. M. Knipe, and P. M. Howley (ed.), Fields virology, 3rd ed. Raven Press, New York, N.Y.
40. Wertz, G. W., S. Whelan, A. LeGrone, and L. A. Ball. 1994. Extent of terminal complementarity modulates the balance between transcription and replication of vesicular stomatitis virus RNA. Proc. Natl. Acad. Sci. USA 91: 8587–8591.
41. Whelan, S. P. J., and G. W. Wertz. 1999. Regulation of RNA synthesis by the genomic termini of vesicular stomatitis virus: identification of distinct sequences essential for transcription but not replication. J. Virol. 73:297–306.
42. Wunner, W. H., and C. R. Pringle. 1976. Respiratory syncytial virus proteins. Virology 73:228–243.
43. Yu, Q., R. W. Hardy, and G. W. Wertz. 1995. Functional cDNA clones of the human respiratory syncytial (RS) virus N, P, and L proteins support replication of RSV virus genomic RNA analogs and define minimal *trans*-acting requirements for RNA replication. J. Virol. 69:2412–2419.

JOURNAL OF VIROLOGY, Sept. 1994, p. 5448–5459
0022-538X/94/$04.00+0

Vol. 68, No. 9

Evolutionary Pattern of Human Respiratory Syncytial Virus (Subgroup A): Cocirculating Lineages and Correlation of Genetic and Antigenic Changes in the G Glycoprotein

OLGA GARCÍA,[1] MERCEDES MARTÍN,[1] JOAQUÍN DOPAZO,[2] JUAN ARBIZA,[3] SANDRA FRABASILE,[3] JOSÉ RUSSI,[3] MARIA HORTAL,[3] FILAR PEREZ-BREÑA,[1] ISIDORO MARTÍNEZ,[1] BLANCA GARCÍA-BARRENO,[1] AND JOSÉ A. MELERO[1]*

Centro Nacional de Microbiología, Instituto de Salud "Carlos III," Majadahonda, 28220 Madrid,[1] and Centro Nacional de Biotecnología, CSIC-UAM, 28049 Madrid,[2] Spain, and Laboratorio de Salud Pública, 2720 Montevideo, Uruguay[3]

Received 14 March 1994/Accepted 1 June 1994

The genetic and antigenic variability of the G glycoproteins from 76 human respiratory syncytial (RS) viruses (subgroup A) isolated during six consecutive epidemics in either Montevideo, Uruguay, or Madrid, Spain, have been analyzed. Genetic diversity was evaluated for all viruses by the RNase A mismatch cleavage method and for selected strains by dideoxy sequencing. The sequences reported here were added to those published for six isolates from Birmingham, United Kingdom, and for two reference strains (A2 and Long), to derive a phylogenetic tree of subgroup A viruses that contained two main branches and several subbranches. During the same epidemic, viruses from different branches were isolated. In addition, closely related viruses were isolated in distant places and in different years. These results illustrate the capacity of the virus to spread worldwide, influencing its mode of evolution. The antigenic analysis of all isolates was carried out with a panel of anti-G monoclonal antibodies that recognized strain-specific (or variable) epitopes. A close correlation between genetic relatedness and antigenic relatedness in the G protein was observed. These results, together with an accumulation of amino acid changes in a major antigenic area of the G glycoprotein, suggest that immune selection may be a factor influencing the generation of RS virus diversity. The pattern of RS virus evolution is thus similar to that described for influenza type B viruses, except that the level of genetic divergence among the G glycoproteins of RS virus isolates is the highest reported for an RNA virus gene product.

The study of the molecular evolution of human respiratory syncytial (RS) virus should yield new insights into the epidemiology of this important pathogen. This virus is the leading cause of severe lower respiratory tract infections in very young children (see reference 26 for a review). Early cross-neutralization data with animal hyperimmune sera indicated that RS virus isolates were antigenically heterogeneous (7). More recently, human RS viruses have been subdivided into two antigenic subgroups (A and B) by their reactivities with different panels of monoclonal antibodies (MAbs) (2, 30). Within each subgroup, antigenic differences were predominant in one of the viral surface glycoproteins, namely, the attachment glycoprotein (G) (18).

One-dimensional RNase A fingerprinting of RS virus genes has demonstrated extensive genetic heterogeneity of RS virus isolates, even within the same antigenic subgroup (9, 10, 43). Sequence comparison of reference strains from antigenic subgroups A and B indicated that the G protein was less conserved than were other gene products (21). For each subgroup, the G protein also showed the highest genetic divergence (4, 46). Thus, recent studies on the molecular evolution of RS virus have focused on the G protein gene because of its capacity to differentiate strains that may be identical in other viral genes and because of its antigenic diversity.

The RS virus G protein is responsible for virus binding to the cell surface receptor (24). It is a type II glycoprotein with a single hydrophobic domain between residues 38 and 66 that serves as both signal and transmembrane anchor (41, 50). The protein precursor is synthesized as a 32-kDa polypeptide which is modified by the addition of N- and O-linked sugars to achieve the mature form with an apparent molecular mass of 80 to 90 kDa in sodium dodecyl sulfate-polyacrylamide gel electrophoresis (SDS-PAGE) (8, 15, 51). The protein ectodomain contains four cysteines (residues 173, 176, 182, and 186) which are conserved in all RS virus isolates and a short segment (residues 164 to 176) of exact sequence identity between the two antigenic subgroups. This region represents the most hydrophobic segment of the G protein ectodomain and has been proposed as the putative receptor binding site (21).

The G glycoprotein is a major target (together with the other surface glycoprotein, F) of the anti-RS virus humoral immune response. Purified G protein (49) or vaccinia virus recombinants that express this antigen (32, 44) induce subgroup-specific protection in experimental animals. In addition, anti-G MAbs confer passive protection to an RS virus challenge (47).

Monoclonal antibodies have identified three types of epitopes in the G molecule (see reference 29 for a review): (i) strain-specific or variable epitopes (2, 18), (ii) subgroup-specific epitopes, and (iii) conserved epitopes, shared by subgroups A and B (2, 30). The strain-specific epitopes have been mapped within the hypervariable C-terminal third of the G protein ectodomain (19, 36). Epitopes of the other two types have been tentatively located near the four-cysteine cluster of the protein ectodomain (1, 37).

To elucidate the genetic basis of G protein diversity and to evaluate the contribution of immune selection to RS virus evolution, we have analyzed the sequences and antigenic

* Corresponding author. Phone: 34-1-638 0011. Fax: 34-1-639 1859.

changes of the G glycoproteins from 76 subgroup A strains isolated during six consecutive epidemics in Montevideo, Uruguay, and Madrid, Spain. The results obtained offer a model of RS virus evolution analogous to the evolution of influenza B virus (54).

MATERIALS AND METHODS

Viruses. HEp-2 cells grown in Dulbecco's modified Eagle's medium supplemented with 10% fetal calf serum were inoculated with nasopharyngeal aspirates from children admitted to some of the main hospitals of Montevideo, Uruguay, and Madrid, Spain. All RS virus-positive cultures (confirmed by immunofluorescence) were kept at −70°C until further use.

Viruses from original isolates were passaged four to five times in HEp-2 cells, until a clear cytopathic effect could be observed within 48 h after inoculation (17). At this time, the cells were resuspended in the virus-containing supernatant and were kept as a working seed at −70°C.

The nomenclature adopted for the strains analyzed in this study indicates the place of isolation (Montevideo [Mon] or Madrid [Mad]), followed by a number and the year of isolation. For instance, Mon/1/87 is the first isolate of 1987 from Montevideo.

Immunochemical assays. One petri dish (100 mm) of HEp-2 cells was infected with each of the viruses used in this study. When an extensive cytopathic effect was evident by the formation of syncytia, the cells were scraped off with a rubber policeman, pelleted by low-speed centrifugation (3,000 × *g*, 5 min), and washed with phosphate-buffered saline (PBS). The cell pellets were then resuspended in 300 μl of extraction buffer (10 mM Tris [pH 7.6], 5 mM EDTA, 140 mM NaCl, 1% Triton X-100, and 1% sodium deoxycholate). The extracts were clarified by centrifugation at 10,000 × *g* for 5 min and were used in the following assays.

(i) Dot test. Extracts were diluted with PBS to 10 μg of protein per ml, and 5 ml was spotted onto strips of Immobilon paper (Millipore). After air drying, the paper was saturated with 5% nonfat dry milk in PBS and was developed with the MAbs indicated in the figures, by using biotinylated anti-mouse immunoglobulin, streptavidin-peroxidase, and 4-chloro-1-naphthol according to the recommendations of the manufacturer (Amersham Corp.).

(ii) Western immunoblot. Thirty micrograms of protein from each cell extract was separated by SDS-PAGE (45), electrotransferred to Immobilon paper (48), and developed with MAbs as in the dot test assay.

The anti-G MAbs used in this study were raised against either the Long (63G, 68G, 78G, and 25G) (18) or Mon/3/88 strains (labelled with the prefix "021/") (26a).

RNase A digestion of heteroduplexes and product analysis. The procedure has been described in detail previously (9, 25, 53). Briefly, total RNA was obtained by the isothiocyanate-CsCl method (6) from five petri dishes of HEp-2 cells infected with each virus isolate in parallel with those used for the preparation of protein extracts. Ten micrograms of RNA was hybridized to an in vitro-synthesized radiolabelled RNA probe (negative sense) of the G protein gene from the Long strain (9). After RNase A digestion (60 μg/ml) at 30°C for 30 min, the probe fragments were separated by electrophoresis in an 8% polyacrylamide–7 M urea sequencing gel and were visualized by autoradiography.

Nucleic acid sequencing. Synthesis and cloning of G gene cDNAs were done essentially as described by Cane et al. (4). Briefly, 20 μg of total RNA was used for the synthesis of first-strand DNA with reverse transcriptase (avian myeloblastosis virus) and the oligonucleotide LG3⁻ (5′-GGCCCGG GAAGCTTTTTTTTTTTTTTT-3′), which has an *Aval* site (underlined) for cloning purposes. This DNA was amplified with 2.5 U of *Taq* DNA polymerase (Perkin-Elmer) and the primers LG3⁻ and LG5⁻ (5′-GGATCCCGGGGCAAATGC AAACATGTCC-3′), which has the *Aval* site and the first 20 nucleotides (in boldface) of the G protein gene from the Long strain (19). The amplifications involved 25 cycles of denaturation at 93°C, hybridization at 37°C, and elongation at 72°C (each step lasted 1.5 min). The amplified DNAs were digested with the restriction enzymes *Aval* (site included in the primers) and *Pst*I (which cuts after nucleotide 535 of the G protein gene of all RS virus strains), ligated to pGEM4 vector (Promega), digested with the same enzymes, and used to transform competent *Escherichia coli* DH5. Recombinant plasmids with cDNA inserts of the two G gene segments were selected and sequenced by the dideoxy method (40).

In some cases, the G mRNA was sequenced directly by the dideoxy method by using 2 μg of selected poly(A⁺) RNA, 5′-^{32}P-labelled oligonucleotides, and reverse transcriptase, followed by a chase with terminal transferase (11).

Statistical analysis. The nucleotide and amino acid sequences were aligned by using the program CLUSTAL (20). The percentages of nucleotide and amino acid similarities were calculated for each pair of viruses. The distance between pairs of nucleotide sequences was calculated with the formula $d = -(3/4)\ln(1-4p/3)L$ where p is the proportion of nucleotide changes between two sequences and L is the sequence length after the alignment (22). Phylogenetic analysis was done by the method of neighbor joining (38, 42). The topological accuracy of each tree was estimated by the bootstrap method, with 500 replicates (13). The consensus topology and the confidence limit for each tree nodule were calculated with the program CONSENSE (PHYLIP) (14). The proportion of synonymous to nonsynonymous nucleotide changes was calculated with the algorithm of Nei and Gojobori (31).

Nucleotide sequence accession number. The nucleotide sequences reported in this manuscript have been submitted to the EMBL Data Library with accession numbers Z33414 to Z33432, Z33454 to Z33456, and Z33493 to Z33494.

RESULTS AND DISCUSSION

Analysis of the G proteins from RS viruses isolated in Montevideo between 1987 and 1992. Thirty-seven strains of human RS virus (subgroup A) isolated in Montevideo during six consecutive epidemics (1987-1992) were entered in this study. The viruses were isolated from hospitalized children (generally less than 1 year old) in the Montevideo area who were suffering from either pneumonia or bronchiolitis.

To speed up the genetic analysis of virus isolates, a screening of their G protein genes was done by the RNase A mismatch cleavage method, using a full-length antisense RNA probe of the Long strain (9, 10). The results obtained (Fig. 1) demonstrated that the probe was essentially protected when hybridized to homologous RNA (Long) but produced a characteristic band pattern for each strain when hybridized to heterologous RNA. Since partial digestion conditions were used in the assay (9), the sum of all protected bands in each lane exceeded the probe size; however, more stringent conditions increased the background in the lane of the homoduplex (Long), making interpretation of the results more difficult. Nevertheless, the one-dimensional fingerprints obtained with each strain RNA were highly reproducible. For instance, Mon/1/87 generated identical patterns of RNA fragments in the three separate assays represented in Fig. 1.

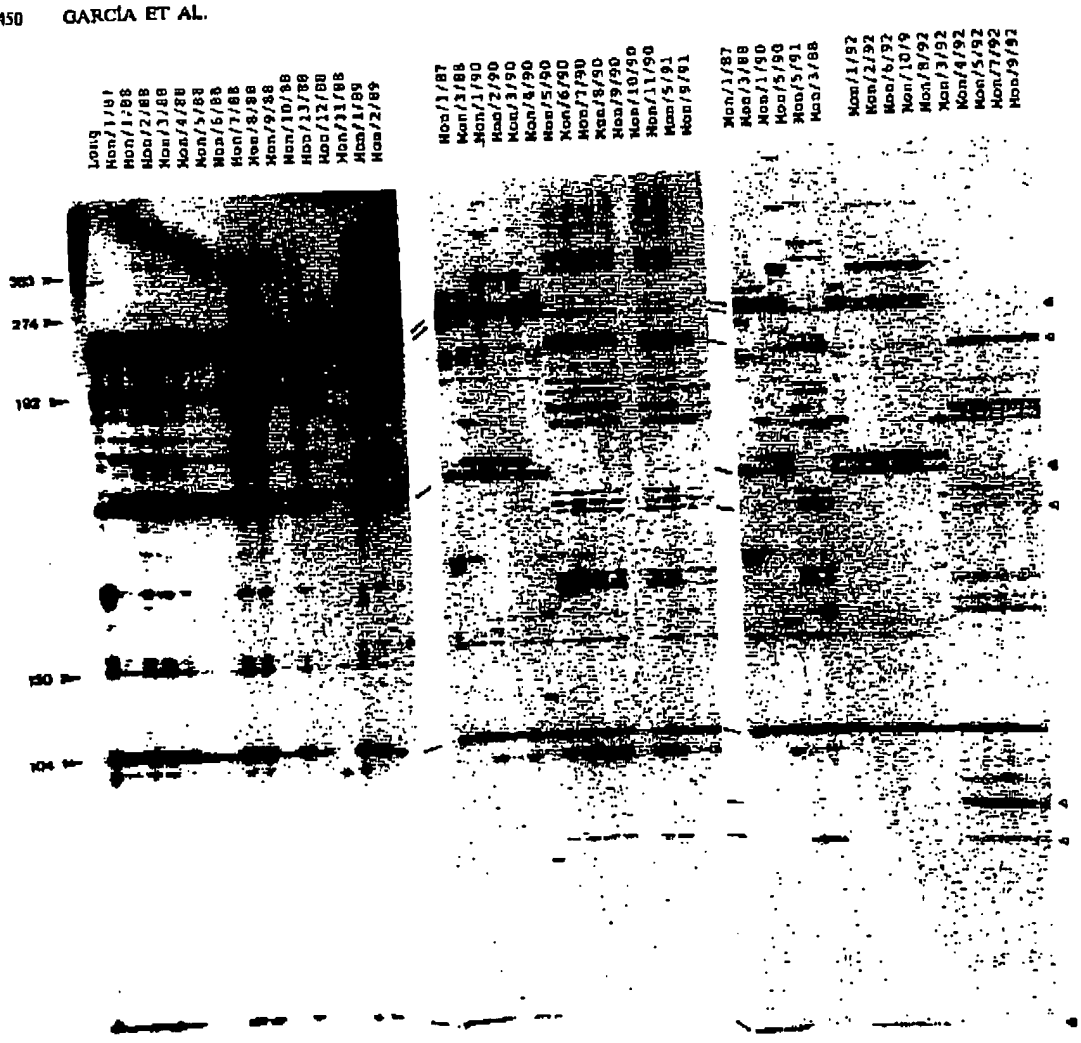

FIG. 1. RNase A fingerprints of the G protein gene from Montevideo isolates. The viruses entered in the analysis are indicated at the top of each lane. The RNase A digestion of RNA-RNA heteroduplexes was done as indicated in Materials and Methods. Each panel represents a different experiment. To compare the results of different assays, some strains were included in all three separate experiments. Molecular size markers (nucleotide length) are indicated at the left, and the positions of some diagnostic bands (◁ and ◀) are indicated at the right. The band difference mentioned in the text, between Mon/3/88 and Mon/1/89, is marked with an asterisk at the right of the first panel. Although the band pattern of Mon/8/90 was not visible in this assay, it was identical to that of Mon/8/90 in other experiments.

The RNase A fingerprints shown in Fig. 1 revealed extensive genetic heterogeneity among the G protein genes of the Montevideo isolates. Identical fingerprints were observed only with isolates from the same year. However, this was not always the case, and viruses that generated different fingerprints could be isolated during the same epidemic. The fingerprints of the different viruses could be grouped into two main patterns that shared some diagnostic bands (Fig. 1, ◁ and ◀). The capacity of RNase A fingerprinting to discriminate between closely related strains can be assessed from the following data: Mon/2/88 and Mon/3/88 viruses, whose nucleotide sequences of the G protein gene differed in only 1 nucleotide (see below), generated identical fingerprints; however, Mon/3/88 and Mon/1/89 viruses, whose sequences were 99.7% identical (see below), generated fingerprints that were very similar but distinguishable by a diagnostic band (left panel of Fig. 1, *). Thus, RNase A fingerprinting distinguished G protein genes with sequences which had close to 100% identity. From this point

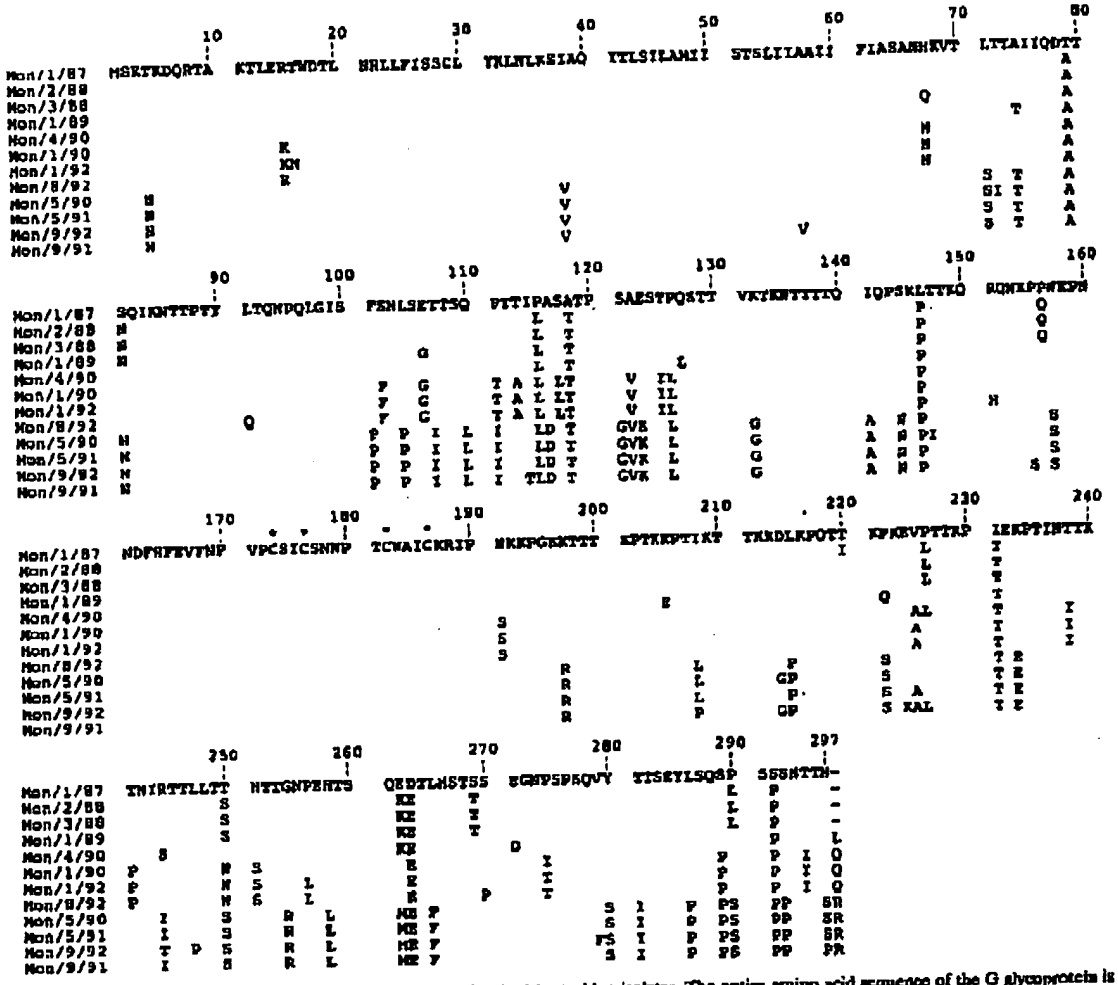

FIG. 2. Sequence alignment of the deduced G proteins for the Montevideo isolates. The entire amino acid sequence of the G glycoprotein is shown for Mon/1/87 in the one-letter code. Amino acid differences are shown for the other viruses. The four cysteines of the protein ectodomain are indicated by asterisks.

on, we assumed that viruses which share their RNase A fingerprints have essentially identical G protein gene sequences. In addition, a good correlation, deduced from either G gene sequences or the number of shared bands in the fingerprints, has been found between the degrees of genetic relatedness among strains (12a).

Twelve viruses were selected on the basis of their RNase A fingerprints for an in-depth sequence analysis of their genetic relatedness. Eleven of those viruses generated different fingerprints. In addition, Mon/2/88 and Mon/3/88, which shared RNase A fingerprints, were selected to assess the degree of sequence identity between viruses with the same fingerprint. cDNA clones of the G protein genes were sequenced by the dideoxy method (see Materials and Methods). When unusual sequence changes were observed, they were confirmed for other cDNA clones and were eventually confirmed for the G mRNA by using reverse transcriptase and appropriate primers. In all cases, the sequences obtained from cDNAs and mRNAs (including the entire sequence of Mon/2/88 G gene) were identical. Thus, the sequences reported here represent the consensus sequence for each isolate.

The deduced G protein sequences of the twelve Montevideo isolates, with those of Mon/1/87 as the standard, are shown in Fig. 2. All sequence changes were the result of either amino acid replacements or changes in the stop codon position. Some strains, which encode proteins of 297 amino acids, have two consecutive termination codons after nucleotide 906 of the G protein gene. Other strains, however, which encode proteins of

298 amino acids, have mutated the first termination codon to a coding triplet. Similar changes in the stop codon, associated with important antigenic changes, have been found in certain RS virus escape mutants selected with anti-G MAbs that recognized strain-specific epitopes (29, 36).

In agreement with previous studies (4, 46), the amino acid changes in the G protein gene of the Montevideo isolates accumulated preferentially in two regions of the protein ectodomain: (i) the region between amino acids 100 and 130 and (ii) the C-terminal third of the protein. The four cysteines and the amino acids between residues 160 and 190 of the G protein ectodomain, which constitute the putative receptor binding site, were conserved in the 12 isolates. For each virus pair, the percentage of sequence identity was higher at the nucleotide level than at the amino acid level (data not shown).

The nucleotide sequences of the G protein gene from the 12 Montevideo isolates were used to build the phylogenetic tree shown in Fig. 3. The viruses that generated identical RNase A fingerprints are shown at the end of each branch with the strain whose sequence was actually determined (shown underlined). The different isolates were distributed between two main lineages. In some epidemics (e.g., that of 1988), most viruses were included in the same branch, whereas in others (e.g., that of 1990), viruses were distributed between different branches.

To correlate the genetic diversity of the G proteins from the Montevideo isolates with changes at the antigenic level, extracts of cells infected with the different viruses were tested with a panel of anti-G MAbs. The viruses could be grouped into two main antigenic categories, according to their reactivities with antibodies. Certain strains reacted with antibodies 25G, 78G, and 68G, raised against the Long G protein, whereas others did not react with those antibodies but reacted with some or all of the MAbs raised against the Mon/3/88 G protein (prefix "021/"). These two antigenic categories correlated with the two main branches of the phylogenetic tree. In addition, other antigenic changes could be related to virus diversification in minor branches. For instance, the viruses Mon/1/90, Mon/1/92, and Mon/8/92, which were placed in the same minor branch of the tree, had altered or lost the epitopes 021/7G, 021/4G, 021/16G, and 021/14G. Thus, a clear relationship was observed between the degrees of genetic identity for the Montevideo isolates and their antigenic similarities.

Analysis of the G protein from RS viruses isolated in Madrid between 1988 and 1993. The same strategy used for the analysis of the Montevideo isolates was employed to study 39 viruses (subgroup A) isolated in Madrid during six consecutive epidemics (1988 to 1993). After a first assessment of their genetic heterogeneity by RNase A fingerprinting (data not shown), 15 isolates were selected for sequence analysis of their G protein genes. Figure 4 shows the alignment of these sequences, with those of Mad/1/88 as the standard. In this case, the protein length ranged from 297 to 299 amino acids. As with the Montevideo isolates, the Madrid viruses that encoded G proteins of 297 amino acids had two contiguous stop codons, whereas those that encoded proteins of 298 amino acids had only the second termination triplet. The strain Mad/4/91, which encoded a G protein of 299 amino acids, had two triplets inserted after nucleotide 588 (amino acids 193 and 194) and two termination codons. The amino acid replacements in the Madrid viruses were also clustered in the two hypervariable regions of the G protein (4, 46). The four cysteines of the G protein ectodomain and the region between amino acids 160 and 190 were conserved in all the isolates.

The phylogenetic tree obtained for the Madrid isolates is shown in Fig. 5, denoting at the end of each branch those viruses that generated identical RNase A fingerprints. Two main branches were also observed in this case, but one of the branches had only two viruses (Mad/2/88 and Mad/8/89), whereas the other had multiple minor branches with viruses isolated between 1988 and 1993. The reactivities of the Madrid isolates with certain anti-G MAbs were clearly related to their positions in the phylogenetic tree. It is interesting to note that the viruses isolated between 1988 and 1990, which were included in the largest branch, reacted with all the antibodies raised against the G protein of the Mon/3/88 strain (isolated in Montevideo in 1988). However, antigenic changes occurred in later years that altered the epitopes 021/4G, 021/5G, 021/7G, 021/14G, and 021/16G and split the evolutionary main branch into three. This result is indicative of antigenic drift occurring during consecutive epidemics within the same lineage. One virus (Mad/10/92), however, showed a pattern of antibody reactivity markedly different from that of other closely related viruses (Mad/1/93 or Mad/6/92).

Evolutionary pattern of human RS virus (subgroup A). The sequences of the Montevideo and Madrid isolates were added to those published for the reference strains, Long (isolated in Baltimore in 1956) and A2 (isolated in Melbourne in 1961), and for six viruses from Birmingham (isolated in the United Kingdom in 1989), to derive the phylogenetic tree shown in Fig. 6. Again, two main branches were observed, but the historical strains (Long and A2) were distantly related to recent isolates. It is remarkable that most minor branches contained viruses isolated in such distant geographical locations as Montevideo, Madrid, and Birmingham. This result reinforces the conclusions reached by Cane and coworkers (5) from analysis of N gene restriction patterns and partial G and SH protein gene sequences. These authors found that viruses isolated at similar times in Hannover and Montevideo or in Birmingham, Hannover, and Kuala Lumpur were very similar. It should also be noted that viruses isolated in the same place during the same epidemic (e.g., Mon/4/90 and Mon/5/90) may be more distantly related than are viruses isolated in two distant places and in different epidemics (e.g., Mon/1/87 and Mad/1/89).

The geographical distribution of the subgroup A isolates and their prevalence in different epidemics suggest that RS virus, like other respiratory viruses (e.g., influenza virus), can spread from one place to another. Consequently, the shape of the phylogenetic tree for RS viruses isolated worldwide should be determined by at least two parameters: (i) the rapidity with which viruses originating in one place move to distant places and (ii) the viral genetic drift due to the accumulation of mutations. It is interesting to note that in the tree in Fig. 6, not all isolates from the three places were equally represented in the branches. For instance, the minor branch that included Bir/5/89, Bir/3/89, Bir/6/89, Mad/4/91, Mad/5/92, and Mad/3/92 lacked viruses isolated in Montevideo. Similarly, only one Madrid isolate (Mad/2/88) was placed in one of the major branches. This result may be due to a sampling error but may also indicate certain limitations of viruses in spreading from one place to another.

The phylogenetic tree in Fig. 6 suggests a model of RS virus evolution similar to that of influenza B virus (54). In the latter case, several cocirculating lineages coexist for extended periods of time (two discrete lineages have coexisted since 1983), but within each lineage new viruses emerge after successive epidemics, replacing the older strains (23, 34, 35, 54). A linear accumulation of genetic changes with time is observed in influenza B virus isolates, and this is correlated with an antigenic drift within each lineage of the virus hemagglutinin (3, 23, 33–35). However, the extent of sequence divergence in the G glycoprotein of human RS virus subgroup A isolates (up

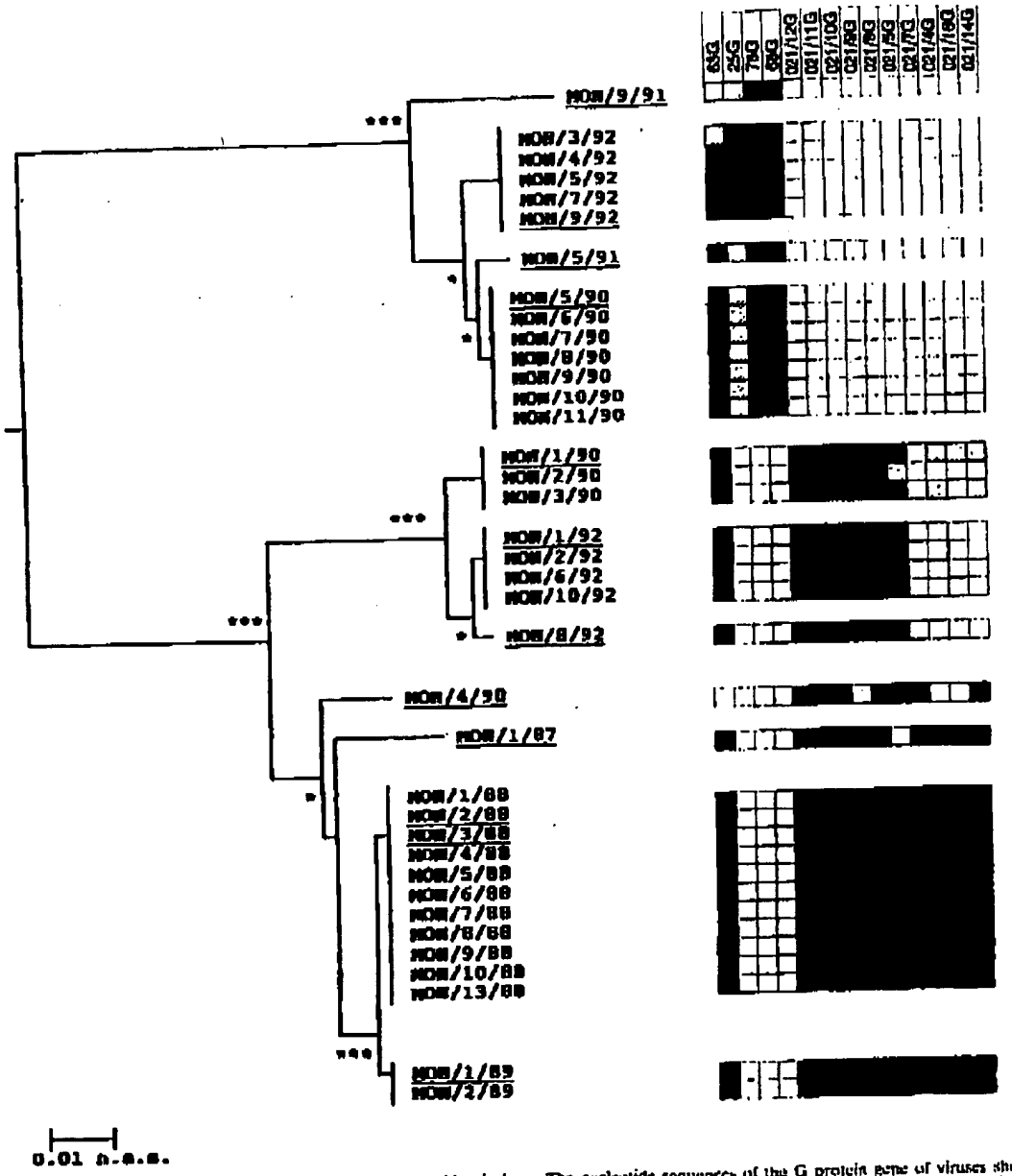

FIG. 3. Phylogenetic and antigenic analysis of the Montevideo isolates. The nucleotide sequences of the G protein gene of viruses shown underlined were used to construct the evolutionary tree by the method of neighbor joining (see Materials and Methods). Listed at the end of each branch are the viruses that generated identical RNase A fingerprints, including Mon/2/88 and Mon/3/88, which had a single nucleotide difference and are separated in Fig. 6. The length of horizontal lines is proportional to the genetic distance between viruses. The bar represents 0.01 nucleotide substitutions per site. Three asterisks and one asterisk denote branch points with confidence limits of >90.9% and >95%, respectively. The reactivities of viruses in a dot test with the MAbs indicated at the top, relative to reactivities of the reference strains, are shown at the right (positive, ■; intermediate, ▨; or negative, □). These were Long virus for antibodies 63G, 25G, 08G, and 78G and Mon/3/88 for the antibodies with the prefix "021/". Ambiguous results of the dot tests were resolved in Western blot assays (see Materials and Methods).

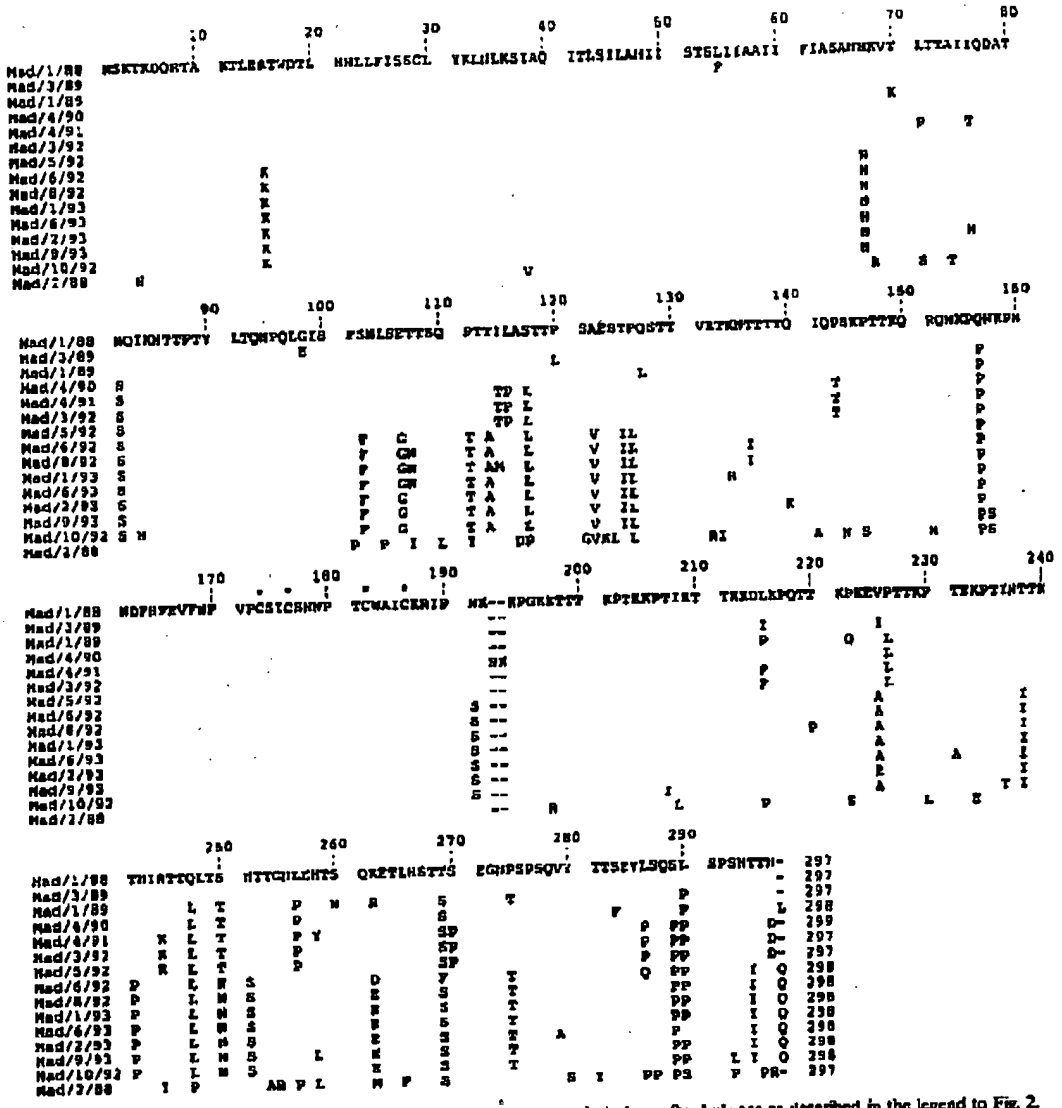

FIG. 4. Sequence alignment of the deduced G proteins for the Madrid isolates. Symbols are as described in the legend to Fig. 2.

to 20%) is higher than that among influenza B virus hemagglutinins (up to 10%). This result highlights the extreme tolerance of the RS virus G protein to sequence changes.

Antigenic structure of the RS virus G glycoprotein and its natural antigenic variation. Previous studies with escape mutants of the Long strain resistant to certain MAbs had identified residues, within the C-terminal third of the G protein, essential for the integrity of some strain-specific epitopes (29, 36). An extreme situation was found in mutants resistant to MAb 63G, which had altered the C-terminal amino acid sequence of the G glycoprotein because of frameshift mutations (19). These mutants had lost all the strain-specific epitopes of the Long G glycoprotein.

The antibodies used for the antigenic analysis of RS virus isolates reacted in a Western blot with the G glycoprotein of the strain used as immunogen, suggesting that they recognized essentially nonconformational epitopes. Thus, comparison of the amino acid changes selected in the escape mutants with the

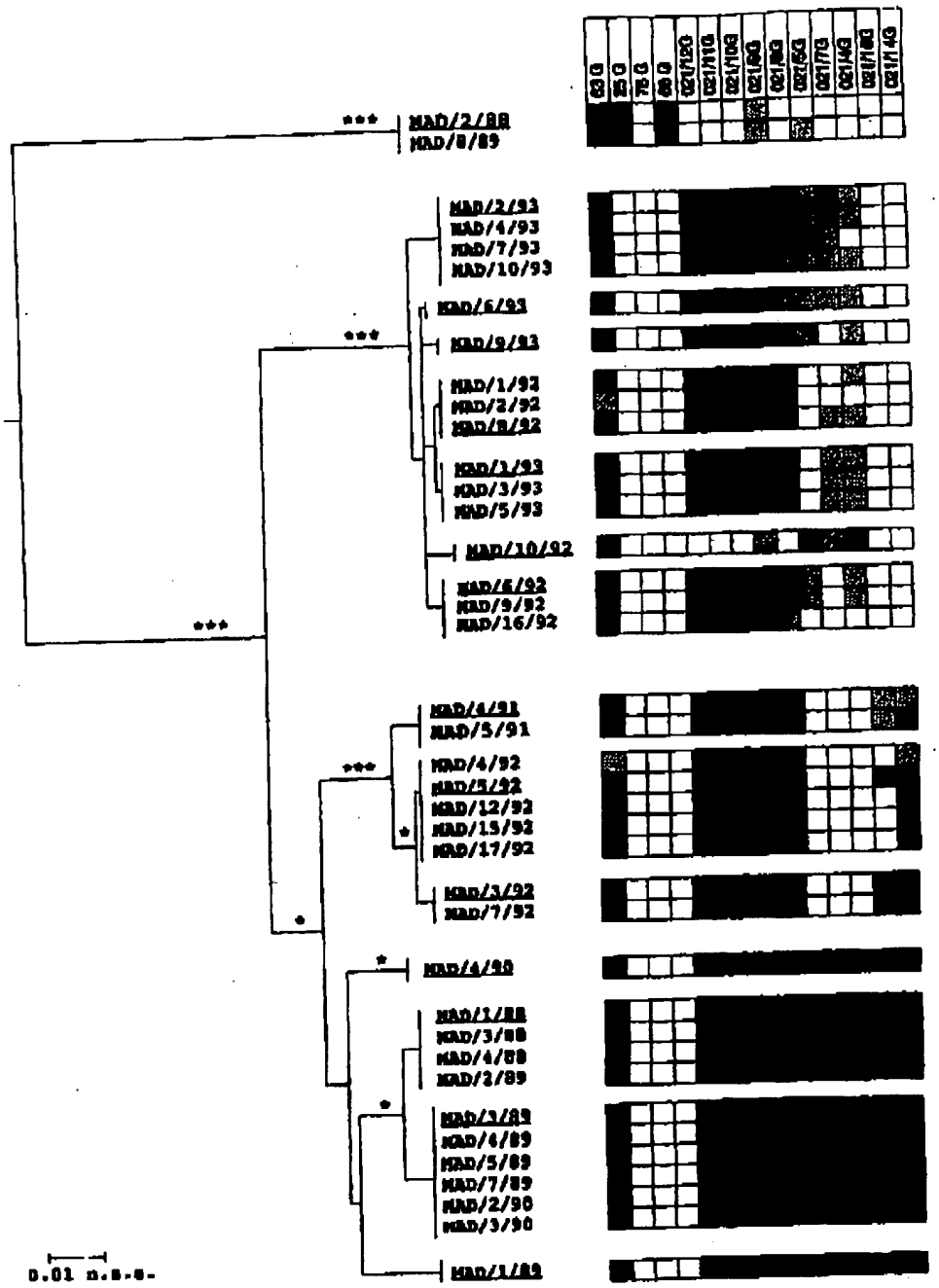

FIG. 5. Phylogenetic and antigenic analyses of the Madrid isolates. Symbols are as described in the legend to Fig. 3.

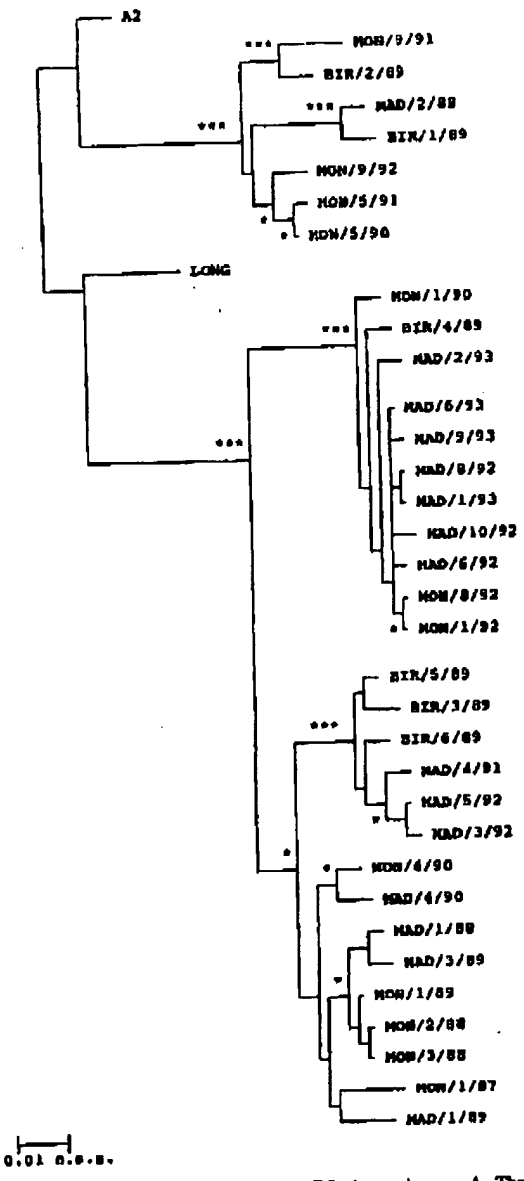

FIG. 6. Phylogenetic analysis of the RS virus subgroup A. The nucleotide sequences of the G protein genes of the Montevideo and Madrid isolates were added to those of the Long (19) and A2 (50) strains and to those of six isolates from Birmingham (4) with the following original nomenclature: RSB-642 (Bir/1/89), RSB-1734 (Bir/2/89), RSB-5857 (Bir/3/89), RSB-6190 (Bir/4/89), RSB-6257 (Bir/5/89), and RSB-6614 (Bir/6/89). The phylogenetic tree was obtained by the neighbor joining method. Symbols are as described in the legend to Fig. 3.

TABLE 1. Amino acid changes associated with epitope loss in escape mutants and natural isolates of human RS virus[a]

Epitope	Changes selected in escape mutants	Changes associated in natural isolates
63G	205K-N 206P-Q 207T-P 208F-S 209K-R 210T-Q 211T-P	205K-E
68G	232E-V 234P-S	233E-K 244T-R(S)
78G	284E-V	280S-Y 293P-S(L)
25G	265F-L 275L-P	265F-L

[a] The relevant amino acid differences with respect to the Long strain are indicated. The seven amino acid changes in a mutant resistant to MAb 63G were generated by a double reading frame shift (19). The changes selected in mutants resistant to MAb 25G have been reported (36). The changes in mutants resistant to MAbs 68G and 78G are unpublished (37a).

G protein sequences reported in this article allowed us to tentatively associate certain amino acid substitutions of natural isolates with the loss of epitopes 63G, 25G, 68G, and 78G (Table 1). The sequence 205-KPTFKTT-211 of the Long strain was replaced by 205-NQPSRQP-211 in a mutant (R63/2/4/1) resistant to MAb 63G (19); the only amino acid change in that sequence of natural isolates that was linked to the loss of epitope 63G was 205K-E in Mon/4/90. Mutants resistant to MAb 68G had changed either 232E-V or 234P-S, whereas nearby changes in natural isolates associated with the loss of epitope 68G were 233E-K and 244T-R (or S). The change selected in one mutant resistant to 78G was 284E-V, whereas the changes in natural isolates associated with the loss of that epitope were 280S-Y and 293P-S (or L). The only change in RS virus isolates that coincided with the change selected in escape mutants was 265F-L, associated with the loss of epitope 25G.

These results indicate that in most cases the mutations associated with epitope changes in natural isolates were located close together but did not coincide with the changes selected in escape mutants. This situation, similar to the one found for human influenza virus type A hemagglutinin (52), is in contrast to that observed in some icosahedral viruses, where changes in the structural proteins of natural antigenic variants often coincide with changes selected in escape mutants (28). It is likely that these differences reflect greater structural restrictions in the proteins of icosahedral viruses—which interact tightly with other particle components—than in viral membrane proteins of envelope viruses.

Considerations on the genetic differences found in RS virus isolates and factors influencing its mode of evolution. It was reported previously that certain escape mutants of the Long strain selected in vitro contained deletions or insertions of adenosine (A) in runs of 6 or 7 of the G protein gene (19). A similar double frameshift mutation—deletion of an A, followed seven triplets later by an A insertion—has also been found in two natural isolates of RS virus subgroup B (46). It was thus unexpected that mutations of this type were not found in natural isolates of subgroup A, suggesting that there may be restrictions for frameshift changes during RS virus propagation in its natural host. This result may be related to our recent finding that RS virus mutants with single reading frame changes, generated by deletions or insertions of an A, have

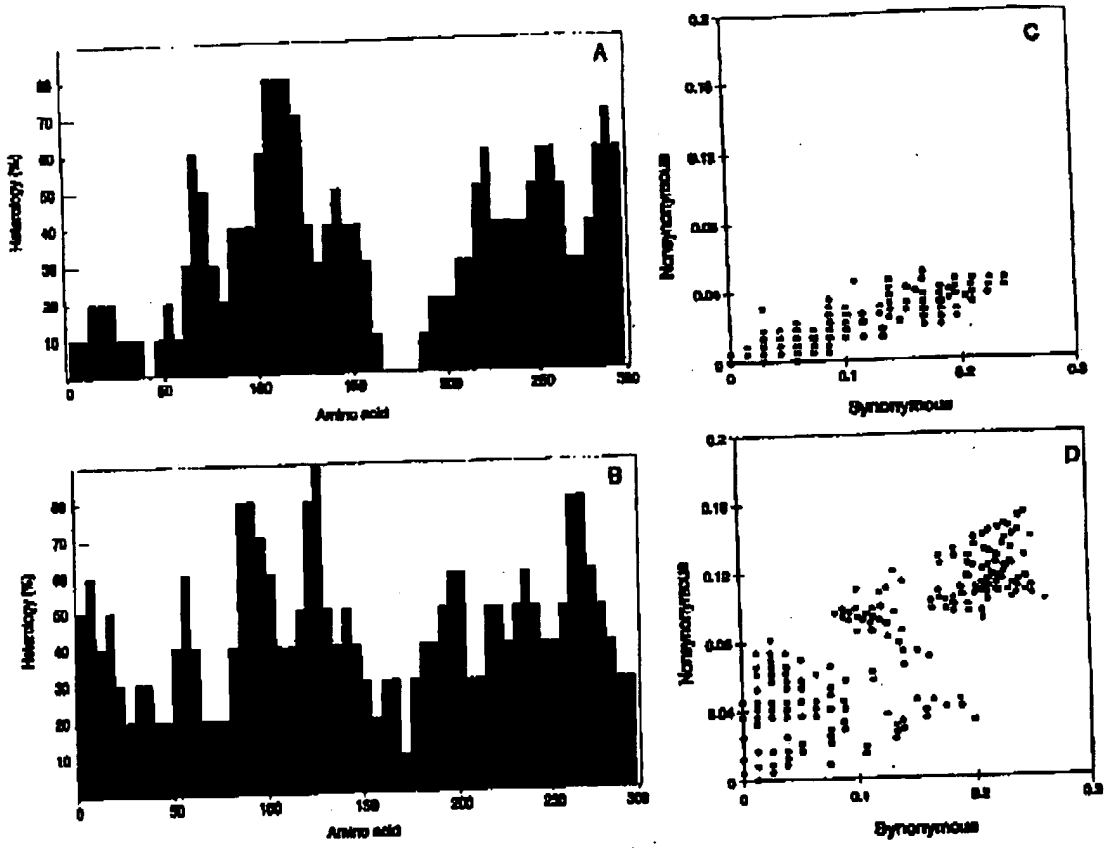

FIG. 7. Sequence changes throughout the G protein gene. The heterology along the G glycoprotein (percentage of sequence differences between viruses) was calculated with a window of 10 codons overlapping five triples, for amino acid changes (A) and synonymous changes (B). The index of synonymous and nonsynonymous changes between pairs of G protein gene sequences was calculated by using the algorithm of Nei and Gojobori (31) for the regions encoding amino acids 1 to 99 (C) and 200 to 298 (D).

reduced fitness to replicate in vitro compared with wild-type virus (19a).

Changes in the position of the stop codon of the G protein gene are not exclusive to the viruses entered in this study. Even larger variations have been reported for limited sets of viruses from human subgroup B (46) and bovine RS viruses (27). It should be noted that changes in the stop codon position were generally associated with the emergence of certain branch points in the evolutionary tree in Fig. 6. A similar result has been reported for the attachment protein (HN) of another paramyxovirus, namely, Newcastle disease virus (39). It is tempting, then, to speculate that the use of alternative termination codons may play a role in the long-term evolution of paramyxovirus attachment type II glycoproteins. The amino acid changes in the G glycoprotein of human RS virus isolates accumulated preferentially in two hypervariable regions of the protein ectodomain (4, 46). This is clearly illustrated by the results shown in Fig. 7A, where the percent amino acid differences among strains (heterology) is represented along the G protein sequence. However, when the heterology was calculated only for synonymous nucleotide changes (Fig. 7B), the values along the G protein gene were not statistically different from a uniform distribution.

These results indicated either a positive selection of amino acid changes in the hypervariable regions of the G protein ectodomain or a greater tolerance of those regions to sequence changes. Since these results may be influenced by a bias in the codon usage, the numbers of synonymous and nonsynonymous changes were calculated for two regions of the G protein gene (encoding amino acids 1 to 99 and 200 to 298) by using the algorithm of Nei and Gojobori (31), which introduces corrections for the genetic code degeneracy. As shown in Fig. 7C and D, the rate of accumulation of nonsynonymous changes in the C-terminal third of the G protein gene was higher than in the segment encoding the first 99 amino acids, independent of codon use.

As mentioned before, the strain-specific (or variable) epitopes of the RS virus G glycoprotein accumulate in its C-terminal third (19, 29, 36). The correlation of genetic and antigenic changes in the G glycoprotein of human RS virus isolates (Fig. 3 and 5) suggests that the accumulation of sequence changes in the protein C-terminal third (Fig. 7) may be determined by immune selection of new antigenic variants. This situation parallels that in the hemagglutinin of influenza A viruses (16), in which amino acid replacements in antigenic sites through immune surveillance are fixed at higher rates than in other parts of the molecule. However, not all sequence changes in the RS virus G protein are associated with antigenic changes. In fact, there is no indication that the hypervariable region between residues 100 and 130 contains any relevant epitope.

It should be borne in mind that the MAbs used for epitope mapping were raised in mice and that the antigenicity of the region between residues 100 and 130 in humans is unknown. Thus, at least three alternative explanations can be offered for the accumulation of amino acid changes in that region of the G molecule: (i) that the region from residues 100 to 130 is immunogenic in humans but not in mice, (ii) that the sequence changes accumulated in that region of natural isolates compensate for those selected in other parts of the G protein gene or the viral genome, and (iii) that the region from residues 100 to 130 has an extreme tolerance to amino acid changes which are selected by random drift (discussed for other RNA viruses in reference 12).

In summary, the RS virus G glycoprotein shows one of the highest degrees of tolerance to amino acid changes among the structural proteins of RNA viruses. At least two major cocirculating lineages of subgroup A viruses, distributed worldwide, have coexisted for an extended period of time. The genetic diversification of RS viruses is tightly associated with antigenic changes in the G glycoprotein. This mode of evolution, which resembles the pattern of influenza B virus evolution, is likely determined by many factors, including RS virus spreading from one place to another and the emergence of new variants through immune selection.

ACKNOWLEDGMENTS

We thank P. A. Cane and C. R. Pringle for providing the oligonucleotides for PCR and the cloning protocol, E. Domingo for critical reading of the manuscript, and A. del Pozo for the artwork.

This research was funded in part by grants from the Commission of the European Communities (J. A. Melero and M. Hortal) and from Comisión Interministerial de Ciencia y Tecnología (SALUD-0042) (J. A. Melero). O. García and M. Martín were the recipients of predoctoral training fellowships from Fondo de Investigaciones Sanitarias and Ministerio de Educación y Ciencia, respectively. J. Dopazo was supported by a Fundación Ramón Areces-CSIC contract.

REFERENCES

1. Akerlind-Stopner, B., U. Utter, M. A. Mufson, C. Örvell, R. A. Lerner, and E. Norrby. 1990. A subgroup-specific antigenic site in the G protein of respiratory syncytial virus forms a disulfide-bonded loop. J. Virol. 64:5143–5148.
2. Anderson, L. J., J. C. Heirholzer, C. Tsou, R. M. Hendry, B. N. Fernie, V. Stone, and K. McIntosh. 1985. Antigenic characterization of respiratory syncytial virus strains with monoclonal antibodies. J. Infect. Dis. 151:626–633.
3. Berton, M. T., C. W. Naeve, and R. G. Webster. 1984. Antigenic structure of the influenza B virus hemagglutinin: nucleotide sequence analysis of antigenic variants selected with monoclonal antibodies. J. Virol. 52:919–927.
4. Cane, P. A., D. A. Matthews, and C. R. Pringle. 1991. Identification of variable domains of the attachment (G) protein of subgroup A respiratory syncytial viruses. J. Gen. Virol. 72:2091–2096.
5. Cane, P. A., D. A. Matthews, and C. R. Pringle. 1992. Analysis of relatedness of subgroup A respiratory syncytial viruses isolated worldwide. Virus Res. 25:15–22.
6. Chirgwin, J. M., A. E. Przybyla, R. J. MacDonald, and W. J. Rutter. 1979. Isolation of biologically active ribonucleic acid from sources enriched in ribonuclease. Biochemistry 18:5294–5299.
7. Coates, H. V., D. W. Alling, and R. M. Chanock. 1966. An antigenic analysis of respiratory syncytial virus isolates by a plaque reduction neutralization test. Am. J. Epidemiol. 83:299–313.
8. Collins, P. L., and G. Mottet. 1992. Oligomerization and post-translational processing of glycoprotein G of human respiratory syncytial virus: altered O-glycosylation in the presence of brefeldin A. J. Gen. Virol. 73:849–863.
9. Cristina, J., J. A. López, C. Albo, B. García-Barreno, J. García, J. A. Melero, and A. Portela. 1990. Analysis of genetic variability in human respiratory syncytial virus by the RNase A mismatch cleavage method: subtype divergence and heterogeneity. Virology 174:126–134.
10. Cristina, J., A. Moya, J. Arbiza, J. Rutal, M. Hortal, C. Albo, B. García-Barreno, O. García, J. A. Melero, and A. Portela. 1991. Evolution of the G and F genes of human respiratory syncytial virus (subgroup A) studied by the RNase A mismatch cleavage method. Virology 184:210–218.
11. DeBarde, D. C., C. W. Naeve, M. L. Herlocher, and H. F. Maassab. 1986. Resolution of a common RNA sequencing ambiguity by terminal deoxynucleotidyl transferase. Anal. Biochem. 157:275–282.
12. Domingo, E., J. Diez, M. A. Martínez, J. Hernández, A. Holguín, B. Borrego, and M. G. Mateu. 1995. New observations on antigenic diversification of RNA viruses. Antigenic variation is not dependent on immune selection. J. Gen. Virol. 76:2039–2045.
12a. Dopazo, J., et al. Unpublished data.
13. Felsenstein, J. 1985. Confidence limits of phylogenies: an approach using the bootstrap. Evolution 39:783–791.
14. Felsenstein, J. 1990. PHYLIP manual, version 3.3. University Herbarium, University of California, Berkeley.
15. Fernie, B. F., G. Dapolito, P. J. Cote, Jr., and J. L. Gerin. 1985. Kinetics of respiratory syncytial virus glycoproteins. J. Gen. Virol. 66:1983–1990.
16. Fitch, W. M., J. M. E. Leiter, X. Li, and P. Palese. 1991. Positive Darwinian evolution in human influenza A viruses. Proc. Natl. Acad. Sci. USA 88:4270–4274.
17. García-Barreno, B., J. L. Jurcano, T. Aukenbauer, C. López-Galíndez, and J. A. Melero. 1988. Participation of cytoskeletal intermediate filaments in the infectious cycle of human respiratory syncytial virus (RSV). Virus Res. 9:307–322.
18. García-Barreno, B., C. Palomo, C. Peñas, T. Delgado, P. Pérez-Breña, and J. A. Melero. 1989. Marked differences in the antigenic structure of human respiratory syncytial virus F and G glycoproteins. J. Virol. 63:925–932.
19. García-Barreno, B., A. Portela, T. Delgado, J. A. López, and J. A. Melero. 1990. Frame shift mutations as a novel mechanism for the generation of neutralization resistant mutants of human respiratory syncytial virus. The EMBO J. 9:4181–4187.
19a. García-Barreno, B., T. Delgado, and J. A. Melero. 1994. Oligo(A) sequences of human respiratory syncytial virus G protein gene: assessment of their genetic stability in frameshift mutants. J. Virol. 68:5460–5468.
20. Higgins, D. G., and P. M. Sharp. 1988. CLUSTAL: a package for performing multiple sequence alignment on a microcomputer. Gene 73:237–244.
21. Johnson, P. R., M. K. Spriggs, R. A. Olmsted, and P. L. Collins. 1987. The G glycoprotein of human respiratory syncytial viruses of subgroups A and B: extensive sequence divergence between antigenically related proteins. Proc. Natl. Acad. Sci. USA 84:5625–5629.
22. Jukes, T. H., and C. R. Cantor. 1969. Evolution of protein molecules, p. 21. *In* H. M. Munro, (ed.), Mammalian protein metabolism. Academic Press, New York.
23. Kanegae, Y., S. Sugita, A. Endo, M. Ishida, S. Senya, K. Osaka, K. Nerome, and A. Oya. 1990. Evolutionary pattern of the hemagglutinin gene of influenza B viruses isolated in Japan: cocirculating lineages in the same epidemic season. J. Virol. 64:2860–2865.

24. Levine, S., R. Klaiber-Franco, and P. R. Paradiso. 1987. Demonstration that glycoprotein G is the attachment protein of respiratory syncytial virus. J. Gen. Virol. 68:2521–2524.
25. López-Galíndez, C., J. A. López, J. A. Melero, L. De La Fuente, C. Martínez, J. Ortín, and M. Perucha. 1988. Analysis of genetic variability and mapping of point mutations in influenza virus by the RNase A mismatch cleavage method. Proc. Natl. Acad. Sci. USA 85:3522–3526.
26. Mallipaddi, S. K., and S. K. Samal. 1993. Sequence variability of the glycoprotein gene of bovine respiratory syncytial virus. J. Gen. Virol. 74:2001–2004.
26a. Martínez, I., et al. Unpublished data.
27. Mateu, M. G., J. Hernández, M. A. Martínez, D. Feigelstock, S. Lee, J. J. Pérez, E. Giralt, D. Stuart, E. L. Palma, and E. Domingo. 1994. Antigenic heterogeneity of a foot-and-mouth disease virus serotype in the field is mediated by very limited sequence variation at several antigenic sites. J. Virol. 68:1407–1417.
28. McIntosh, K., and R. M. Chanock. 1990. Respiratory syncytial virus, p. 1045–1072. *In* B. N. Fields and D. M. Knipe (ed.), Virology, 2nd ed. Raven Press, New York.
29. Melero, J. A., P. Rueda, and B. García-Barreno. 1993. Antigenic variation of human respiratory syncytial virus G glycoprotein: genetic mechanisms and evolutionary significance, p. 141–149. *In* L. Carrasco, E. Wimmer, and N. Sonenberg (ed.), Regulation of gene expression in animal viruses. Plenum Press, New York.
30. Mufson, M. A., C. Örvell, B. Rafnar, and E. Norrby. 1985. Two distinct subtypes of human respiratory syncytial virus. J. Gen. Virol. 66:2111–2124.
31. Nei, M., and T. Gojobori. 1986. Simple methods for estimating the number of synonymous and nonsynonymous nucleotide substitutions. Mol. Biol. Evol. 3:418–426.
32. Olmsted, R. A., N. Elango, G. A. Prince, B. R. Murphy, P. R. Johnson, B. Moss, R. M. Chanock, and P. L. Collins. 1986. Expression of the F glycoprotein of respiratory syncytial virus by a recombinant vaccinia virus: comparison of the individual contributions of the F and G glycoproteins to host immunity. Proc. Natl. Acad. Sci. USA 83:7462–7466.
33. Oxford, J. S., A. J. Kilmov, T. Corcoran, Y. Z. Ghendon, and G. C. Schild. 1984. Biochemical and serological studies of influenza B viruses: comparisons of historical and recent isolates. Virus Res. 1:241–258.
34. Rota, P. A., M. A. Hemphill, T. Whistler, H. L. Regnery, and A. P. Kendal. 1992. Antigenic and genetic characterization of the haemagglutinins of recent cocirculating strains of influenza B virus. J. Gen. Virol. 73:2737–2742.
35. Rota, P. A., T. R. Wallis, M. W. Harmon, J. S. Rota, A. P. Kendal, and K. Nerome. 1990. Cocirculation of two distinct evolutionary lineages of influenza B virus since 1983. Virology 175:59–68.
36. Rueda, P., T. Delgado, A. Portela, J. A. Melero, and B. García-Barreno. 1991. Premature stop codons in the G glycoprotein of human respiratory syncytial viruses resistant to neutralization by monoclonal antibodies. J. Virol. 65:3374–3378.
37. Rueda, P., B. García-Barreno, and J. A. Melero. 1994. Loss of conserved cysteine residues in the attachment (G) glycoprotein of two human respiratory syncytial virus escape mutants that contain multiple A-G substitutions (hypermutations). Virology 198:653–662.
37a. Rueda, P., et al. Unpublished data.
38. Saitou, N., and M. Nei. 1987. The neighbor-joining method: a new method for reconstructing phylogenetic trees. Mol. Biol. Evol. 4:406–425.
39. Sakaguchi, T., T. Toyoda, B. Gotoh, N. M. Inocencio, K. Kuma, T. Miyata, and Y. Nagai. 1989. Newcastle disease virus evolution. I. Multiple lineages defined by sequence variability of the hemagglutinin-neuraminidase gene. Virology 169:260–272.
40. Sanger, F., S. Nicklen, and A. R. Coulson. 1977. DNA sequencing with chain-terminating inhibitors. Proc. Natl. Acad. Sci. USA 74:5463–5467.
41. Satake, M., J. E. Coligan, N. Elango, E. Norrby, and S. Venkatesan. 1985. Respiratory syncytial virus envelope glycoprotein (G) has a novel structure. Nucleic Acids Res. 13:7795–7812.
42. Saurdis, J., and M. Nei. 1988. Relative efficiencies of the maximum parsimony and distance-matrix methods in obtaining the correct phylogenetic tree. Mol. Biol. Evol. 5:298–311.
43. Storch, G. A., C. S. Park, and D. E. Dobson. 1989. RNA fingerprinting of respiratory syncytial virus using ribonuclease protection. Application to molecular epidemiology. J. Clin. Invest. 83:1894–1902.
44. Stott, E. J., G. Taylor, L. A. Ball, K. Anderson, K.-Y. Young, A. M. Q. King, and G. W. Wertz. 1987. Immune and histopathological responses in animals vaccinated with recombinant vaccinia viruses that express individual genes of human respiratory syncytial virus. J. Virol. 61:3855–3861.
45. Studier, F. W. 1972. Analysis of bacteriophage T7 early mRNAs and proteins in slab gels. J. Mol. Biol. 79:237–248.
46. Sullender, W. M., M. A. Mufson, L. J. Anderson, and G. W. Wertz. 1991. Genetic diversity of the attachment protein of subgroup B respiratory syncytial viruses. J. Virol. 65:5425–5434.
47. Taylor, G., E. J. Stott, M. Bew, B. F. Fernie, P. J. Cote, A. P. Collins, M. Hughes, and J. Jebbett. 1984. Monoclonal antibodies protect against respiratory syncytial virus infection in mice. Immunology 52:137–142.
48. Towbin, H., T. Staehelin, and J. Gordan. 1979. Electrophoretic transfer of proteins from polyacrylamide gels to nitrocellulose sheets: procedure and some applications. Proc. Natl. Acad. Sci. USA 76:4350–4354.
49. Walsh, E. E., C. B. Hall, M. Briselli, M. W. Brandriss, and J. J. Schlesinger. 1987. Immunization with glycoprotein subunits of respiratory syncytial virus to protect cotton rats against viral infection. J. Infect. Dis. 155:1198–1204.
50. Wertz, G. W., P. L. Collins, Y. Huang, C. Gruber, S. Levine, and L. A. Ball. 1985. Nucleotide sequence of the G protein of human respiratory syncytial virus reveals an unusual type of viral membrane protein. Proc. Natl. Acad. Sci. USA 82:4075–4079.
51. Wertz, G. W., M. Krieger, and L. A. Ball. 1989. Structure and cell surface maturation of the attachment glycoprotein of human respiratory syncytial virus in a cell line deficient in O-glycosylation. J. Virol. 63:4767–4776.
52. Wiley, D. C., I. A. Wilson, and J. J. Skehel. 1981. Structural identification of the antibody-binding sites of Hong Kong influenza hemagglutinin and their involvement in antigenic variation. Nature (London) 289:373–378.
53. Winter, E., F. Yamamoto, C. Almoguera, and M. Perucho. 1985. A method to detect and characterize point mutations in transcribed genes: amplification and overexpression of the mutant c-Kis-ras allele in human tumor cells. Proc. Natl. Acad. Sci. USA 82:7575–7579.
54. Yamashita, M., M. Krystal, W. M. Fitch, and P. Palese. 1988. Influenza B virus evolution: co-circulating lineages and comparison of evolutionary pattern with those of influenza A and C viruses. Virology 163:112–122.

Protein Engineering vol.15 no.5 pp.365–371, 2002

Modelling the structure of the fusion protein from human respiratory syncytial virus

Brian J.Smith[1,2], Michael C.Lawrence[3] and Peter M.Colman[1]

[1]Biomolecular Research Institute, 343 Royal Parade, Parkville, Victoria 3052, Australia

[2]Present address: The Walter & Eliza Hall Institute of Medical Research, P.O. Royal Melbourne Hospital, Parkville, Victoria 3050, Australia

[3]Present address: CSIRO, Division of Health Science and Nutrition, 343 Royal Parade, Parkville, Victoria 3052, Australia

[3]To whom correspondence should be addressed

The fusion protein of respiratory syncytial virus (RSV-F) is responsible for fusion of virion with host cells and infection of neighbouring cells through the formation of syncytia. A three-dimensional model structure of RSV-F was derived by homology modelling from the structure of the equivalent protein in Newcastle disease virus (NDV). Despite very low sequence homology between the two structures, most features of the model appear to have high credibility, although a few small regions in RSV-F whose secondary structure is predicted to be different to that in NDV are likely to be poorly modelled. The organization of individual residues identified in escape mutants against monoclonal antibodies correlates well with known antigenic sites. The location of residues involved in point mutations in several drug-resistant variants is also examined.

Keywords: fusion/homology modelling/Newcastle disease virus/respiratory syncytial virus

Introduction

Respiratory syncytial virus (RSV) is the leading cause of lower respiratory tract infection in infants and children, with almost all children becoming infected by the age of 2 years. Primary infection does not induce immunity and recurrent infection occurs throughout life. The virus is also an important pathogen in immunocompromised adults and the elderly (Collins *et al.*, 1996).

RSV is a member of the *Pneumovirus* genus of the family of *Paramyxoviridae*. The *Paramyxoviridae* also include the human pathogens measles, mumps and parainfluenza virus types 1–4. Other members include Sendai virus, Newcastle disease virus (NDV), simian virus 5 (SV5), pneumonia virus of mice (PVM) and turkey rhinotracheitis virus (TRT). RSV has a single strand of negative-sense RNA, encoding for 10 viral proteins. Three of these are exposed on the surface of virion and infected cells; the F (fusion) protein, the G (attachment) protein and SH (small hydrophobic) integral membrane protein, the first two being the major immunogenic proteins.

The G protein is responsible for attachment of the viral particle to the host, a role adopted by the haemagglutinin of other members of the family (although G itself does not bind sialic acid). Following attachment, fusion of the viral particle with its host is achieved by F. While F is able to mediate fusion in recombinant viruses lacking G and SH, efficient fusion is obtained only when all three surface proteins are coexpressed (Karron *et al.*, 1997). The F protein also promotes infection of neighbouring cells by the formation of syncytia.

The F protein is synthesized as a single *N*-glycosylated polypeptide precursor of 574 amino acids (F_0), that is assembled in the rough endoplasmic reticulum into a homo-oligomer and cleaved by a cellular protease into two disulphide-linked chains, F_2 and F_1, before reaching the cell surface. The peptide is anchored in the viral membrane by a transmembrane segment found toward the C-terminus of F_1. At the N-terminus of F_1, ~20 residues compose a highly hydrophobic domain (fusion peptide) that is believed to insert into the target membrane during the fusion process. The F proteins of all *Paramyxoviridae* family display heptad repeat sequences. One of these (HR-A) extends from the C-terminus of the fusion peptide approximately 56 residues to a conserved cysteine residue, while the second is N-terminal to the transmembrane anchoring domain. The X-ray structure of NDV-F shows that the helix of HR-A extends a further 22 residues C-terminal to the conserved cysteine residue. A third heptad repeat region (residues 53–100) identified in the sequence of the F_2 chain of RSV-F (Lambert *et al.*, 1996) maps to the HR-C helix observed in the X-ray structure of NDV-F. The structures of a complex of regions of HR-A and HR-B from both RSV-F (Zhao *et al.*, 2000) and SV5-F (Baker *et al.*, 1999) show a trimeric coiled-coil core formed by HR-A, with three HR-B α-helices packed anti-parallel within the grooves formed by adjacent HR-A segments. This hexameric motif has now been observed in a large number of viral fusion proteins and may reflect a common mechanistic element (Lentz *et al.*, 2000).

The hexameric coiled-coil structure observed for the HR-A/HR-B complex probably corresponds to the stable post-fusion conformation. The three-dimensional atomic structure of the remainder of the RSV-F protein is at present unknown. Single-molecule electron microscopy images of RSV-F (Calder *et al.*, 2000) suggest two morphologies, 'cone' shape and 'lollipop' shape. These probably relate to the pre-fusion metastable and post-fusion forms of the protein, respectively, analogous to those seen for haemagglutinin from influenza virus (Skehel and Wiley, 2000).

The structure of the F protein from NDV, however, has been determined recently (Chen *et al.*, 2001). The molecule is trimeric and is organized into three regions, head, neck and stalk (Figure 1). In the head, each monomer comprises an immunoglobulin type β-sandwich domain and a highly twisted β-sheet domain. Residues 171–221 (NDV-F numbering), that include HR-A, form a central coiled-coil spanning both neck and stalk regions; residues 465–495 (HR-B) are disordered in the structure. The neck includes all of HR-C (77–105) that forms an α-helix in which the first 15 residues (77–91) pack parallel against the central coiled-coil, a mixed four-stranded β-sheet and an irregular bundle of four α-helices. The structure is fenestrated by three radial channels between the head and neck regions. These connect to a wide central channel that extends ~50 Å down through the head region.

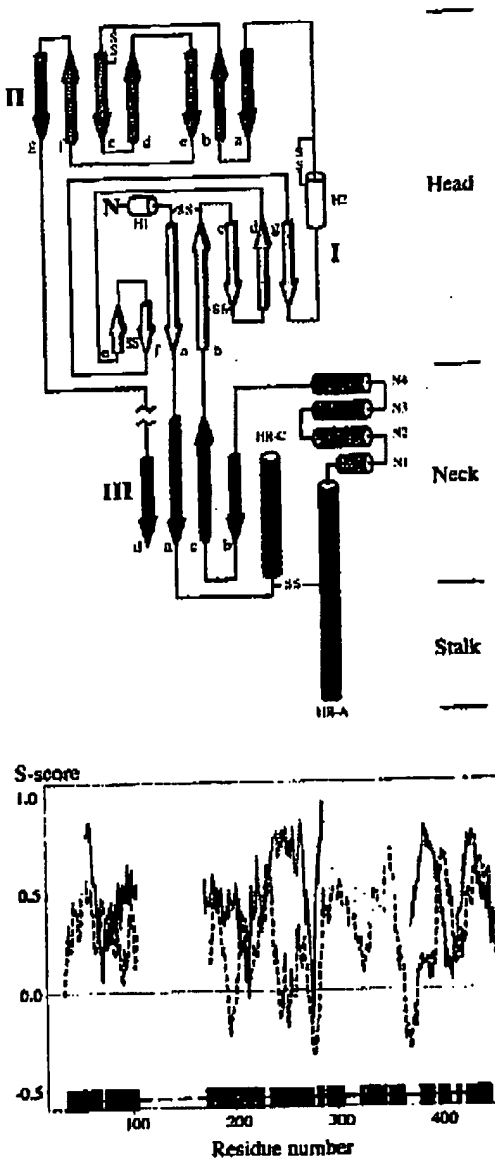

Fig. 1. Schematic secondary structure diagram of the RSV-F model based on Chen *et al.* (Chen *et al.*, 2001) and structure compatibility plot from Profiles-3D for NDV-F (solid coloured line) and the model of RSV-F (black dashed line). The compatibility trace is colour coded according to the individual domains: the β-barrel domain I and immunoglobulin-like domain II are coloured yellow and green, respectively, the β-domain II, helix HR-C and central coiled-coil HR-A are coloured blue and the irregular four-helix bundle is coloured pink. The secondary structure elements of NDV-F are indicated by the coloured boxes along the lower edge of the panel (colour coded: green, helix; red, strand).

The sequence homology of F proteins within the *Paramyxoviridae* family is generally fairly low although, within any one subfamily, the level of homology can be high. The sequence homology between F proteins from NDV and RSV is particularly low, <15%, certainly well below the so-called twilight zone (Rost, 2000) for homology modelling. There are, however, several features that allow the generation of a realistic model of RSV-F based on the structure of NDV-F: they are known to have the same function, their overall morphology is the same and key sequence/structural features are present in both in identical positions within their sequences. The presence of such features improves the chances of obtaining a successful model (Colman *et al.*, 1993; Crennell *et al.*, 2000). We report here our efforts in deriving a model of RSV-F and an appraisal of this model.

Methods

Alignments of representative sequences from several members of the *Paramyxoviridae* family were performed using ClustalW (Thompson *et al.*, 1994) implemented in the BioEdit program (Hall, 1999). Minor manual changes were performed to ensure maximum overlap of predicted secondary structure with no insertions in these regions. These changes were restricted primarily to the N-terminal region of F_2 and residues in the regions 329–346 and 385–391 (RSV-F numbering). Secondary structure prediction was performed through the PHD server (Rost and Sander, 1993, 1994).

The model of RSV-F was first generated by homology with NDV-F using the Modeller package (Šali and Blundell, 1993) within the InsightII program (Molecular Simulations). Compatibility of the model with the sequence was evaluated with Profiles-3D (Luthy *et al.*, 1992). Three-fold symmetry was applied by superimposing the α-carbon atoms of one RSV-F monomer on to the other two related monomers. The trimer resulting from this assembly was then energy minimized using the Discover program (Molecular Simulations) with all backbone atoms held fixed. The molecular mechanics minimization used the AMBER force field and an electrostatic cut-off of 18 Å. The method of steepest descents was applied until the gradient fell below 10.0 kcal/mol.Å, at which point the conjugate gradients method was applied until the gradient fell below 0.01 kcal/mol.Å. The final model was again assessed using Profiles-3D and Procheck (Laskowski *et al.*, 1993).

Results

The alignment of sequences from several members of the *Paramyxoviridae* family is presented in Table I. Also indicated in Table I is the secondary structure observed in the three-dimensional X-ray crystal structure NDV-F. The sequence identity matrix based on this alignment is presented in Table II. Secondary structure was correctly predicted by PHD for 78% of the residues in NDV-F. Residues involved in the β-bulges (Chan *et al.*, 1993) in strands Ia and Ib were not predicted as strand although the flanking regions were. Residues 314–318 and 322–326 had secondary structure incorrectly assigned (i.e. assigned strand when the structure was helix and vice versa). Notably, the X-ray structure near residues 311–314 is poorly defined. The residues in strand Ig were predicted to be coil. Residues 371–377 were incorrectly predicted to be strand (although they do not form of a β-sheet they do adopt an extended conformation).

The success of PHD in predicting the secondary structure in NDV-F provides encouragement for the prediction in RSV-F. The predicted secondary structure for the F proteins from NDV, SV5, HPIV 1–4, mumps, Sendai and measles

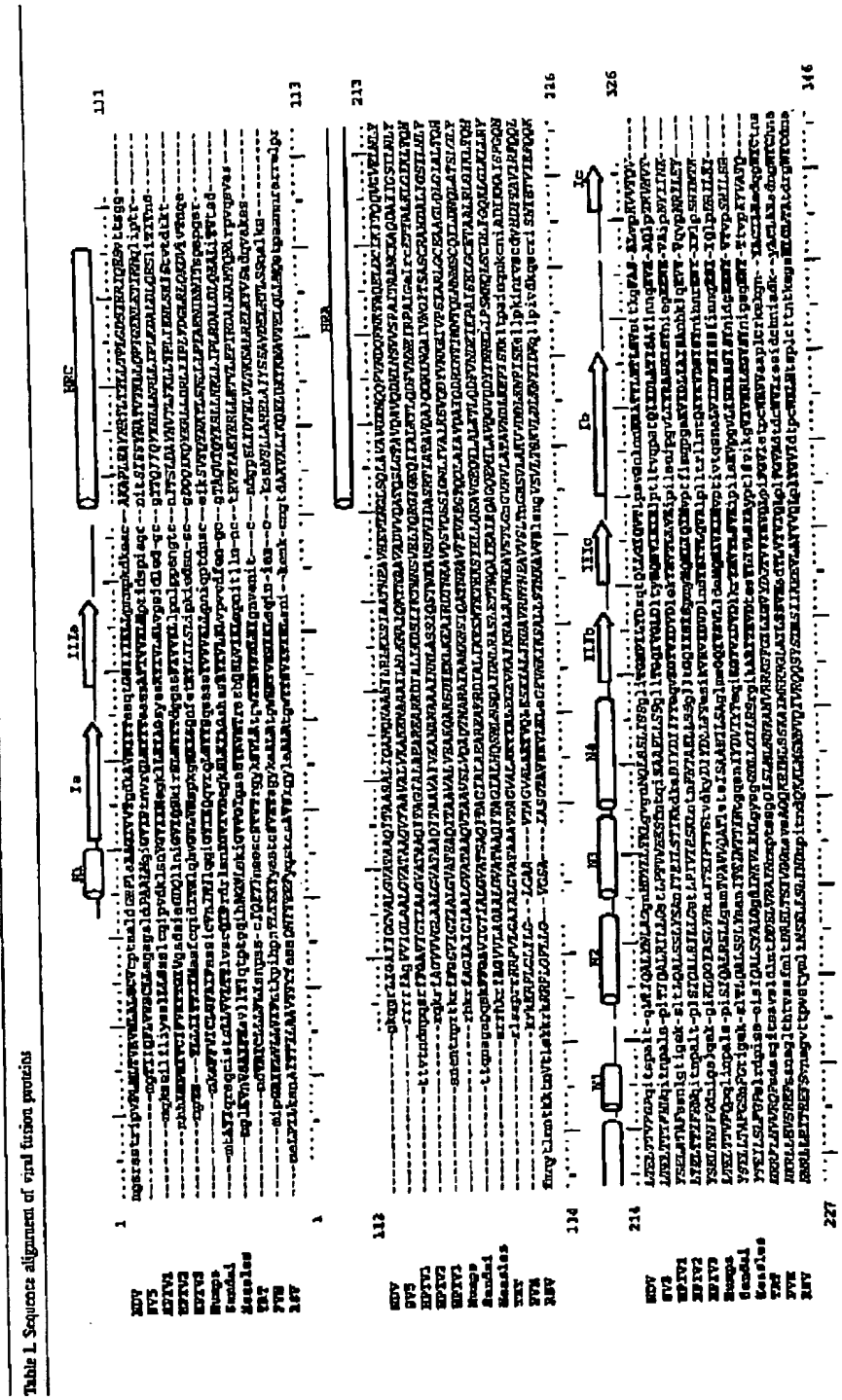

Table 1. Sequence alignment of viral fusion proteins

Table 1. Continued

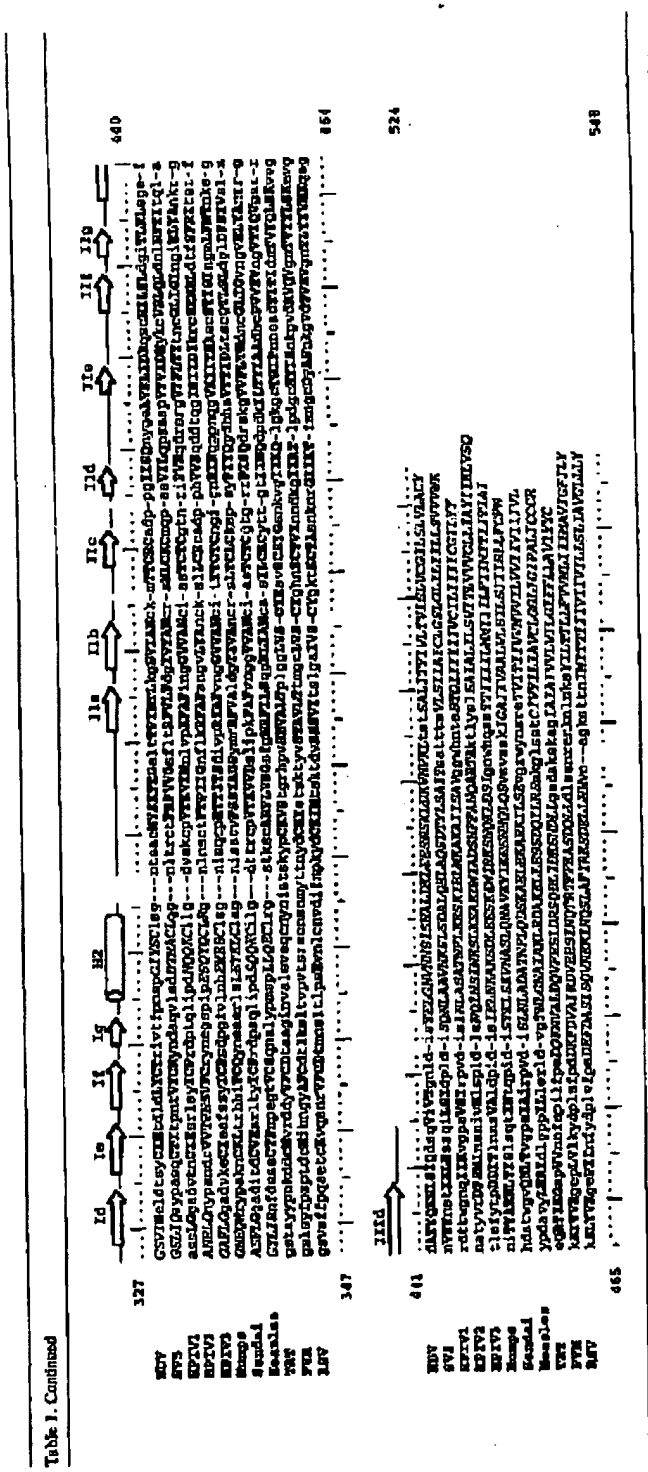

Sequence alignment was performed by rubinal manual adjustment of ClustalW alignment. Amino acids in bold uppercase and italic uppercase are predicted strand and helix, respectively, by PHD. Cylinders and arrows indicate helices and strands, respectively, observed in NDV-F labelled according to Chen *et al.* (Chen *et al.*, 2001). Amino acid numbering is for NDV (top) and RSV (bottom). NDV (Queensland, AAF42837); SV5 (W3, P04849); HPIV1 (C39 P12606); HPV12 (Tochiba, P26629); HPV3 (OP, BAA32573); Mumps (SBL-1, P19716); Sendai (Z, P27564); Measles (AIK-C, P35975); TKT (UK53/83, P24014); PVM (J3599/49); RSV (LongA, P12568). Strain and Genbank codes in parentheses. Sequences extracted from http://www.ncbi.nlm.nih.gov.

Table II. Sequence identity matrix of members of the family *Paramyxoviridae* (based on the sequence alignment presented in Table I)

Subfamily		NDV	SV5	HPIV1	HPIV2	HPIV3	Mumps	Sendai	Measles	TRT	PVM
Paramyxovirinae	SV5	0.311									
	HPIV1	0.226	0.236								
	HPIV2	0.304	0.478	0.224							
	HPIV3	0.252	0.245	0.447	0.243						
	Mumps	0.303	0.439	0.223	0.388	0.253					
	Sendai	0.241	0.241	0.701	0.224	0.426	0.200				
	Measles	0.253	0.284	0.277	0.251	0.257	0.258	0.276			
Pneumovirinae	TRT	0.157	0.149	0.161	0.143	0.179	0.158	0.161	0.136		
	PVM	0.147	0.150	0.129	0.134	0.157	0.127	0.134	0.131	0.394	
	RSV	0.135	0.124	0.129	0.136	0.172	0.136	0.142	0.120	0.339	0.411

uppears to be highly conserved, despite pairwise sequence identities being as low as 20%. The members of the Pneumovirinae subfamily (that includes TRT, PVM and RSV) also share a high degree of similarity in their predicted secondary structure, but there are clear differences between the F proteins from this genus and the members of the Paramyxovirinae subfamily. This dichotomy is also reflected in the level of sequence identity, ranging from as low as 12% to a maximum of only 18%. In particular, the sequence identity between NDV-F, a member of the rubulavirus family and RSV-F is only 13.5%.

The predicted secondary structure of RSV-F (Table I) differs significantly from that predicted for NDV-F in several regions: (1) in HR-A, 13 residues (202–214) are not predicted to adopt a helical structure, although there is a cysteine present that is strictly conserved; (2) in the 4-helix bundle, where the helices N2–N4 were successfully predicted in NDV-F, only two helices are predicted for RSV; (3) in RSV, strand IIIb is predicted to be significantly shorter, with an intervening helical segment between strands IIIb and IIIc; (4) residues in strand Ic, incorrectly predicted by PHD as helix in NDV-F, are predicted to be strand in RSV-F; and (5) the residues in helix H2 of NDV-F are predicted to be random coil in RSV-F.

The homology model of RSV-F was based on the sequence alignment in Table I. The r.m.s. difference in α-carbon positions between individual monomers of RSV-F and NDV-F is 0.9 Å. In the X-ray structure of NDV-F, five disulphide linkages are observed in each monomer. In the sequence alignment presented in Table I, eight of the disulphide-forming cysteine residues are aligned with cysteine residues in RSV-F. While the likelihood of disulphide formation in the model is reasonably unambiguous in a few cases, as judged by the close proximity of the constituent cysteine residues, the cysteine-rich nature of the head region makes unambiguous assignment in that region somewhat more difficult. In particular, a shift in the sequence alignment by just two residues of cysteines 322 and 393 would bring them within a distance capable of forming a disulphide link, at the loss of the NDV-F equivalent disulphide link between residues 382 and 393 (362 and 370, NDV-F numbering). Similar shifts in sequence alignment of cysteines 37, 416 and 439 could also change the disulphide pattern in RSV-F. Several alternative disulphide linkages were explored and their suitability was assessed by examining the Profiles-3D score in the region of the newly formed disulphide link. The Profiles-3D score was significantly poorer for all models in which an NDV-F equivalent disulphide link was removed. In the final model all NDV-F equivalent disulphide links were therefore maintained. Residues 37, 322 and 439 all lie in close proximity: the disulphide link between 37 and 322 provided the better Profiles-3D score.

Disulphide links were therefore built between the following pairs of cysteine residues in the RSV-F model, 37:322, 313:343, 69:212, 358:367, 382:393 and 416:422. The latter four links correspond to those observed in the structure of NDV-F; the link between cysteine residues 401 and 424 (NDV-F numbering) is not present in RSV-F. The former two links are additional to those observed in NDV-F; they connect, respectively, the loop between helix H1 and strand Ia with the C terminus of strand Ib and the loop between the central region of strand Ib with the C terminus of strand Ic. Two inter-chain disulphide links are predicted for RSV-F, between cysteine pairs 37:322 and 69:212; the former of these has no corresponding partner in NDV-F.

The residue compatibility score (S-score) from Profiles-3D for both the X-ray structure of NDV-F and the model structure of RSV-F proteins is presented in Figure 1 (only the score for one of the monomers is presented, the profile for the other monomers being very similar). The compatibility score for NDV-F falls below zero for residues Asp277 and Ser278, at the C-terminus of strand IIIb. The compatibility score for the RSV-F model falls below zero in five regions, four of which are where the secondary structure prediction by PHD differs for NDV-F and RSV-F (region 1, Val207–Ser215; region 2, Leu257–Met274; region 3, Tyr286–Val296; and region 5, Leu381–Asp392), while the fifth occurs at Lys470–Asp479 (region 4).

Several resides fall into disallowed regions of the Ramachandran plot (Cys37, Arg235, Thr324, Asp344, Cys416, Ser436). Residue Thr324 corresponds to Thr310 in NDV-F, which also lies in the disallowed region of the Ramachandran diagram in the X-ray structure of NDV-F. Both cysteine residues (37 and 416) have been modelled in disulphide links.

The proline residue involved in the wide β-bulge, responsible for introducing a twist into the connection between strands IIIc and Ib (Pro290 NDV-F, Pro304 RSV-F), is strictly conserved in all sequences. Apart from cysteine residues, the only other residues that are strictly conserved in the alignment presented in Table I are Gly145, Ala147, Gly411 and Asp486. Only Gly411 is observed in the structure of NDV-F; this residue is in a type I′ (inverse common) β-turn (Chou and Fasman, 1977; Richardson and Richardson, 1989) connecting stands IIa and IIb, found at the outside opening of the radial channel. Asp486 is located on the surface of coiled-coil HR-A/HR-B complex (Zhao *et al.*, 2000).

The sequence of RSV-F differs from all other sequences in that it has a large insertion prior to the fusion peptide cleavage

Table III. Hydrophobic heptad repeat in HR-A helix from NDV, SV5 and RSV

NDV-F	172	3 4 3 4 4 3 4 3 4 3 4 4 a d a d d a d a d a d a LSQLAVAVGKMQQPVNDQFNKTAQELDCIKITQQVGVELNLYLTELTTVF	221
SV5-F	168	3 4 3 4 4 3 4 a d a d d a d TQSLGTAVQAVQDHINSVVSPAITAANC	185
RSV-F	185	3 4 3 4 4 4 a a a d d d a VSVLTSKVLDLKNYIDKQLLPIVNKQSCRISNIETVIEFQQKNNRLLEIT	234

Observed heptad spacing (3 or 4) and core residue positions (*a* or *d*) for the triple-stranded coiled-coil indicated above sequences of NDV-F (Chen *et al.*, 2001). SV5-F (Baker *et al.*, 1999) and RSV-F (Zhao *et al.*, 2000). Underlined residues in RSV indicate previously predicted core positions (Chambers *et al.*, 1992).

site. This region contains three potential N-linked glycosylation sites (at Asn116, Asn120 and Asn126). Proteolytic removal of this region appears to be necessary for activation of the fusion protein (Zimmer *et al.*, 2001). Three other potential N-linked glycosylation sites are at Asn27, Asn70 and Asn500. Only Asn70 has been included in the current model, located at the N-terminus of helix HR-C at the base of the neck region.

The heptad repeat pattern of hydrophobic amino acids in the *a* and *d* positions in HR-A observed in NDV-F is shown in Table III. Two stutters are found in this region (Brown *et al.*, 1996). There is predicted to be a disruption of the helix in HR-A between residues 202 and 214 of RSV-F [also previously noted by Chambers *et al.* (Chambers *et al.*, 1992)]. In the alignment with NDV-F this region contains various residues in positions that are likely to be unfavourable towards the formation of a coiled coil (Lupas *et al.*, 1991), specifically Leu204 in a *b* position, Val207 in an *e* position and Arg213 in a *d* position. In addition, Pro205 (conserved between SV5-F and RSV-F) could introduce a kink into the helix (Chang *et al.*, 1999) further disrupting the coiled-coil. In the sequence alignment presented in Table I, the observed structure of NDV-F and the HR-A/HR-B complex from RSV-F have 24 residues in common through HR-A (Gly184–Lys209). The HR-A helix in NDV-F contains a shorter (3–4–4–3) stutter than that observed (3–4–4–4–3) in the N-terminus of both RSV-F and SV5-F HR-A helices (Table III). The longer stutter, however, may be induced by the artificial nature of the constructs employed in the last two structures. The difference in heptad repeat pattern corresponds roughly with onset of poor Profiles-3D compatibility scores in region I.

A 21-residue peptide, corresponding to residues 255–275 of RSV-F, adopts a helix–loop–helix conformation in 30% trifluoroethanol (Toiron *et al.*, 1996). The secondary structure matches very well the prediction from PHD for this region, but as was noted above, this is different to that observed in the X-ray structure of NDV-F. It is likely, therefore, for the structures of RSV and NDV fusion proteins to differ in this region.

The spatial location of various antigenic sites on the surface of RSV-F has been provided through EM images of monoclonal antibodies (MAbs) of known specificity in complex with full length F (Calder *et al.*, 2000). The angle at which each MAb binds F is compared with the position of the altered residue of the resistant mutants in the model of RSV-F in Table IV. Angles in the model were calculated from the α-carbon of each residue to a point −30 Å from the top of the head of the trimeric assembly lying on the molecular symmetry axis. The agreement is very good, with most comparisons lying within a few degrees. All residues that confer antibody resistance through mutation are exposed on the surface of the protein in the model. Residues forming antigenic site II are found in helices N3 and N4, on the exterior of the neck and at the

Table IV. Organization of antigenic sites in RSV-F[a]

MAb	Site[b]	Residue	Angle (°)	
			Model	Expt.[c]
2F	I	389	135	150
47F	II	262	68	85–90
		272	82	
		268	86	
		275	71	
56F	IV	429	102	95–100
7.957	V	432	110	110–115
		433	115	
		447	98	
7.916	VI	436	123	120

[a]Angles were calculated from the α-carbon of each residue to a point −30 Å from the top of the head of the trimeric assembly lying on the molecular symmetry axis.
[b]Site classification according to the literature (Arbiza *et al.*, 1992; López *et al.*, 1998).
[c]Experimental angles from Calder *et al.* (Calder *et al.*, 2000).

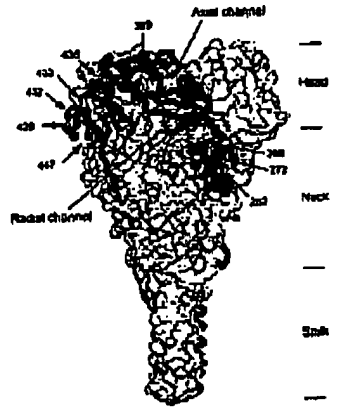

Fig. 2. Surface diagram of the model of RSV-F: two monomers shown in surface representation and the third as an α-carbon worm. Residues forming antigenic sites are indicated. Figure generated using DINO (Philippsen, 2000) and Raster-3D (Merritt and Bacon, 1997).

mouth of the radial channel. Site I is near the top of the head, while sites IV, V and VI lie at the apex of the trimeric structure of the head. These sites are indicated in Figure 2.

A segment from the C-terminal region of HR-A from the Sendai virus fusion protein has been shown to be able to induce membrane fusion (Peisajovich *et al.*, 2000). This segment corresponds to residues 221–242 in RSV-F and encompasses the C-terminus of HR-A and all of helix N1. In the present model, several residues in N1 are surface exposed at the base of the axial channel. These residues could become exposed to the target membrane after opening and disassembly of the head (Chen *et al.*, 2001).

Polypeptides from the HR-B domain of RSV demonstrate antiviral activity, inhibiting syncytia formation (Lambert *et al.*, 1996). These are believed to function by interfering with the association of HR-B with HR-A. The HR-B region is not observed in the structure of NDV-F; however, the overlay of the HR-A/HR-B complex from RSV-F suggests an onward extension of the coiled-coil from HR-A with HR-B packed into the grooves. It is anticipated that the association of HR-B with HR-A, which brings together the transmembrane and fusion peptides, occurs only in the post-fusion form of the protein. The polypeptide that inhibits syncytia formation could associate with the extended α-helical N-terminal region of HR-A, preventing it from adopting its correct post-fusogenic association with HR-B.

Several small-molecule inhibitors of RSV have been developed recently that function either by inhibiting fusion or by interfering with formation of the multimeric state or early processing of RSV-F (Anlabaugh, *et al.*, 2000; Meanwell and Krystal, 2000). In a few cases, resistant viruses have led to an indication of the site of interaction. Resistance to the compound RD3-0028 was mapped to residue N276Y in RSV-F (Sudo *et al.*, 1998). This compound presumably acts by interfering with the synthesis or intracellular processing of the F protein. Residue 276 lies in helix N4, at the interface between head and neck regions. Benzimidazole derivatives have demonstrated potent antiviral activity (Andries *et al.*, 2000); resistant mutants to these compounds have single point mutations at residues S398L and D486N. Residue 486 has not been included in the present model, while residue 398 lies N-terminal to the immunoglobulin-like β-sandwich domain and is found surface exposed on the rim of the axial channel at the junction between two monomers.

Conclusions

The recently determined three-dimensional structure of NDV-F has permitted the construction of a reasonably reliable model of RSV-F. The model of RSV-F, however, is clearly inadequate in several regions. We have shown that the heptad repeat pattern in HR-A of NDV-F and RSV-F differs. The secondary structure prediction in RSV-F in this region is also not consistent with the structure observed in NDV-F. Similarly, the secondary structure prediction for RSV-F in the region of the 4-helix bundle differs from what is observed in the structure of NDV-F, but is consistent with the structure of a small polypeptide taken from this region. Other regions where the secondary structure prediction in RSV-F differs from the X-ray structure of NDV-F also have poor Profiles-3D structure compatibility scores and are likely to be poorly modelled. Despite these reservations, the model is consistent with the known three-dimensional arrangement of antigenic sites and provides an indication of the location of residues involved in drug-resistant variants and hence should provide a useful framework for future investigations in these areas.

Acknowledgement

The support by Biota Holdings (Melbourne, Australia) for some of the work described here is gratefully acknowledged.

References

Andries,K., Moeremans,M., Gevers,T., Willebrords,R., Lacrampe,J. and Janssens,F. (2000) Abstract from 40th International Conference on Antimicrobial Chemotherapy, September 17–20, 2000, Ontario, Canada.
Arbiza,J. *et al.* (1992) *J. Gen. Virol.*, 73, 2225–2234.
Anlabaugh,A. *et al.* (2000) *Virology*, 271, 122–131.
Baker,K.A., Dutch,R.E., Lamb,R.A. and Jardetzky,T.S. (1999) *Mol. Cell.* 3, 309–319.
Brown,J.H., Cohen,C. and Parry,D.A.D. (1996) *Proteins*, 26, 134–145.
Calder,L.J., Gonzalez-Reyes,L., Garcia-Barreno,B., Wharton,S.A., Skehel,J.J., Wiley,D.C., Melero,J.A. (2000) *Virology*, 271, 122–131.
Chambers,P., Pringle,C.R. and Easton,A.J. (1992) *J. Gen. Virol.*, 73, 1717–1724.
Chan,A.W.E., Hutchinson,E.G., Harris,D. and Thornton,J.M (1993) *Protein Sci.*, 2, 1574–1590.
Chang,D.K., Cheng,S.F., Trivedi,V.D. and Lin,K.L. (1999) *J. Struct. Biol.*, 128, 270–279.
Chen,L., Gorman,J.J., McKimm-Breshkin,J., Lawrence,L.J., Tulloch,P.A., Smith,B.J., Colman,P.M. and Lawrence,M.C. (2001) *Structure*, 9, 255–266.
Chou, P.Y. and Fasman, G.D. (1977) *J. Mol. Biol.*, 115, 135–175.
Collins,P.L., McIntosh,K. and Chanock,R.M. (1996) In Fields,B.N., Knipe,D.M., Howley,P.M., Chanock,R.M., Melnick,J.L., Monath,T.P., Roizman,B., Straus,S.E. (eds), *Fields Virology*, 3rd edn, Lippincott-Raven, Philadelphia, PA., pp. 1313–1351.
Colman,P.M., Hoyne,P.A. and Lawrence,M.C. (1993) *J. Virol.*, 67, 2972–2980.
Crennell,S., Takimoto,T., Portner,A. and Taylor,G. (2000) *Nature Struct. Biol.*, 7, 1068–1074.
Qazumyan,A., Mirzabekov,T. and Ellestad,G.A. (2000) *Curr. Pharm. Des.*, 6, 525–546.
Hall,T., Hall,T.A. (1999) *Nucl. Acids Symp. Ser.* 41, 95–98.
Karron,R.A. *et al.* (1997) *Proc. Natl Acad. Sci. USA*, 94, 13961–13966.
Lambert,D.M., Barney,S., Lambert,A.L., Guthrie,K., Medinas,R., Davis,D.E., Bucy,T., Erickson,J., Merutka,G. and Petteway,S.R. (1996) *Proc. Natl Acad. Sci. USA*, 93, 2186–2191.
Laskowski,R.A., MacArthur,M.W., Moss,D.S. and Thornton,J.M. (1993) *J. Appl. Crystallogr.*, 26, 283–291.
Lenz,D.R., Melinin,V., Haque,M.E. and Evans,K. (2000) *Curr. Opin. Struct. Biol.*, 10, 607–615.
López, J.A., Bustos,R., Orvell,C., Berois,M., Arbiza,J., García-Barreno,B. and Melero,J.A. (1998) *J. Virol.*, 72, 6922–6928.
Lupas,A., van Dyke,M. and Stock,J. (1991) *Science*, 252, 1162–1164.
Luthy,R., Bowie,J.U. and Eisenberg,D. (1992) *Nature*, 356, 83–85.
Meanwell,N.A. and Krystal,M. (2000) *Drug Discov. Today*, 5, 241–252.
Merritt,E.A. and Bacon,D.J. (1997) *Methods Enzymol.* 277, 505–524.
Peisajovich,S.G., Samuel,O. and Shai,Y. (2000) *J. Mol. Biol.*, 296, 1353–1365.
Philippsen, A. (2000) *DINO: Visualizing Structural Biology*. http://www.biozz.unibas.ch/~xray/dino.
Richardson, J.S. and Richardson, D.C. (1989) In Fasman, G.D. (ed.), *Prediction of Protein Structure and the Principles of Protein Conformation*. Plenum Press, New York pp. 1–98.
Rost, B. (2000) *Protein Eng.*, 12, 85–94.
Rost,B. and Sander,C. (1993) *J. Mol. Biol.*, 233, 584–599.
Rost,B. and Sander,C. (1994) *Proteins*, 19, 55–72.
Sali,A. and Blundell,T.L. (1993) *J. Mol. Biol.*, 234, 779–815.
Skehel,J.J and Wiley,D.C. (2000) *Annu. Rev. Biochem.*, 69, 531–569.
Sudo,K., Konno,K., Shigeta,S. and Yokota,T. (1998) *Antiviral Res.*, 37, A89.
Toiron,C., Lopez,J.A., Rivas,G., Andreu,D., Melero,J.A. and Bruix,M. (1996) *Biopolymers*, 39, 537–548.
Thompson,J.D., Higgins,D.G and Gibson,T.J. (1994) *Nucleic Acids Res.*, 22, 4673–4680.
Zhao,X., Singh,M., Malashkevich,V.N., Kim,P.S. (2000) *Proc. Natl Acad. Sci. USA*, 97, 14172–14177.
Zimmer,G., Budz,L. and Herrler,G. (2001) *J. Biol. Chem.*, 276, 31642–31650.

Received October 5, 2001; accepted January 4, 2002

JOURNAL OF VIROLOGY, Sept. 2002, p. 9218–9224
0022-538X/02/$04.00+0 DOI: 10.1128/JVI.76.18.9218–9224.2002

Vol. 76, No. 18

Cleavage at the Furin Consensus Sequence RAR/KR^{109} and Presence of the Intervening Peptide of the Respiratory Syncytial Virus Fusion Protein Are Dispensable for Virus Replication in Cell Culture

Gert Zimmer,[1] Karl-Klaus Conzelmann,[2] and Georg Herrler[1]*

Institut für Virologie, Tierärztliche Hochschule Hannover, D-30559 Hannover,[1] and Max-von-Pettenkofer-Institut and Genzentrum der Ludwig-Maximillians-Universität, D-81377 Munich,[2] Germany

Received 22 April 2002/Accepted 17 June 2002

Proteolytic processing of the respiratory syncytial virus F (fusion) protein results in the generation of the disulfide-linked subunits F1 and F2 and in the release of pep27, a glycopeptide originally located between the two furin cleavage sites FCS-1 (RKRR^{136}) and FCS-2 (RAR/KR^{109}). We made use of reverse genetics to study the importance of FCS-2 and of pep27 for BRSV replication in cell culture. Replacement of FCS-2 in the F protein of recombinant viruses by either of the sequences NANR^{109}, RANN^{109} or SANN^{109}, respectively, abolished proteolytic processing at this position, whereas the cleavage of FCS-1 was not affected. All mutants replicated in calf kidney and Vero cells in the absence of exogenous trypsin, although somewhat higher titers of BRSV containing the NANR^{109} or the RANN^{109} motif were achieved in the presence of trypsin. The virus mutants showed a reduced cytopathic effect which was lowest in the case of the SANN^{109} mutant. These findings demonstrate that cleavage at FCS-2 is dispensable for replication of respiratory syncytial virus in cell culture. A deletion mutant containing FCS-1 but lacking FCS-2 and most of pep27 replicated in cell culture as efficiently as the parental virus, indicating that this domain of the F protein is not essential for virus maturation and infectivity.

Human respiratory syncytial virus (HRSV) and *Bovine respiratory syncytial virus* (BRSV) are closely related members of the genus *Pneumovirus* within the family *Paramyxoviridae*. HRSV is the most important viral agent of pediatric respiratory tract disease worldwide, causing bronchiolitis and pneumonia (7). A very similar disease is caused by BRSV in calves (1, 2, 20, 33).

The envelope of the respiratory syncytial viruses (RSV) contains three glycoproteins: the attachment protein G, the small hydrophobic protein SH, and the fusion protein F. Several studies indicate that both the G and the SH proteins are dispensable for virus replication in cell culture but may have some accessory function in the host (4, 18, 19, 35, 39). The F protein mediates fusion between the viral and cellular membrane and is therefore essential for virus replication. Since fusion does not require low pH, cells infected with RSV can fuse with adjacent cells resulting in multinucleated syncytia. Syncytium formation can also be observed with cells transfected with the F gene, although coexpression of F together with G and/or SH protein has been reported to enhance fusion activity (16, 29). Recent studies suggest that certain glycosaminoglycans of the cell surface are required for HRSV infection (13, 14, 23, 27). The G protein, as well as the F protein, have been demonstrated to bind to these carbohydrate structures (10, 11, 18, 23).

The primary sequence of the F protein from different serotypes of HRSV and BRSV is highly conserved but shows only little homology with other paramyxovirus fusion proteins. However, with respect to size, locations of hydrophobic domains, heptad repeats, and cysteine residues the RSV F protein shares many structural features with other paramyxovirus fusion proteins. A property that is even more common and also found with other virus families is the synthesis of the fusion protein as an inactive precursor F_0 that has to be proteolytically cleaved to become fusion active (21, 22). This posttranslational modification results in the exposition of a hydrophobic fusion peptide at the N terminus of the membrane-anchored fragment. The fusion peptide is supposed to play a crucial role in the fusion process. The majority of viral fusion proteins, including the RSV F proteins, contain a multibasic cleavage motif of the consensus sequence RX(K/R)R immediately upstream of the fusion peptide. This sequence is recognized by the ubiquitous subtilisin-like endoprotease furin of the trans-Golgi network (21, 22). A few viruses are not activated by furin. Their fusion proteins usually contain a monobasic cleavage site that is cleaved by trypsin-like proteases. The type of the cleavage motif has been shown to be an important determinant for virus pathogenicity (21). A unique feature of the RSV F proteins is the cleavage of F_0 at two conserved furin consensus sequences, RAR/KR^{109} (FCS-2) and KKRKRR^{136} (FCS-1), resulting in the generation of three proteolytic fragments, the large membrane-anchored subunit F_1 with the hydrophobic fusion peptide at its N terminus, the small subunit F_2 which is linked to F_1 via a disulfide bridge, and a small peptide composed of 27 amino acids (pep27) originally located between the two cleavage sites (12, 41). All three products have been shown to contain N-linked oligosaccharide side

* Corresponding author. Mailing address: Institut für Virologie, Tierärztliche Hochschule, Hannover, Bünteweg 17, D-30559 Hannover, Germany. Phone: 49-511-953-8857. Fax: 49-511-953-8898. E-mail: Georg.Herrler@tiho-hannover.de.

chains (40, 41). Analysis of the two cleavage sites by site-directed mutagenesis revealed that efficient syncytium formation in transfected cells requires cleavage at both sites (12, 41). Moreover, complete cleavage at both sites was shown to be associated with a conformational change in the molecule (12). In the present study, we made use of reverse genetics to analyze the role of the second furin motif and the intervening peptide in proteolytic activation of BRSV.

MATERIALS AND METHODS

Cells. BSR-T7/5 cells were grown in Eagle minimal essential medium with Earle salts (EMEM) supplemented with 5% fetal calf serum, nonessential amino acids, and 0.5 mg of G418 sulfate (Calbiochem-Novabiochem)/ml. Vero cells were maintained in Dulbecco modified Eagle medium with 5% fetal calf serum. Proximal tubule cells of calf kidney (PT-11 cells) were kindly provided by R. Riebe (Bundesanstalt für Viruserkrankungen der Tiere, Insel Riems, Germany). The cells were grown in EMEM containing 10% fetal calf serum.

Plasmid construction. The BRSV (strain ATue51908) antigenomic plasmid was described previously (3). The unique restriction sites for *Bst*EII and *Nhe*I in this plasmid define a 2,700-bp fragment containing the M2 and almost the whole F gene lacking only the first 130 nucleotides of its open reading frame. This fragment was cloned into a modified pCR3.1 vector (Invitrogen) containing a new single *Bst*EII restriction site. The single *Eco*RI restriction site of pCR3.1 was removed by the cloning step. The resulting plasmid was designated BRSV-F/M2-cassette. The BRSV fusion protein mutants bF:R106N/K108N and bF: K108N/R109N assembled in the pTM1 expression vector have been previously described (41). A *Bst*EII/*Eco*RI-fragment of 540 bp containing the mutations was used to replace the corresponding region in the BRSV-F/M2 cassette. The mutant bF:R106S/K108N/R109N was generated in the same vector by using an overlapping PCR technique. Two PCR products were amplified from the bF: K108N/R109N template by using *Pfu* DNA polymerase (Promega). Nucleotides 1 to 327 of the F open reading frame were amplified by using forward primer bF-S(1-27) (5′-AATCCATGGGCAACACAACCATGAGGATGATC; start codon underlined) and a reverse mutagenesis primer (5′-CGTTGTTTGCTGA ACTGAAGGAGC). Nucleotides 304 to 744 of the *F* gene were amplified by using a forward mutagenesis primer (5′-GCCTCCTTCAGTTCAGCAAACAA CGGC) and reverse primer bF-AS(724-744) (5′-ACTGACAAGGTGTGGTAA TACC). The two PCR products were separated by agarose gel electrophoresis and purified by gel extraction. Equimolar amounts of the purified fragments were combined, heated for 2 min at 95°C for denaturation, and annealed to each other at 60°C for 30 s. Oligonucleotide-primed DNA synthesis with *Pfu* DNA polymerase resulted in a completely double-stranded DNA fragment that was amplified by PCR after addition of the bF-S(1-27) and bF-AS(724-744) primers. The product was digested with *Bst*EII and *Eco*RI and used to replace the corresponding fragment in the BRSV-F/M2 cassette. The whole region that was replaced was sequenced to confirm the nucleotide exchanges. The F protein deletion mutant bF-Δ10-130 lacking nucleotides 316 to 390 was assembled in a similar way by using the oligonucleotides 5′-GAACCGGCCTCCTTCAGTAA GAAGAGAAAAAGGAGATTTTTAGGATTC and 5′-TCTCCTTTTTCTCT TCTTACTGAAGGAGGCCGGTTCATTTTGCATAAG as forward and reverse mutagenesis primers, respectively. Finally, each of the *Bst*EII/*Nhe*I fragments of the parental and mutated BRSV-F/M2 cassettes were used to replace the corresponding region in the BRSV antigenomic plasmid.

Recovery of recombinant BRSV. Recombinant BRSVs were rescued from the supernatant of BSR-T7/5 cells transfected with the antigenomic plasmid, together with four plasmids directing the expression of the viral polymerase complex (3). The viruses were propagated on PT-11 cells. At 5 to 6 days after infection, when the cytopathic effect became obvious, the supernatants were taken; adjusted to 50 mM HEPES (pH 7.5), 0.1 $MgSO_4$, and 10% fetal calf serum; and subjected to low-speed centrifugation to remove cell debris. The supernatants were divided into aliquots, flash-frozen in liquid nitrogen, and stored at −80°C. Low-passage stocks (maximum of four passages) were used throughout all experiments. The identity of the recombinant viruses was verified by reverse transcription-PCR (RT-PCR; see below) and DNA sequencing of the PCR products.

Growth kinetics and virus titration. Multistep replication of the recombinant BRSVs was analyzed by using PT-11 and Vero cells. Confluent cell monolayers seeded the day before in six-well plates were inoculated at 37°C for 3 h with each virus at a multiplicity of infection (MOI) of 0.1. Four wells were infected in parallel with each virus. After adsorption, the inoculum was removed and the cells were washed three times with medium before the addition of 2.5 ml of medium (without fetal calf serum). Two wells of each infection received medium containing 0.5 μg of acetylated trypsin (Sigma)/ml. At the indicated times, aliquots of 250 μl were taken and replaced by the same volume of fresh medium. The aliquots were adjusted to 0.1 M $MgSO_4$, 50 mM HEPES (pH 7.5), and 10% fetal calf serum; flash-frozen in liquid nitrogen; and stored at −80°C until titration.

The viruses were titrated in duplicate on Vero cells grown in 24-well dishes to 90% confluence. The cells were inoculated with 10-fold dilutions of each virus for 3 h at 37°C and overlaid with medium containing 2% fetal calf serum and 0.99% methylcellulose (Sigma). After incubation for 3 days, the medium was removed and the cells were washed twice with phosphate-buffered saline (PBS) and then fixed with 3% paraformaldehyde for 20 min at room temperature. Excess paraformaldehyde was quenched with 0.1 M glycine in PBS for 5 min. The cells were permeabilized with 0.2% Triton X-100 in PBS for 5 min at room temperature and then incubated for 90 min at room temperature with a monoclonal antibody directed to the RSV matrix protein (monoclonal antibody 18G6D1; diluted 1:40 in PBS). The cells were washed three times with PBS and incubated for 1 h at room temperature with a horseradish peroxidase-linked goat antiserum directed to mouse immunoglobulin (1:300 in PBS). After three wash steps, the cells were incubated for 10 min with AEC peroxidase substrate (1.7 mM 3-amino-9-ethylcarbazole and 0.1% H_2O_2 in 50 mM sodium acetate buffer [pH 5.0]). Immunostained cells were counted under an inverse light microscope.

RT-PCR. Total RNA was prepared from Vero cells 2 days after infection (RNeasy [Qiagen]) and reverse transcribed by using Expand reverse transcriptase (Roche Diagnostics) and random hexamers for priming. Nucleotides 1 to 744 of the F gene were amplified from the cDNA by PCR with oligonucleotides bF-S(1-27) and bF-AS(724-744) and according to the following protocol: initial denaturation at 94°C for 1.5 min, followed by 35 two-step cycles (each composed of denaturation at 94°C for 30 s and annealing-elongation at 60°C for 30 s), with a final elongation step at 72°C for 7 min. The PCR products were separated on a 2% agarose gel, stained with ethidium bromide, and analyzed on a UV transluminator.

Radioimmunoprecipitation. Confluent monolayers of PT-11 cells grown on 35-mm dishes (ca. 10^6 cells per dish) were inoculated with 250 μl of serum-free EMEM containing rBRSV at an MOI of 0.1. After 2 h of adsorption, the inoculum was replaced by 2.5 ml of EMEM containing 5% fetal calf serum. At 40 h postinfection, the cells were washed twice with PBS, starved for 1 h in methionine-cysteine-deficient EMEM, and then incubated for 1 h with 250 μl of the same medium supplemented with 50 μCi of [^{35}S]methionine-[^{35}S]cysteine (Trans-^{35}S-label [ICN]). Immunoprecipitation of the F protein from cell lysates was performed as recently described (41).

Western blot. Confluent monolayers of PT-11 cells grown in 25-cm^2 flasks were inoculated in duplicate with the indicated recombinant BRSVs (MOI of 0.1) for 3 h at 37°C. After removal of the inoculum, the cells were maintained in medium with 10% fetal calf serum for 24 h at 37°C, washed three times with PBS, and then maintained in medium without fetal calf serum for a further 96 h. The duplicate cells received medium supplemented with 0.5 μg of acetylated trypsin/ml. At 5 days postinfection, the cell culture supernatants were harvested and subjected to low-speed centrifugation (2,000 × *g*, 15 min, 4°C) to remove detached cells. An aliquot of each supernatant was taken and titrated by plaque assay as described above. Viruses in the remaining supernatant (ca. 4.5 ml) were pelleted through a 25% sucrose cushion by ultracentrifugation (105,000 × *g*, 60 min, 4°C) and dissolved in sodium dodecyl sulfate (SDS) sample buffer. The volume was adjusted corresponding to the calculated virus titers. Aliquots (10 μl) of the viruses were run on an SDS–10% polyacrylamide gel under nonreducing conditions and transferred to nitrocellulose by the semidry blotting technique (24). The membrane was incubated overnight at 4°C with PBS containing 1% bovine serum albumin, washed three times with PBS containing 0.1% Tween 20, and incubated for 1 h at room temperature with a mixture of three different monoclonal antibodies directed to the RSV F protein (each diluted 1:1,000 in PBS). The antibodies used were RSV3216 (Serotec) and clones 7.90I and 47F kindly provided by Jose Antonio Melero (Madrid, Spain) and Clara Orvell (Stockholm, Sweden), respectively. The blots were washed as described above, and primary antibody was detected by incubation with a biotinylated goat anti-mouse immunoglobulin serum (1:1,000 in PBS; Amersham-Pharmacia), followed by three wash steps and incubation with a streptavidin-peroxidase complex (1:2,000 in PBS; Amersham-Pharmacia). Both incubations were performed for 60 min at 4°C. Finally, the nitrocellulose was washed as described above and incubated for 1 min with a chemiluminescent peroxidase substrate (BM chemiluminescence blotting substrate, Roche Diagnostics). The resulting light emission was visualized by short exposure of the membrane to an Biomax autoradiography film.

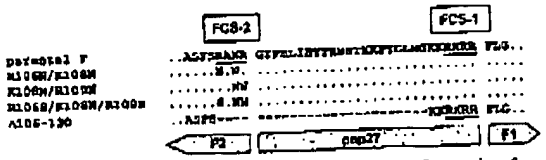

FIG. 1. Amino acid changes introduced into the F protein of recombinant BRSVs. A section of the BRSV fusion protein comprising amino acids 102 to 139 is shown. The furin consensus sequences are underlined, and the positions of the amino acids located N terminally of the furin cleavage site are indicated. Identical amino acids are represented by dots, and dashes indicate deleted amino acids. The three proteolytic cleavage products F_1, F_2, and pep27 are indicated by bars.

RESULTS

The RSV fusion protein contains two conserved furin consensus sequences: FCS-1 is located immediately upstream of the fusion peptide, whereas FCS-2 is separated from the fusion peptide by a stretch of 27 amino acids, designated pep27 (Fig. 1). Previously, we reported that changing FCS-2 of the HRSV ($RARR^{109}$) or the BRSV ($RAKR^{109}$) fusion protein to either $NANR^{109}$ or $NANR^{109}$ abolished cleavage by furin, whereas cleavage at FCS-1 was not affected (41). In the modified FCS-2 motifs, single arginine residues either at position 106 or position 109 were preserved making these sites susceptible to trypsin-like proteases. To evaluate the role of FCS-2 in the proteolytic activation of RSV, we generated two recombinant BRSV mutants, rBRSV-F(R106N/K108N) and rBRSV-F(K108N/R109N), differing from the parental virus in the same amino acid exchanges described above (Fig. 1). The mutants were rescued after transfection of BSR-T7/5 cells with the modified antigenomic plasmid together with four plasmids directing the expression of the polymerase complex (3). Since we first hypothesized that cleavage at FCS-2 might be required to activate fusion activity of the virus mutants, we added trypsin to the cell culture supernatant. However, the recovery of the mutants was also successful in the absence of exogenous trypsin. To exclude the possibility that endogenous trypsin-like proteases could cleave at the preserved arginine residues, we generated another recombinant BRSV, rBRSV-F(R106S/K108N/R109N), in which FCS-2 was replaced by the amino acid sequence $SANN^{109}$ (Fig. 1). Like the other two mutants, this virus was efficiently recovered from transfected BSR-T7/5 cells. In addition to mutants containing amino acid exchanges, we constructed and rescued a recombinant virus, rBRSV-F(Δ106-130), with a deletion of 25 amino acids in the F protein. The deletion comprised FCS-2 and most of pep27, retaining only FCS-1 and the two basic amino acids at positions 131 and 132 (Fig. 1). Virus stocks were prepared by two passages on PT-11 (bovine calf kidney) cells. To verify the identity of the recombinant virus mutants, total RNA was extracted from infected cells and the region between nucleotides 5570 and 6313 of the RNA genome was amplified by RT-PCR. Although the PCR product derived from the parental virus genome was ca. 750 bp long, the deletion mutant was characterized by a PCR product of 670 bp, thus confirming the deletion within the F gene (data not shown). All changes introduced into the F gene were also verified by sequencing of the RT-PCR products.

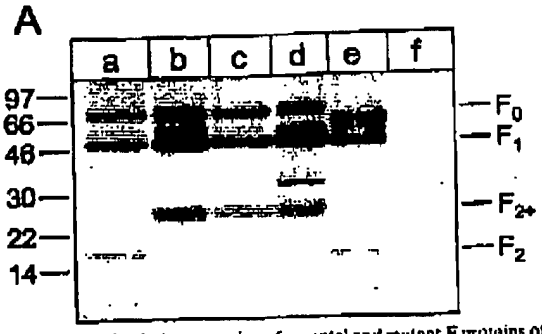

FIG. 2. Proteolytic processing of parental and mutant F proteins of recombinant BRSVs. (A) PT-11 cells were infected with recombinant BRSVs at an MOI of 0.1. At 40 h after infection, the cells were metabolically labeled with [^{35}S]methionine-[^{35}S]cysteine for 1 h, and F protein was immunoprecipitated from the cell lysates. The immunoprecipitates were separated by Tricine–SDS–10% polyacrylamide gel electrophoresis under reducing conditions and detected by autoradiography [lane a, rBRSV-F(parental); lane b, rBRSV-F(R106N/K108N); lane c, rBRSV-F(K108N/R109N); lane d, rBRSV-F(R106S/K108N/R109N); lane e, rBRSV-F(Δ106-130); lane f, noninfected cells]. (B) PT-11 cells were infected with recombinant BRSVs at an MOI of 0.1 and maintained in medium either in the absence or presence of trypsin (as indicated at the top of the gel). After 4 days, the viruses were harvested from the cell culture supernatant and then pelleted by ultracentrifugation. The viruses were solubilized by SDS sample buffer and run on an SDS–8% polyacrylamide gel under nonreducing conditions [lanes a and b, rBRSV-F(parental); lanes c and d, rBRSV-F(R106N/K108N); lanes e and f, rBRSV-F(K108N/R109N); lanes g and h, rBRSV-F(R106S/K108N/R109N); lanes i and j, rBRSV-F(Δ106-130)]. F protein was detected by conventional Western blot technique with a mixture of three monoclonal antibodies directed to this protein. The relative positions of standard proteins (with the molecular masses indicated in kilodaltons) are shown on the left.

We have previously shown that FCS-2 cleavage mutants are characterized by a large size F_2 subunit designated F_2+ (41). The difference in molecular weight between F_2 and F_2+ is due to the glycosylated pep27 that remains attached to F_2. This phenotypical marker allowed us to distinguish between parental and mutant rBRSVs. The F proteins were immunoprecipitated from metabolically labeled PT-11 cells 2 days after infection and analyzed by Tricine-SDS-PAGE under reducing conditions (Fig. 2A). The parental F protein (lane a) appeared as three distinct bands: the precursor F_0 (72 kDa), the large subunit F_1 (50 kDa), and the small subunit F_2 (17 kDa). Instead of F_2, all three FCS-2 mutants showed the characteristic F_2+ band of 26 kDa (lanes b to d), indicating that the modified motifs were resistant to furin cleavage. Immunoprecipitation of the F deletion mutant revealed a different pattern. Due to the absence of the glycosylated pep27, F(Δ106-130) differed from the parental F protein in the smaller size of its precursor F_0 (lane e).

Since the FCS-2 mutants might be activated by cellular proteases secreted into the medium, we also analyzed the F proteins incorporated into mature virus particles. At 4 days postinfection, the virions were pelleted from the clarified supernatants through a 25% sucrose cushion, separated by

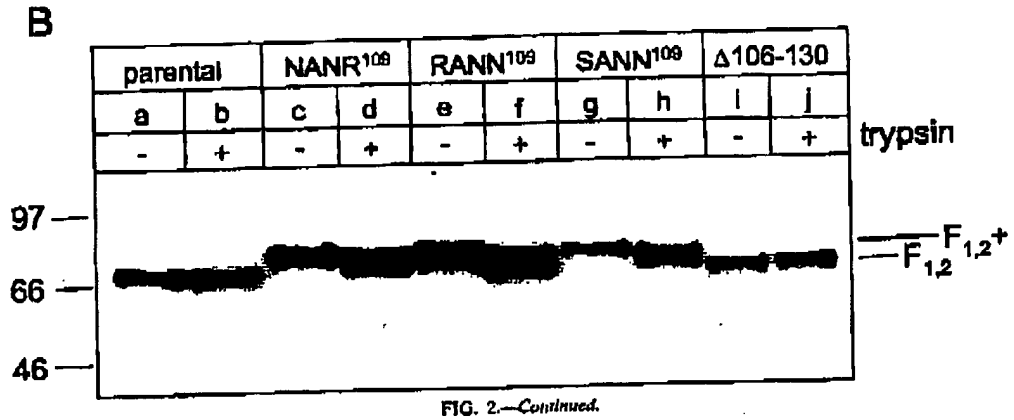

FIG. 2.—*Continued.*

SDS-polyacrylamide gel electrophoresis under nonreducing conditions, and analyzed by the Western blot technique (Fig. 2B). The F protein of the parental rBRSV appeared as a 72-kDa disulfide-linked complex ($F_{1,2}$) composed of F_1 and F_2 (lane a). Addition of trypsin to the cell culture supernatant did not change this pattern (lane b). The presence of F_2+ in the FCS-2 cleavage mutants caused a molecular weight shift of the disulfide-linked complex to ca. 82 kDa ($F_{1,2}$+) (lanes c, e, and g). A 72-kDa band that would indicate cleavage by endogenous proteases was not detected with any of the mutants. However, the addition of trypsin to the cell culture medium led to a partial cleavage of rBRSV-F(R106N/K108N) (lane d) and rBRSV-F(K108N/R109N) (lane f) and also of rBRSV-F(R106S/K108N/R109N) (lane h). However, cleavage of the latter mutant did not result in the $F_{1,2}$ complex of 72 kDa, indicating that cleavage has occurred at another basic amino acid within pep27. The deletion mutant showed the same pattern as the parental virus (compare lanes a and b with lanes i and j). After proteolytic release of pep27 from the parental F protein, there is no major difference between the two F proteins that could be detected by the Western blot.

The growth characteristics of the parental and mutant rBRSVs were analyzed by using the bovine kidney PT-11 cell line, as well as African green monkey kidney (Vero) cells. The cells were infected in duplicate with the viruses at an MOI of 0.1, and supernatants were collected over a 6-day period at 24-h intervals. The virus titers were quantitated in duplicate by a plaque assay facilitated by immunological staining of the matrix protein. In the absence of trypsin (Fig. 3A), the FCS-2 cleavage mutants showed a somewhat reduced virus release in the beginning, but at day 6 postinfection they reached the titers of the parental virus. In the case of the mutants rBRSV-F(R106N/K108N) and rBRSV-F(K108N/R109N), this growth retardation was compensated for by the addition of acetylated trypsin (0.5 μg/ml) to the cell culture supernatant (Fig. 3B). In contrast, trypsin did not affect replication of either the parental virus or the mutant rBRSV-F(R106S/K108N/R109N) (Fig. 3C). The deletion mutant rBRSV-F(Δ106-130) replicated in PT-11 cells with a kinetics comparable to that of the parental virus. Likewise, the presence of trypsin had no effect on replication of this virus. Very similar growth kinetics were observed with Vero cells, although BRSV generally grew to lower titers in this cell line (not shown). On the other hand, BRSV caused a much more pronounced cytophatic effect in Vero cells than in PT-11 cells. At day 3 postinfection, we observed giant multinucleated cells in the Vero cell monolayer infected with the parental rBRSV (Fig. 4). Syncytium formation was also induced by the FCS-2 cleavage mutants; however, the syncytia were of smaller size and contained much fewer nuclei, indicating that the mutations introduced into the FCS-2 cleavage site affect cell-to-cell fusion. The syncytia formed by the mutants rBRSV-F(R106N/K108N) and rBRSV-F(K108N/R109N) grew to almost the parental virus level during the following 24 h. In striking contrast, the size of syncytia formed by the mutant rBRSV-F(R106S/K108N/R109N) did not change with time (data not shown). The deletion mutant showed a phenotype similar to that of the triple mutant, e.g., formation of very small syncytia that did not increase in size after longer incubation. Taken together, these results indicate that both FCS-2 and the intervening peptide pep27 are dispensable for virus replication in cell culture.

DISCUSSION

The fusion protein of RSV resembles many other viral fusion proteins in the location of a furin recognition site immediately upstream of the fusion peptide. Cleavage at this site by furin or a related cellular protease results in the location of the fusion peptide at the N terminus of the membrane-anchored subunit and is associated with a conformational change as shown for influenza virus hemagglutinin and the fusion proteins of simian virus 5 and RSV (6, 9, 12). Many viral fusion proteins require this posttranslational modification in order to become fusion active (21, 22). For example, blocking this step by specific furin inhibitors has been shown to reduce the infectivity of human immunodeficiency virus type 1 (15). In addition, recombinant measles was demonstrated to require an exogenous trypsin for activation of infectivity if the furin motif of the viral fusion protein was changed into a trypsin-like motif (26). However, reverse genetics showed that the conserved

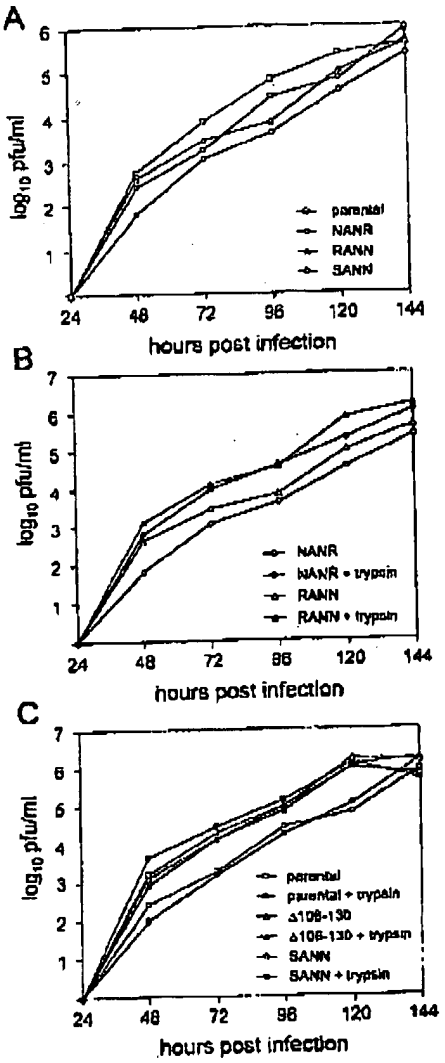

FIG. 3. Multistep replication of recombinant BRSV mutants in PT-11 cells. Duplicate cell monolayers in six-well dishes were infected with the indicated viruses at an MOI of 0.1 and incubated at 37°C with medium either in the absence (open symbols) or presence (solid symbols) of 0.5 μg of acetylated trypsin/ml. Aliquots were taken at the indicated times, stored at −80°C, and titrated in parallel by plaque assay on Vero cells. Each point shown is the mean titer from two wells of infected cells. For reasons of presentation, the figure has been divided into three parts. (A) Comparison of parental rBRSV (parental) with rBRSV-F(R106N/K108N) (NANR), rBRSV-F(K108N/R109N) (RANN), and rBRSV-F(R106S/K108N/R109N) (SANN); (B) effect of trypsin on replication of the mutants rBRSV-F(R106N/K108N) (NANR) and rBRSV-F(K108N/R109N) (RANN); (C) effect of trypsin on replication of parental virus (parental), rBRSV-F(Δ106-130) (Δ106-130), and rBRSV-F(R106S/K108N/R109N) (SANN).

furin motifs found in the Ebola virus glycoprotein and in the human cytomegalovirus glycoprotein B are dispensable for virus growth in cell culture (28, 34). A major difference between these and the former viruses is the location of the furin cleavage site distantly from the postulated hydrophobic fusion domains.

A unique feature of RSV is the additional cleavage of the F protein at a second furin consensus sequence, FCS-2, separated from the fusion peptide by 27 amino acids. Previous studies by using a plasmid-driven or vaccinia virus-based expression system revealed that F-mediated syncytium formation was significantly affected when either FCS-1 or FCS-2 were changed into a furin-resistant motif by site-directed mutagenesis, indicating that cleavage at both sites might be important for activation of the RSV fusion protein (12, 41). In the present study, we learned from reverse genetics that cleavage at FCS-2 is not essential for virus infectivity though the FCS-2 cleavage mutants did not grow as efficiently as the parental virus during the first replication cycles. If a single arginine was left with the modified motif ($NANR^{109}$ or $RANN^{109}$), the addition of trypsin to the cell culture supernatant compensated for this growth retardation, whereas it had no supporting effect on rBRSV-F(R106S/K108N/R109N) that did not contain any arginine or lysine residues in the modified FCS-2. Accordingly, trypsin treatment caused a partial cleavage of the mutants rBRSV-F(R106N/K108N) and rBRSV-F(K108N/R109N), whereas there was no evidence for cleavage by endogenous trypsin-like proteases. However, the mutant F protein of rBRSV-F(R106S/K108N/R109N) was also cleaved by trypsin but probably at a different site. Potential cleavage sites within pep27 are Arg^{110} and $Lys\text{-}Lys^{124}$. The amino acid changes made with the FCS-2 also led to a reduced syncytium formation by the recombinant BRSV mutants. These findings suggest that the fusion activity of the FCS-2 mutants is not abolished but impaired. Probably, the glycosylated pep27 that remains attached to the F_2 subunit of the FCS-2 cleavage mutants interferes with conformational rearrangements necessary for optimal fusion activity (12). In accordance with this view, the deletion mutant lacking pep27 did not show any growth retardation and addition of trypsin had no supporting effect on this virus. Nevertheless, the deletion mutant also showed a drastically reduced syncytium formation activity in Vero cells. It should be noted that the mature parental F protein differs from the deletion mutant with respect to the C terminus of its F_2 subunit. Although the former ends with the sequence $RAKR^{109}$, the latter has two additional amino acids and terminates with the sequence $KKRKRR^{111}$. This C terminus did not impair the infectivity (virus-to-cell fusion) of rBRSV-F(Δ106-130) as indicated by the growth kinetics. However, it might interfere with cell-to-cell fusion, suggesting that the structural requirements for these two processes differ from each other. Differences between virus-to-cell fusion and syncytium formation have also been reported for the fusion protein of other enveloped viruses (8, 32, 37).

The second furin consensus sequence RAK/RR^{109} in the RSV fusion protein is highly conserved in all HRSV and BRSV strains isolated so far, suggesting that this cleavage site has a role in the viral life cycle. Our results indicate that cleavage at FCS-2 is not critical for virus replication in cell culture. However, it might be advantageous for RSV replication in vivo.

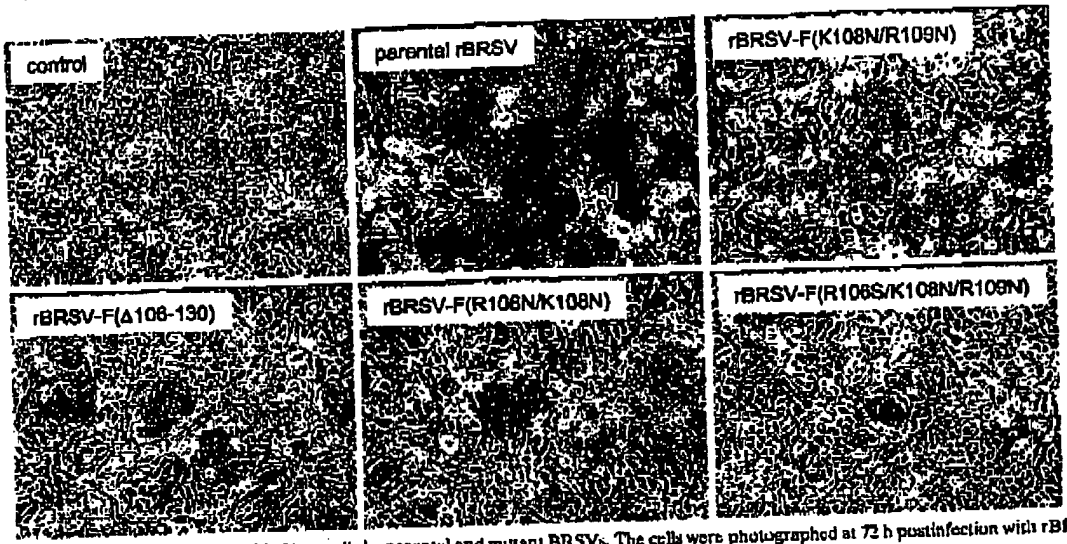

FIG. 4. Cytophatic effect induced in Vero cells by parental and mutant BRSVs. The cells were photographed at 72 h postinfection with rBRSVs containing the indicated mutant F proteins (MOI = 0.1).

One possible function of pep27 and the dual cleavage might be related to the host immune response. The RSV fusion protein has recently been shown to inhibit proliferation of T cells by cell-to-cell contact (31). In analogy to measles virus (38), proteolytic activation of RSV F might be necessary for this function. It will be interesting to determine, by using the mutants described here, how the proteolytic processing of the fusion protein may influence its inhibitory activity. Another possible function might be related to pep27 itself, the intervening peptide released upon furin cleavage at FCS-2 and FCS-1. Like FCS-2, this peptide is dispensable for virus replication in cell culture. However, the motif FYGLM[129] in pep27 of BRSV suggests a possible role in the host. FYGLM[129] matches the signature sequence FXGLM characteristic for the tachykinin family of bioactive peptides (36). Substance P and other members of this family exhibit multiple activities, including the induction of bronchoconstriction, mucus secretion, histamine release, vasodilation, and others (5, 17, 25, 30). It remains to be experimentally shown whether pep27 of BRSV or a further processed form of it exhibits a similar tachykinin-like activity. Although the pep27 peptides of all known BRSV isolates are highly homologous to one another, they show only little similarity with the pep27 of HRSV. In particular, the latter lacks the tachykinin motif, indicating that the pep27 peptides of BRSV and HRSV might exhibit different activities. Whatever the function of the two different peptides exactly is, we should take into account that both peptides might contribute to the pathogenicity of RSV. This idea is especially important for the development of live attenuated RSV vaccines or other virus vectors expressing the RSV F protein, as well as for DNA vaccines which are based on the F gene. In this regard, the deletion mutant rBRSV-F(Δ106-130) is of particular interest since it is expected to lack the proposed activity of pep27. Another feature of this mutant that makes it an interesting vaccine candidate is the reduced cytopathic effect in infected cells. Finally, this virus will help us to study the role of pep27 in infection of the host.

ACKNOWLEDGMENTS

We thank R. Riebe for providing the PT-11 cell line. We acknowledge the help of Jose Antonio Melero and Claes Örvell, who made monoclonal antibodies available to us.

This work was supported by grants from the European Community (QLK2-CT-1999-00843) and the Deutsche Forschungsgemeinschaft (HE 1168/11-1/2) to G.H.

REFERENCES

1. Baker, J. C. 1991. Human and bovine respiratory syncytial virus: immunopathologic mechanisms. Vet. Q. 13:47–59.
2. Baker, J. C., T. R. Ames, and R. J. F. Markham. 1986. Seroepizootiologic study of bovine respiratory syncytial virus in a dairy herd. Am. J. Vet. Res. 47:240–245.
3. Buchholz, U. J., S. Finke, and K.-K. Conzelmann. 1999. Generation of bovine respiratory syncytial virus (BRSV) from cDNA: BRSV NS2 is not essential for virus replication in tissue culture, and the human RSV leader region acts as a functional BRSV genome promoter. J. Virol. 73:251–259.
4. Bukreyev, A., S. S. Whitehead, B. R. Murphy, and P. L. Collins. 1997. Recombinant respiratory syncytial virus from which the entire SH gene has been deleted grows efficiently in cell culture and exhibits site-specific attenuation in the respiratory tract of the mouse. J. Virol. 71:8973–8982.
5. Campos, M. M., and J. B. Calixto. 2000. Neurokinin mediation of edema and inflammation. Neuropeptides 34:314–322.
6. Chen, J., K. H. Lee, D. A. Steinhauer, D. J. Stevens, J. J. Skehel, and D. C. Wiley. 1998. Structure of the hemagglutinin precursor cleavage site, a determinant of influenza pathogenicity and the origin of the labile conformation. Cell 95:409–417.
7. Collins, P. L., K. McIntosh, and R. M. Chanock. 1996. Respiratory syncytial virus, p. 1313–1351. *In* B. N. Fields, D. M. Knipe, and P. M. Howley (ed.), Virology, 3rd ed. Raven Press, New York, N.Y.
8. Dedera, D., and L. Rainer. 1991. Demonstration of two distinct cytopathic effects with syncytium formation-defective human immunodeficiency virus type 1 mutants. J. Virol. 65:6129–6136.
9. Dutch, R. E., R. N. Hagglund, M. A. Nagel, R. G. Paterson, and R. A. Lamb. 2001. Paramyxovirus fusion (F) protein: a conformational change on cleavage activation. Virology 281:138–150.
10. Feldman, S. A., R. M. Hendry, and J. A. Beeler. 1999. Identification of a linear heparin binding domain for human respiratory syncytial virus attachment glycoprotein G. J. Virol. 73:6610–6617.

11. Feldman, S. A., S. Audet, and J. A. Beeler. 2000. The fusion glycoprotein of human respiratory syncytial virus facilitates virus attachment and infectivity via an interaction with cellular heparan sulfate. J. Virol. 74:6442–6447.
12. Gonzalez-Reyes, L., M. B. Ruiz-Argüello, B. García-Barreno, L. Calder, J. A. Lopez, J. P. Albar, J. J. Skehel, D. C. Wiley, and J. A. Melero. 2001. Cleavage of the human respiratory syncytial virus fusion protein at two distinct sites is required for activation of membrane fusion. Proc. Natl. Acad. Sci. USA 98:9859–9864.
13. Hallak, L. K., D. Spillmann, P. L. Collins, and M. E. Peeples. 2000. Glycosaminoglycan sulfation requirements for respiratory syncytial virus infection. J. Virol. 74:10508–10513.
14. Hallak, L. K., P. L. Collins, W. Knudson, and M. E. Peeples. 2000. Iduronic acid-containing glycosaminoglycans on target cells are required for efficient respiratory syncytial virus infection. Virology 271:264–275.
15. Hallenberger, S., V. Bosch, H. Angliker, E. Shaw, H.-D. Klenk, and W. Garten. 1992. Inhibition of furin-mediated cleavage activation of HIV-1 glycoprotein gp160. Nature 360:358–361.
16. Hemmerway, B. R., Y. Yu, Y. Tsukha, K. G. Perrine, E. Gustafson, M. Bernstein, and M. S. Galinski. 1994. Analysis of respiratory syncytial virus F, G and SH proteins in cell fusion. Virology 200:801–805.
17. Jeon, G. F., K. O. Sweet, and R. A. Pauwels. 2001. Airway inflammation and tachykinins: prospects for the development of tachykinin receptor antagonists. Eur. J. Pharmacol. 429:239–250.
18. Karger, A., U. Schmidt, and U. J. Buchholz. 2001. Recombinant bovine respiratory syncytial virus with deletions of the G or SH genes: G and F proteins bind heparin. J. Gen. Virol. 82:631–640.
19. Karron, R. A., D. A. Buonagurio, A. F. Georgiu, S. S. Whitehead, J. E. Adamus, M. L. Clements-Mann, D. O. Harris, V. B. Randolph, S. A. Udem, B. R. Murphy, and M. S. Sidhu. 1997. Respiratory syncytial virus (RSV) SH and G proteins are not essential for viral replication in vitro: clinical evaluation and molecular characterization of a cold-passaged, attenuated RSV subgroup B mutant. Proc. Natl. Acad. Sci. USA 94:13961–13966.
20. Klenness, T. G., and F. Westenbrink. 1990. Immunity to human and bovine respiratory syncytial virus. Arch. Virol. 112:1–25.
21. Klenk, H.-D., and W. Garten. 1994. Host cell proteases controlling viral pathogenicity. Trends Microbiol. 2:39–43.
22. Klenk, H.-D., and W. Garten. 1994. Activation of viral spike proteins by host proteases, p. 241–280. *In* E. Wimmer (ed.), Cellular receptors for animal viruses. Monograph 28. Cold Spring Harbor Laboratory Press, Cold Spring Harbor, N.Y.
23. Krusat, T., and H.-J. Streckert. 1997. Heparin-dependent attachment of respiratory syncytial virus (RSV) to host cells. Arch. Virol. 142:1247–1254.
24. Kyhse-Andersen, J. 1984. Electroblotting of multiple gels: a simple apparatus without buffer tank for rapid transfer of proteins from polyacrylamide to nitrocellulose. J. Biochem. Biophys. Methods 10:203–209.
25. Lecci, A., S. Giuliani, M. Tramontana, F. Carini, and C. A. Maggi. 2000. Peripheral actions of tachykinins. Neuropeptides 34:303–313.
26. Mulmer, A., B. Mrkic, G. Herrler, M. Moll, M. A. Billeter, R. Cattaneo, and H.-D. Klenk. 2000. Recombinant measles virus requiring an exogenous protease for activation of infectivity. J. Gen. Virol. 81:461–449.
27. Martinez, I., and J. A. Melero. 2000. Binding of human respiratory syncytial virus to cells: implication of sulfated cell surface proteoglycans. J. Gen. Virol. 81:2715–2722.
28. Neumann, G., H. Feldmann, S. Watanabe, I. Lukashevich, and Y. Kawaoka. 2002. Reverse genetics demonstrates that proteolytic processing of the ebola virus glycoprotein is not essential for replication in cell culture. J. Virol. 76:406–410.
29. Peeples, M. K., and S. K. Samal. 1997. Analysis of bovine respiratory syncytial virus envelope glycoproteins in cell fusion. J. Gen. Virol. 78:1885–1889.
30. Rogers, D. F. 2001. Motor control of airway goblet cells and glands. Respir. Physiol. 125:129–144.
31. Schlender, J., G. Walliser, J. Fricke, and K.-K. Conzelmann. 2002. Respiratory syncytial virus fusion protein mediates inhibition of mitogen-induced T-cell proliferation by contact. J. Virol. 76:1163–1170.
32. Schmid, E., Zurbriggen, A., Gassen, U., Binz, B., Ter Meulen, V., and J. Schneider-Schaulies. 2000. Antibodies to CD9, a tetraspan transmembrane protein, inhibit canine distemper virus-induced cell-cell fusion but not virus cell fusion. J. Virol. 74:7554–7561.
33. Stott, E. J., and G. Taylor. 1985. Respiratory syncytial virus. Brief review. Arch. Virol. 84:1–52.
34. Sriva, T., E. Barzi, M. Meiserik, and K. Radsak. 2002. Proteolytic processing of human cytomegalovirus glycoprotein B is dispensable for viral growth in culture. J. Virol. 76:1253–1264.
35. Techaarpornkul, S., N. Barretto, and P. E. Peeples. 2001. Functional analysis of recombinant respiratory syncytial virus deletion mutants lacking the small hydrophobic and/or attachment glycoprotein gene. J. Virol. 75:6825–6834.
36. Vanden Broeck, J., H. Torfs, J. Poels, W. Van Poyer, R. Swinnen, K. Ferket, and A. De Loof. 1999. Tachykinin-like peptides and their receptors: a review. Ann. N. Y. Acad. Sci. 897:374–387.
37. van Messling, V., C. Zimmer, G. Herrler, L. Haas, and R. Cattaneo. 2001. The hemagglutinin of canine distemper virus determines tropism and cytopathogenicity. J. Virol. 75:6418–6427.
38. Waldmann, A., A. Meisner, W. Garten, M. Seufert, V. ter Meulen, and S. Schneider-Schaulies. 2000. Proteolytic cleavage of the fusion protein but not membrane fusion is required for measles virus-induced immunosuppression in vitro. J. Virol. 74:1985–1993.
39. Whitehead, S. S., A. Bukreyev, M. N. Teng, C. Y. Firestone, M. St Claire, W. R. Elkins, P. L. Collins, and B. R. Murphy. 1999. Recombinant respiratory syncytial virus bearing a deletion of either the NS2 or SH gene is attenuated in chimpanzees. J. Virol. 73:3438–3442.
40. Zimmer, G., L. Trotz, and G. Herrler. 2001. N-glycans of F protein differentially affect fusion activity of human respiratory syncytial virus. J. Virol. 75:4744–4751.
41. Zimmer, G., L. Budz, and G. Herrler. 2001. Proteolytic activation of respiratory syncytial virus fusion protein: cleavage at two furin consensus sequences. J. Biol. Chem. 276:31642–31650.

This Page is Inserted by IFW Indexing and Scanning Operations and is not part of the Official Record

BEST AVAILABLE IMAGES

Defective images within this document are accurate representations of the original documents submitted by the applicant.

Defects in the images include but are not limited to the items checked:

- ☐ BLACK BORDERS
- ☐ IMAGE CUT OFF AT TOP, BOTTOM OR SIDES
- ☐ FADED TEXT OR DRAWING
- ☐ BLURRED OR ILLEGIBLE TEXT OR DRAWING
- ☐ SKEWED/SLANTED IMAGES
- ☐ COLOR OR BLACK AND WHITE PHOTOGRAPHS
- ☐ GRAY SCALE DOCUMENTS
- ☑ LINES OR MARKS ON ORIGINAL DOCUMENT
- ☐ REFERENCE(S) OR EXHIBIT(S) SUBMITTED ARE POOR QUALITY
- ☐ OTHER: _____

IMAGES ARE BEST AVAILABLE COPY.
As rescanning these documents will not correct the image problems checked, please do not report these problems to the IFW Image Problem Mailbox.